

**Universidade de São Paulo
Escola Politécnica da Universidade de São Paulo**

Diego Dias de Lima Santos

An electric urban tricycle designed for safety

Sao Paulo

2023

Diego Dias de Lima Santos

An electric urban tricycle designed for safety

Dissertation presented to the "Escola Politécnica da Universidade de São Paulo" to obtain the title of Master of Science.

Concentration Area: Project and Manufacturing

Addvisor: Prof. Dr. Marcilio Alves

Revised Version

Sao Paulo

2023

Autorizo a reprodução e divulgação total ou parcial deste trabalho, por qualquer meio convencional ou eletrônico, para fins de estudo e pesquisa, desde que citada a fonte.

Este exemplar foi revisado e corrigido em relação à versão original, sob responsabilidade única do autor e com a anuência de seu orientador.

São Paulo, _____ de _____ de _____

Assinatura do autor: _____

Assinatura do orientador: _____

Catálogo-na-publicação

Santos, Diego Dias de Lima

An electric urban tricycle designed for safety / D. D. L. Santos -- versão corr. -- São Paulo, 2023.

133 p.

Dissertação (Mestrado) - Escola Politécnica da Universidade de São Paulo. Departamento de Engenharia Mecânica.

1.Crashworthiness 2.Design for Safety 3.Tricycle design 4.Electric Vehicle 5.Generative design I.Universidade de São Paulo. Escola Politécnica. Departamento de Engenharia Mecânica II.t.

ACKNOWLEDGEMENTS

I would like to express my heartfelt gratitude to those who have supported and encouraged me to embark on this academic journey.

First and foremost, I would like to thank my advisor, Prof. Dr. Marcílio Alves, for his invaluable guidance, mentorship, and support. His expertise and wisdom have been instrumental in my progress.

I am also thankful to my wife, Bianca, for her love, encouragement, and unwavering support. Her understanding and patience have been a source of strength to me.

My son, Arthur, has brought joy and laughter into my life and has been a constant reminder of what truly matters. I am grateful to have him in my life.

My parents, Eunice and Dirceu, have always been a source of inspiration and encouragement to me. Their love and support have been invaluable.

Finally, I would like to thank my friend Samira, who encouraged me to start this study and has always supported me when I needed it.

I am deeply grateful to have such wonderful people in my life, and I could not have embarked on this journey without their love and support. Thank you from the bottom of my heart.

*“The mind is not a vessel to be filled,
but a fire to be kindled.”*

Lucius Plutarchus (46 – 120 AD)

ABSTRACT

Santos, D. D. L. **An electric urban tricycle designed for safety**. 2023. 133p. Dissertação (Mestrado) - Universidade de São Paulo, Sao Paulo, 2023.

This dissertation presents the design of an electric tricycle for urban use (Trike). The vehicle was developed to mainly meet the needs of transporting people in large cities, having a flexible system for changing transport devices. The structure of the tricycle was optimized, allowing polymers to be used as the main raw material. Seat belts, side curtain airbags and front airbags have been included to increase driver safety. Pilot damage was assessed through explicit analysis, using the finite element method and the Total Human Model for Safety (THUMS).

Keywords: Design for safety, Crashworthiness, Tricycle design, Electric Vehicle, Generative design

RESUMO

Santos, D. D. L. **An electric urban tricycle designed for safety**. 2023. 133p. Dissertação (Mestrado) - Universidade de São Paulo, Sao Paulo, 2023.

Esta dissertação apresenta o projeto de um triciclo elétrico para uso urbano. O veículo foi desenvolvido para atender principalmente a necessidade de transportar cargas ou pessoas em grandes cidades, tendo um sistema flexível para troca dos dispositivos de transporte. A estrutura do triciclo foi otimizada, permitindo que Polímeros fossem utilizados como matéria prima principal. Foram incluídos cinto de segurança, air-bags de cortina nas laterais e air-bag frontal para aumentar a segurança do condutor. Os danos ao piloto foram avaliados por meio de análise explícita, utilizando o método dos elementos finitos e o modelo humano completo para avaliação de segurança (THUMS).

Palavras-chave: Projeto para segurança, Simulação de colisão, Projeto de triciclo, Veículo elétrico, Projeto generativo

LIST OF FIGURES

Figura 1 – Accidents by vehicle type	24
Figura 2 – Deaths by vehicle type	24
Figura 3 – Heat map - Accidents along week	25
Figura 4 – Heat map - Deaths along week	26
Figura 5 – Number of deaths per 100,000 inhabitants	27
Figura 6 – Accidents and deaths over regions	27
Figura 7 – Traffic infractions considering cars, motorcycles, trucks and Bus	28
Figura 8 – Traffic infractions	28
Figura 9 – Studebaker electric car, c. 1905.	31
Figura 10 – Toyota Concept i, presented at Geneva Motor Show as a concept car for 2030.	32
Figura 11 – Relationship between customization, production volume and manufac- turing profitable field	32
Figura 12 – Some of the fields that could be considered on DFX	34
Figura 13 – Electronic Design - Embedded Systems	35
Figura 14 – Digital Twins workflow	36
Figura 15 – Example of parametric and Topology Optimization	36
Figura 16 – Topology optimization applied in a component which will be build by addictive manufacturing process	37
Figura 17 – Example of Generative Design concept	38
Figura 18 – Cost of a product change	44
Figura 19 – Stages of IP^2D^2	45
Figura 20 – Example of QFD Matrix	47
Figura 21 – Design Thinking represented by a double diamond graph	48
Figura 22 – C-K Road Map	50
Figura 23 – C-K Theory - Crazy Concept	50
Figura 24 – Concept and Knowledge spaces - C-K Theory	51
Figura 25 – Morphological Matrix	52
Figura 26 – Sample of Pugh Matrix	53
Figura 27 – The general model for TRIZ problem-solving	54
Figura 28 – The hierarchical view of TRIZ	54
Figura 29 – A CORA road-map	55
Figura 30 – Framework Strategy	56
Figura 31 – Project Chart	58
Figura 32 – Morphological Matrix	65
Figura 33 – Initial Trike Design	67

Figura 34 – Ideated Trike	67
Figura 35 – Load Position	67
Figura 36 – Rider’s dimension scheme)	68
Figura 37 – Rider’s dimension table	69
Figura 38 – Center of mass(Unload motorcycle)	69
Figura 39 – Trike - First road used on dynamic simulation	70
Figura 40 – Trike - First road used on dynamic simulation	70
Figura 41 – Trike - Second road used on dynamic simulation	71
Figura 42 – Trike - Second road used on dynamic simulation	71
Figura 43 – Properties: Front Suspension	71
Figura 44 – Properties: Rear Arm	71
Figura 45 – Adams Results for path 1 - In the left, forces of rear suspension (FX, FY and FZ), in the right Force of front suspension (FX, FY and FZ) .	72
Figura 46 – Adams Results for path 2 - In the left, forces of rear suspension (FX, FY and FZ), in the right Force of front suspension (FX, FY and FZ) .	72
Figura 47 – Adams Results for path 3 - In the left, forces of rear suspension (FX, FY and FZ), in the right Force of front suspension (FX, FY and FZ) .	73
Figura 48 – Longitudinal Speed in constant radius, with longitudinal acceleration .	73
Figura 49 – Roll Angle in constant radius, with longitudinal acceleration	73
Figura 50 – Load Case 1 - Frame	74
Figura 51 – Load Case 2 - Rear Arm	74
Figura 52 – PEKK Properties	75
Figura 53 – EOS P 700 3D Printer	75
Figura 54 – Generative Design Result - Frame	76
Figura 55 – Generative Design Result - Frame	76
Figura 56 – Generative Design Result - Rear Arm	76
Figura 57 – Generative Design Result - Rear Arm	76
Figura 58 – Generative Design Result - Front suspension support	76
Figura 59 – Generative Design Result - Front suspension support	76
Figura 60 – ISOFIX Dimensions	77
Figura 61 – Final tricycle design	78
Figura 62 – Final trike design for goods transportation	78
Figura 63 – Final trike design with passenger transportation - Side view	79
Figura 64 – Final trike design with passenger transportation - Isometric view	79
Figura 65 – Thums model	81
Figura 66 – Experimental test matrix	82
Figura 67 – Model Setup	82
Figura 68 – Experimental test results	83
Figura 69 – Brain Model	83

Figura 70 – From left to right: Low strain rate, Medium strain rate and High strain rate	84
Figura 71 – Knee Joint experiment	85
Figura 72 – Neck Ligaments	85
Figura 73 – Spine Posture prediction	85
Figura 74 – Pre-processing in Hypermesh	86
Figura 75 – In the left, helmet model, in the middle, the helmet with the lower belt and in the right helmet meshed	87
Figura 76 – Thums model positioning with Piper’s software	87
Figura 77 – Complete model pre-processed - Trike, THUMS and Helmet	88
Figura 78 – Frontal Crash simulation - Trike, Thums, Helment and Frontal Airbag	89
Figura 79 – Side Impact simulation - Trike, Thums, Helment and Frontal Airbag	90
Figura 80 – Energy balance	91
Figura 81 – Color Pattern	96
Figura 82 – Application of Color Pattern	97
Figura 83 – Example of divided component in two parts	97
Figura 84 – Neck Injury Criteria	98
Figura 85 – Head Acceleration and equivalent HIC36 - Frontal Impact	98
Figura 86 – Head Acceleration and equivalent HIC36 - Side Impact	99
Figura 87 – Vertebrates C1 and C7	99
Figura 88 – Neck Shear and Tension Force - Frontal Impact	100
Figura 89 – Neck Bending Moment - Frontal Impact	100
Figura 90 – Neck Shear and Tension Force - Side Impact	101
Figura 91 – Neck Bending Moment - Side Impact	101
Figura 92 – Summary of proposed injuries criteria for skull and brain	103
Figura 93 – In the left, Brain First Principal Strain and in the right Brain VonMises Stress for the Frontal Impact	104
Figura 94 – In the left, Brain First Principal Strain and in the right Brain VonMises Stress for the Side Impact	104
Figura 95 – In the left, Skull Maximum Principal Strain and in the right Skull strain energy for the Frontal Impact	105
Figura 96 – In the left, Skull Maximum Principal Strain and in the right Skull strain energy for the Side Impact	105
Figura 97 – Summary of proposed injuries criteria for internal organs	106
Figura 98 – In the left, Heart Maximum Principal Strain for Frontal Impact and in the right Heart Maximum Principal Strain for the Side Impact	106
Figura 99 – In the left, Lung Maximum Principal Strain for Frontal Impact and in the right Lung Maximum Principal Strain for the Side Impact	107
Figura 100 – Summary of proposed injuries criteria for thorax	108

Figura 101–In the left, Thorax First Principal Strain, and in the right Thorax VonMises stress for the Front Impact	108
Figura 102–In the left, Thorax First Principal Strain, and in the right Thorax VonMises stress for the Side Impact	109
Figura 103–Kinematic structure of a motorcycle	117
Figura 104–Geometry of a motorcycle	118
Figura 105–Dimension of the trail for the electric motorcycle	120

LIST OF TABLES

Tabela 1 – Accidents involving motorcycles in 2020	29
Tabela 2 – 5W2H applied to Main Project	59
Tabela 3 – Relative Importance Matrix	60
Tabela 4 – Correlation Matrix	60
Tabela 5 – Top Flop Matrix	62
Tabela 6 – Innovation Table	63
Tabela 7 – What and How table	64
Tabela 8 – Use cases	68
Tabela 9 – Maximum components of forces per user case	74

LIST OF ABBREVIATIONS AND ACRONYMS

AGD	Autodesk Generative Design
ABRAMET	Brazilian Association of Traffic Medicine (Associação Brasileira de Medicina de Tráfego)
CAD	Computer Aided Design - Usually related to define a model built by any CAD Software
CAE	Computer Aided Engineering
CAM	Computer Aided Manufacturing
CAPP	Computer Aided Process Planning
CFD	Computational Fluid Dynamics
DFMA	Design for Manufacturing and Assembly
DFS	Design for Safety
DFC	Design for Compliance
DFMa	Design for Maintainability
DFD	Design for Disassembling
DFEA	Design for Ergonomics Aspects
DFI	Design for Integration
DFEc	Design for Ecology
DFE	Design for Energy
DFW	Design for Wellness
DFCh	Design for Change
DFDs	Design for Discovery
DFTOp	Design for Topology optimization
DFAM	Design for Additive Manufacturing
DFR	Design for Recycling
DFX	Design for Excellence
FEA	Finite Element Analysis
FENABRAVE	Brazilian Federation of Motor Vehicle Distribution (Federação Nacional da Distribuição de Veículos Automotores)
HBM	Human Body Model

PLM	Product Life-cycle Management
PRF	Polícia Rodoviária Federal
SENATRAN	Brazilian Traffic Department (Secretaria Nacional de Trânsito)
SWOT	Strengths, Weaknesses, Opportunities, and Threats
THUMS	Total Human Model for Safety
TRIZ	Theory of Inventive Problem Solving (Teoriya Resheniya Izobretatelskikh Zadatch)
5W2H	Who, What, Where, When, Why, How, and How Much

SUMÁRIO

1	INTRODUCTION	23
1.1	Motorcycle Accidents	23
1.2	An overview of product design	30
1.2.1	Design for customization	31
1.2.2	Design for Excellence	33
2	OBJECTIVES	39
3	METHODOLOGIES FOR PRODUCT DEVELOPMENT	41
3.1	Engineering design	41
3.1.1	1-D Modeling and Simulation	42
3.1.2	Problem Definition	43
3.1.3	Product Design Specification	44
3.1.4	Quality Function Deployment	46
3.2	Design Thinking	47
3.3	C-K Design Theory	48
3.4	Morphological Matrix Method	51
3.5	Ranking and selection of the better solution	52
3.6	TRIZ	53
3.7	CORA	55
3.8	Strategy Frameworks	56
4	TRICYCLE DESIGN BASED ON DFSS	57
4.0.1	Define stage	57
4.0.1.1	Customer needs	57
4.0.2	Measure stage	59
4.0.2.1	Benchmarking	61
4.0.3	Analyse stage	63
4.0.3.1	WHAT /HOW Relationship Matrix	63
4.0.4	Design stage	66
4.0.5	Verify stage	66
4.0.5.1	Generative Designing	74
4.1	Design result	74
5	SAFETY ANALYSIS	81
5.1	THUMS Overview	81
5.1.1	Materials used in human models	82

5.1.1.1	Hard Materials	82
5.1.1.2	Soft Materials	83
5.1.2	Modeling and Pre-Processing	85
5.2	THUMS Evaluation	87
6	RESULTS AND DISCUSSION	93
6.1	Product design	93
6.1.1	Process Planing	95
6.1.1.1	Manufacturing	96
6.2	Safety analysis	97
6.2.1	Injuries evaluation	97
6.2.1.1	Head and Neck	97
6.2.2	Skull and Brain	103
6.2.2.1	Internal Organs	106
6.2.2.2	Thorax	107
6.3	Model complexity	109
7	CONCLUSION AND FUTURE WORK	111
	REFERÊNCIAS	113
	ANEXO A – MOTORCYCLE’S CHARACTERISTICS	117
A.0.1	Trail	119
A.0.2	Turning	120
A.0.3	Leaning	120
A.0.4	Countersteering	122
A.0.5	Maneuverability	122
A.0.6	Acceleration	123
A.0.7	Braking	124
A.0.8	Tires	124
A.0.9	Equation of motion	125
	ANEXO B – MECHANICAL DRAWINGS	127

1 INTRODUCTION

Urban mobility is a fascinating and complex topic as it involves various modes of transportation such as busses, cars, motorcycles, bicycles, and pedestrians. Each technology brings a set of characteristics, which has its advantages and disadvantages.

It is a fact that the investment in the development and improvement of car designs surpasses other categories. If we compare motorcycle accidents with light vehicles, motorcyclists are much more at risk. According to ABRAMET, in Brazil at least 30% of the victims who visit the health care system are due to accidents of this type.

Although the Covid-19 pandemic has led to a decline in motorcycle sales, this market generated a profit of more than R\$700 billion in 2020 with a registration figure of more than 900 thousand motorcycles according to FENABRAVE.

Within this context, this work seeks both to present a project adhering to current product development practices and to perform numerical simulations aimed at reconstructing accidents, keeping the driver as the protagonist of the scenario.

1.1 Motorcycle Accidents

According to a report provided by the Ministry of Infrastructure of Brazil, in 2021 was recorded 4.187.002 traffic accidents, in which 6.434.272 people were injured and 108.506 people died. In other words, the consequences of the accidents were not insignificant.

The relation between accidents and vehicle type can be seen in the figure 1. It is possible to note that 53,22% of accidents is related to automobile and 17,49% involved motorcycles.

Regarding the number of deaths, the accidents involving motorcycle represent the highest number, 35,27%, which correspond to 38.270 obits (See Figure 2.

We note that both the highest number of accidents and the highest number of deaths occur on weekends, at night as is shown at figure 3 and figure 4.

If we consider only accidents involving motorcyclists, we recorded 885,777 incidents in

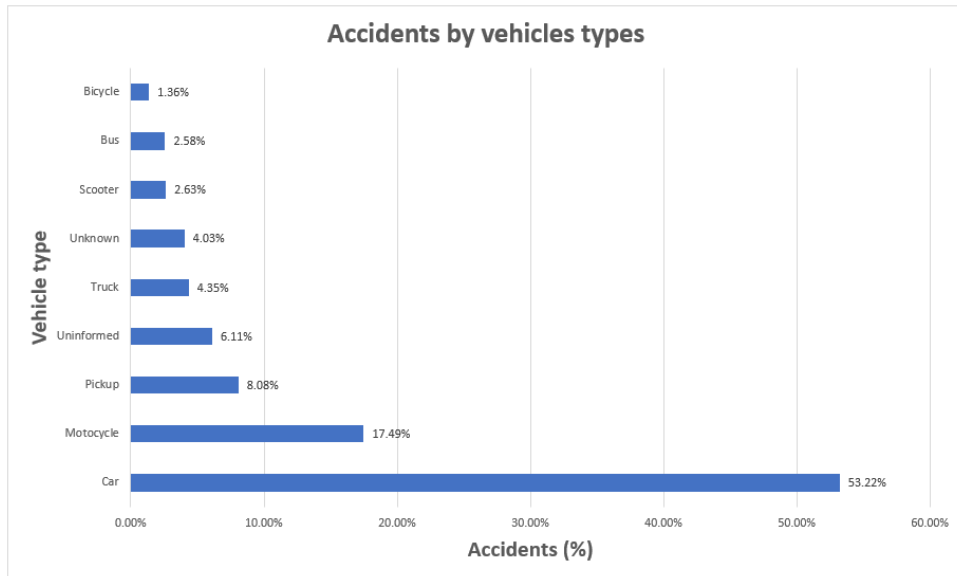


Figura 1 – Accidents by vehicle type

Source: Ministry of Infrastructure of Brazil - webpage: <https://www.gov.br/infraestrutura/pt-br/assuntos/transito/arquivos-senatran/docs/renaest>

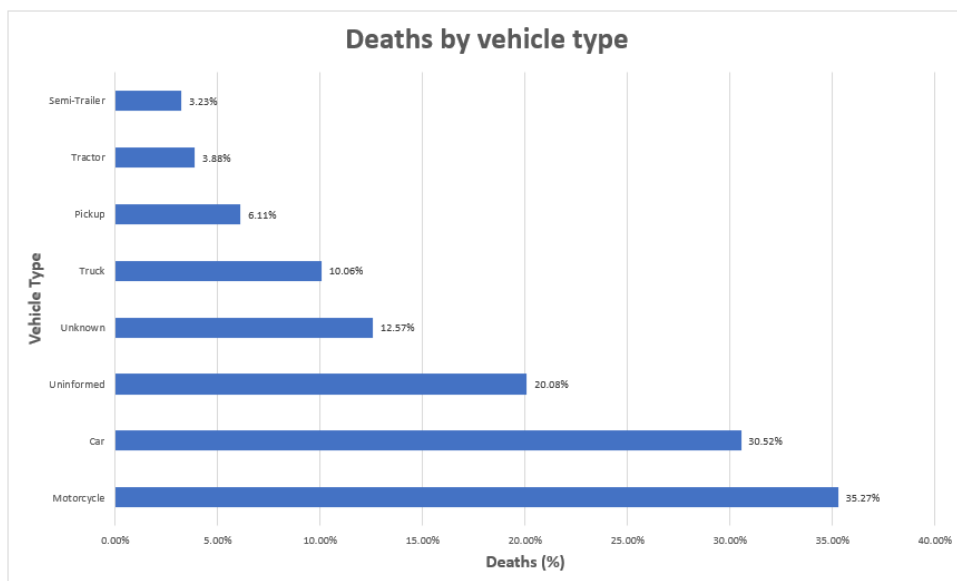


Figura 2 – Deaths by vehicle type

Source: Ministry of Infrastructure of Brazil - webpage: <https://www.gov.br/infraestrutura/pt-br/assuntos/transito/arquivos-senatran/docs/renaest>

2021, with 35,501 deaths (Figure 5).

According to SENATRAN, the total active fleet in Brazil in 2021 was 115,116,532 vehicles, of which 25,743,762 were motorcycles. Although motorcyclists account for 22% of motorists,

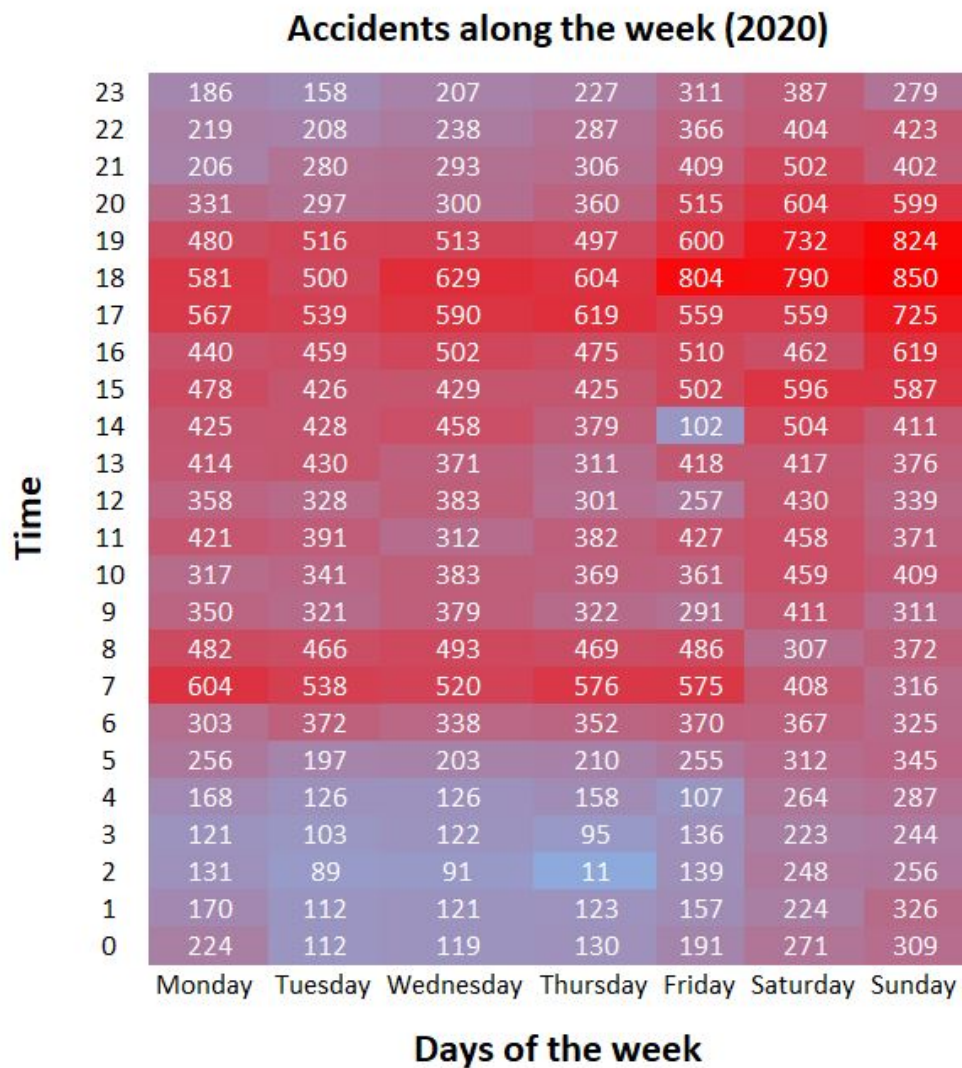


Figura 3 – Heat map - Accidents along week

Source: 2020's Annual Report - PRF

35% of traffic fatalities in Brazil are motorcyclists. It is possible to see in figure 5 as deaths involving motorcycle accidents are higher than involving other vehicles.

The regional distribution shows that the North region of Brazil has the lowest number of accidents, followed by the Midwest. The Northeast, Southeast, and South regions were virtually tied. Table 1 shows the number of motorcycle's riders injured or death in federal highways in Brazil, along the year of 2020. In terms of the number of fatalities, the North region had the lowest number of accidents, followed by the Midwest, with the Northeast region having a negative peak in this regard. See Figure 6.

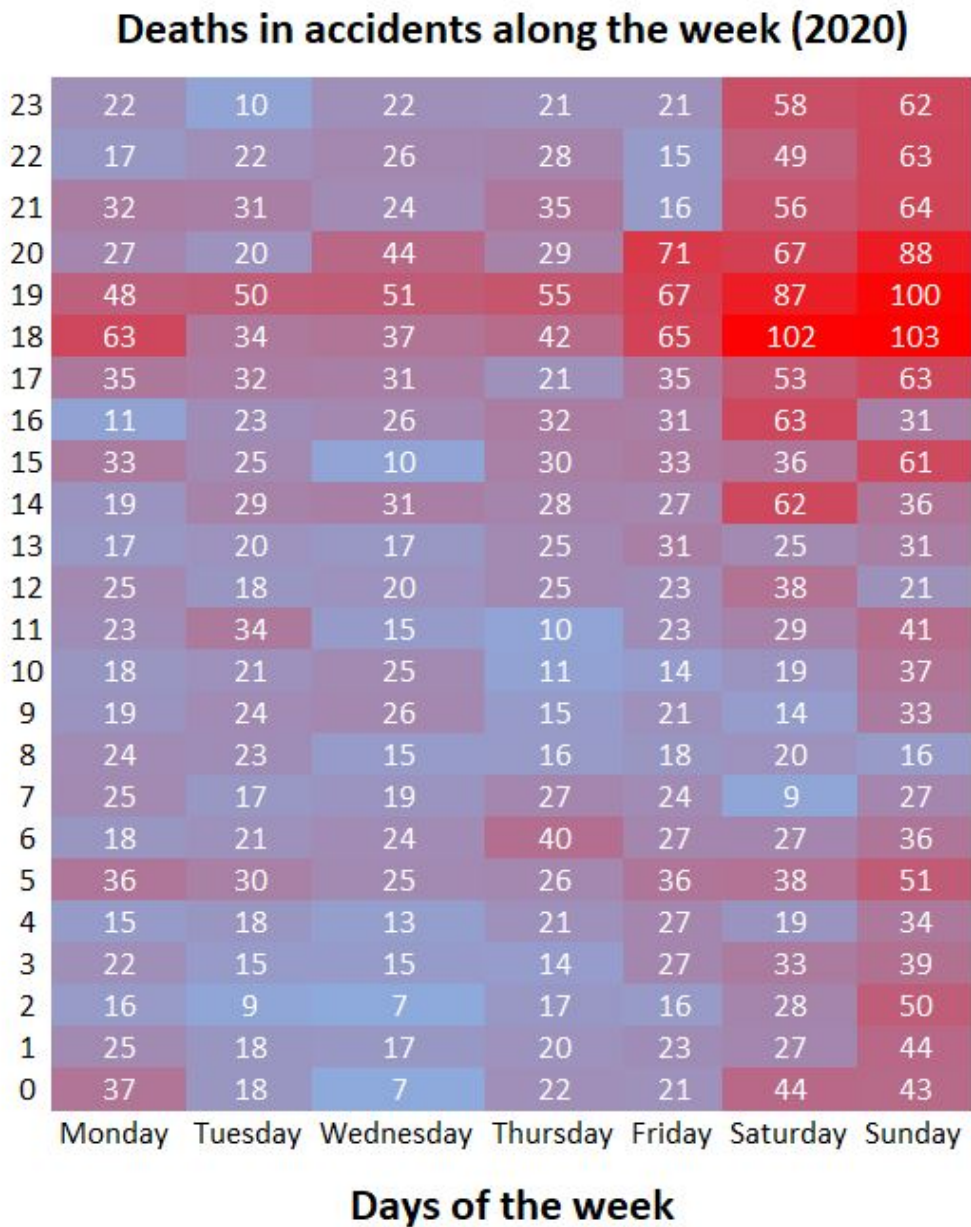


Figura 4 – Heat map - Deaths along week

Source: 2020's Annual Report - PRF

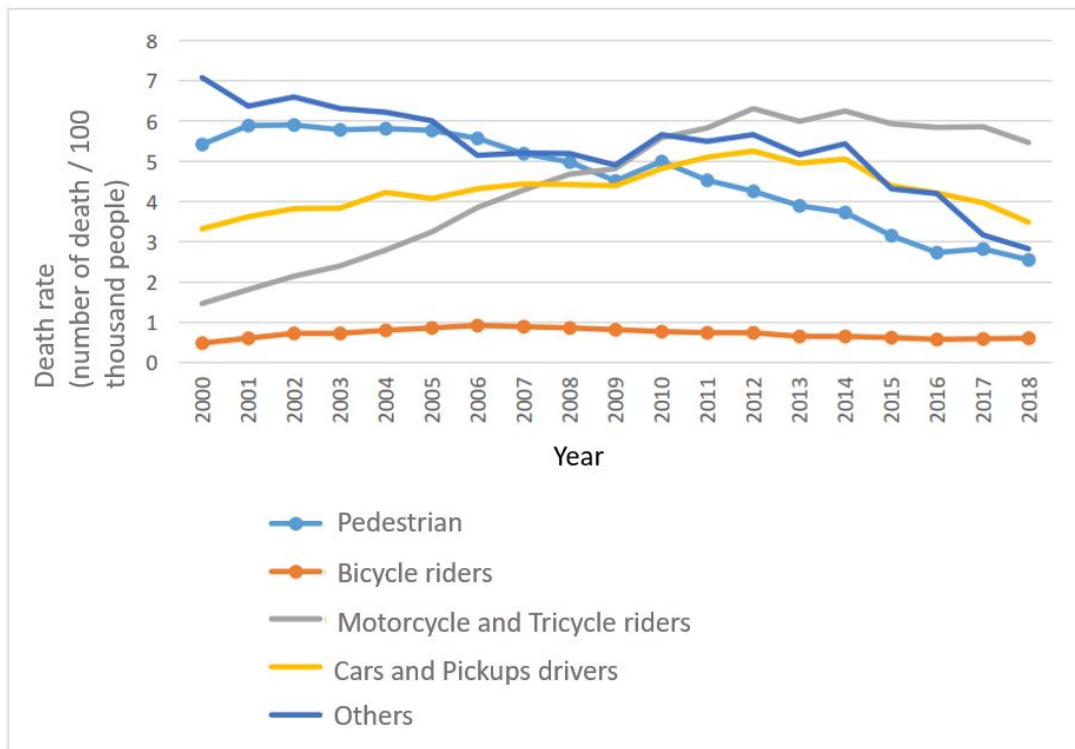


Figura 5 – Number of deaths per 100,000 inhabitants

Brazilian Ministry of Health - SUS Report

Number of deaths by region and group of vehicle (2020)

Car	421	928	202	809	797
Other	46	148	33	121	79
Bus	32	70	9	108	40
Truck	343	720	161	677	554
	Midwest	North East	North	Southeast	South
	Region				

Number of accidents by region and group of vehicle (2020)

Car	5164	8615	2318	12234	13324
Other	267	651	198	859	726
Motorcycle	2684	6137	1890	6840	6841
Truck	2368	3807	1038	5234	4563
	Midwest	North East	North	Southeast	South
	Region				

Figura 6 – Accidents and deaths over regions

Source: 2020's Annual Report - PRF

The number of accidents can be attributed to behavioral characteristics, among others. In this context, the number of reported traffic violations could be a strong indicator. In 2020, more than 70 thousand drivers were identified without helmets, and more than 2 million were driving above the speed limit, as shown in figure 7.

Infractions registered along the years

Year	Alcohol	Helmet	SeatBelt	Overtaking	Maximum Speed	Others
2007	6,619.00	19,073.00	90,067.00	230,544.00	689,367.00	819,800.00
2008	10,210.00	27,970.00	133,121.00	291,426.00	1,023,999.00	946,072.00
2009	22,521.00	35,168.00	182,260.00	323,470.00	1,309,810.00	1,172,380.00
2010	28,665.00	36,542.00	182,641.00	345,094.00	1,261,385.00	1,184,038.00
2011	27,738.00	44,326.00	181,026.00	3,466,157.00	1,095,222.00	1,189,851.00
2012	31,792.00	55,661.00	203,072.00	337,492.00	1,028,479.00	1,187,247.00
2013	38,901.00	56,741.00	248,040.00	375,545.00	1,082,554.00	1,450,022.00
2014	32,286.00	51,635.00	231,546.00	332,603.00	1,300,655.00	1,376,499.00
2015	23,459.00	52,290.00	247,669.00	308,735.00	3,244,773.00	1,532,145.00
2016	17,860.00	50,873.00	233,294.00	277,367.00	3,272,472.00	1,733,091.00
2017	19,083.00	48,140.00	213,347.00	285,538.00	3,053,200.00	2,404,537.00
2018	17,929.00	44,412.00	186,288.00	256,628.00	4,840,535.00	2,010,385.00
2019	18,467.00	46,773.00	209,913.00	247,081.00	3,038,748.00	2,181,141.00
2020	11,901.00	70,606.00	271,418.00	292,162.00	2,375,376.00	2,146,108.00

Figura 7 – Traffic infractions considering cars, motorcycles, trucks and Bus

Source: 2020’s Annual Report - PRF

Historically, these two violations have increased since 2007 (Figure 8), which may reflect the increase in the number of PRF’s officials inspecting these aspects, a greater efficiency in the way of recording incidents, or it may actually express the increase in the

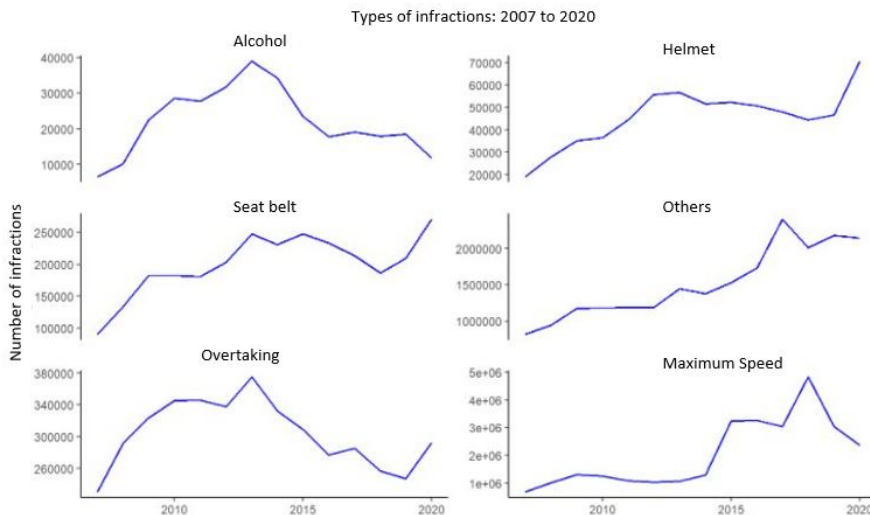


Figura 8 – Traffic infraction

Source: 2020’s Annual Report - PRF

Tabela 1 – Accidents involving motorcycles in 2020

State	Injury	Death
AC	199	7
AL	292	39
AM	53	7
AP	107	2
BA	1323	156
CE	1025	96
DF	473	9
ES	1474	50
GO	1121	65
MA	543	122
MG	2877	130
MS	605	32
MT	818	74
PA	537	60
PB	859	57
PE	1174	145
PI	633	83
PR	2749	132
RJ	1735	64
RN	868	50
RO	1008	38
RR	123	10
RS	1505	47
SC	3546	88
SE	329	17
SP	1771	46
TO	201	30

Source: 2020's Annual Report - PRF

number of violations. The fact is that even considering the first two aspects, the number of violations is not decreasing

Therefore, if we want to strive a state of "zero traffic fatalities", we have a long way to go with public policies strengthening the role and responsibility of individuals for their own safety and those around.

In this sense, this work aims both to look at product development techniques and apply them to the design of a tricycle, which is more stable than a motorcycle e more flexible than a car, and to implement mechanisms that increase the safety of the rider on urban roads.

1.2 An overview of product design

Much has been said about Industry 4.0, the Internet of Things (IoT), artificial intelligence, and machine learning, and how these technologies have brought about disruptive change in various areas of knowledge. Here we will address how these technologies are impacting the design environment in a very broad way, and we will outline some ways to adapt familiar design metrics to the current context. This work draws on both theoretical knowledge and practical experience of the author from years of project development in a variety of domains.

In general, project development is an activity that becomes more complex every day. Take automobiles as an example, which at the beginning of the 20th century were complex machines made of a small combination of mostly metallic materials and moved by a kinematic chain that transferred the mechanical energy from the thermo-chemical source of combustion of the engine (gasoline or diesel) to the steering system, which in turn was completely controlled by the driver (Figure 9). Nowadays they are highly complex systems, equipped with mechanical, electrical, thermo-chemical, magnetic and/or rheological subsystems. They have a control center that regulates fuel quantity, speed limit, driving speed, tire pressure, brakes, and vehicle stability, not to mention the more modern versions from some manufacturers that have an autopilot function (Figure 10). Certainly, designing a car today is a much more complex task than it was in the early 19th century. In contrast, we have a much larger number of tools that not only allow us to evolve significantly with product design, but also to integrate a much larger number of participants into the same project, so that rather than depending on a few people who have reasonable knowledge in many areas, we can count on many people who have specific knowledge in a few areas. This integration exploited the complexity of the system design and created a barrier in terms of evaluating the project as a whole.

Boothroyd, Dewhurst e Knight (2010) have defined Design for Manufacturing and Assembly (DFMA) as a qualitative method for evaluating various aspects of a mechanical design, creating a design paradigm that focuses on manufacturing processes. The criteria of Ullman (1992) are also in this direction, helping us to find a quantitative parameter for project evaluation. The assumption here is that the designer must be an expert in manufacturing processes, since the metrics are based on manufacturing.

It does not mean that studies of Ullman (1992) are not applicable today. On the contrary, the bases are still present, but some extent complementary measures are required.



Figura 9 – Studebaker electric car, c. 1905.

1.2.1 Design for customization

As a rule, the smaller the scale of production, the greater the possibility of customization, since the processes are carried out by professionals in their field. On the other hand, we have components that are manufactured in automated processes and with low flexibility, which means a low level of customization (HUNT; SPROAT; KITZMILLER, 2004).

One of the proposals on Industry 4.0 (along with IoT in household elements) is to enable the best of both worlds. High productivity in automated lines with a high level of customization (ZAWADZKI; ŻYWICKI, 2016). This feature must therefore be taken into account at the conceptual stages of the project in order to make this possibility a reality (Figure 11).



Figura 10 – Toyota Concept i, presented at Geneva Motor Show as a concept car for 2030.

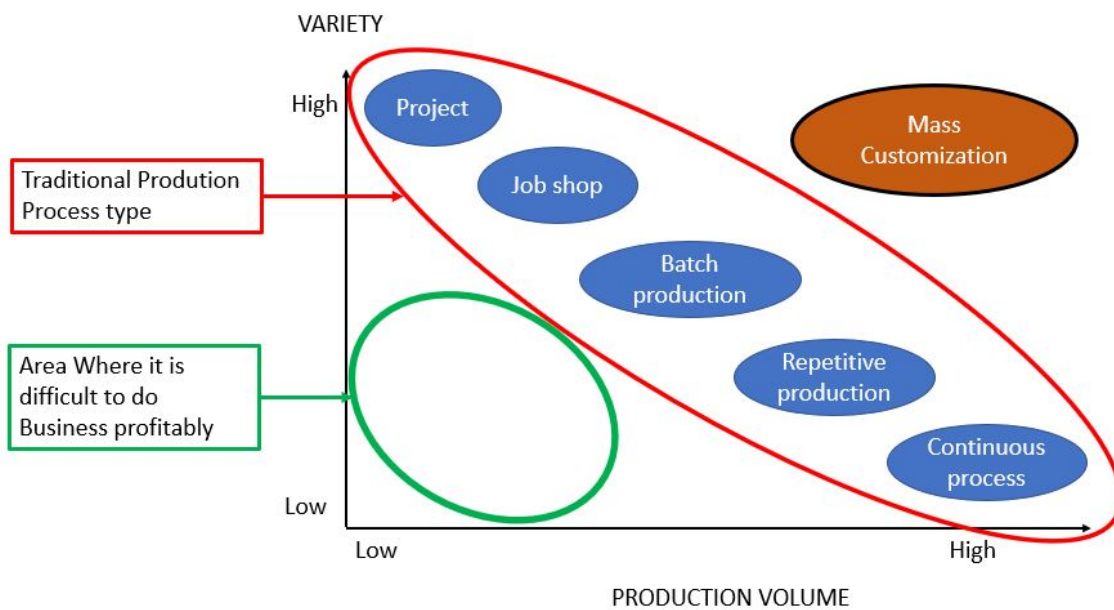


Figura 11 – Relationship between customization, production volume and manufacturing profitable field

Source: Author, adapted from <https://www.logistiikanmaailma.fi/en/production/process-improvement/mass-customization/>

1.2.2 Design for Excellence

Design for Excellence (*DFX*) aims to adapt the tool or method to the project and project functions defined in the initial phases ([EASTMAN, 2012](#)). It covers a wide range of design approaches and studies (Figure 12):

- Design for Manufacturing and assembling (DFMA)
- Design for Safety (DFS)
- Design for Compliance (DFC)
- Design for Maintainability (DFMa)
- Design for Disassembling (DFD)
- Design for Ergonomics Aspects (DFEA)
- Design for Integration (DFI)
- Design for Ecology (DFEc)
- Design for Energy (DFE)
- Design for Wellness (DFW)
- Design for Change (DFCh)
- Design for Discovery (DFDs)
- Design for Topology optimization (DFTOp)
- Design for Addictive Manufacturing (DFAM)
- Design for Recycling (DFR)

The above paradigms can complement each other and must not be mutually exclusive.

Among the various design paradigms mentioned above, three of them have become increasingly important in recent years, and attention will be given to them here.

The first is Design for Integration - DFI ([ANDERL et al., 2018](#)), whose integration can be interpreted in two different ways.

First, we will understand integration as the possibility of connecting a system with other systems or subsystems. Using as an example a vehicle, the project should enable the desired integration (and avoid unwanted integration) between its parts. The car controller

AIA Framework for Design Excellence



Figura 12 – Some of the fields that could be considered on DFX

Source: <https://network.aia.org/blogs/kira-l-gould/2019/09/17/defining-design-excellence>

(control module) needs to be integrated with the electronic steering system, the electronic transmission, the fuel injection system, the ABS brake system, the suspension control system, among others. However it cannot allow the integration with external devices (unwanted integration), such as computers and cell phones, to prevent vehicles from being hacked. Favoring the desired integration and preventing unwanted integration needs to be a design metric, for which it must be considered a validation metric. The creation of a simple check-list can be the difference between developing a vulnerable system or designing a robust system (Figure 13).

Another way of looking at DFI is to think about integration during the development of the project. In this case, we are not dealing with the integration of sub-systems, but with tools and their sub-products.

For a vehicle, once the design is being created, the product must go through the due structural simulations, multi-physics, crash tests among others. The vehicle design is likely to be developed using CAD software, connected to a PLM (Product Life-cycle Management) system, and equipped with CAM and/or CAE tools. In this way, the project's development history is not lost, and the lessons learned are used in future projects (RAMÓN-RAYGOZA; GUERRA-ZUBIAGA; TOMOVIC, 2008).

However, process planning and control steps, factory, and process simulation can eventually be left behind. Simulations of entire factories, made up of robotic and/or fully automated systems, offer a great advantage in terms of installation time and new equipment insertion, predictability regarding the possibility of changes (DFCH - Design For Change) of products

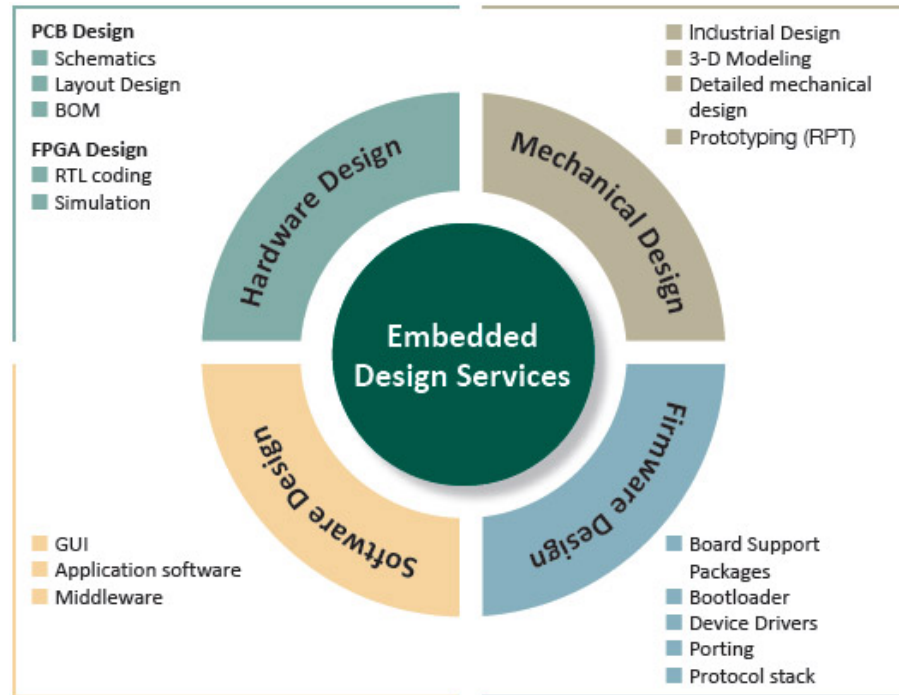


Figura 13 – Electronic Design - Embedded Systems

Source: <https://www.mindteck.com/electronic-design-services-embedded-systems-and-applications>

that are already in production, as well as enable the optimization of logistical flow and/or production time. The project also needs to take this into account from its earliest stages, creating for every subsystem its digital twin. This is the electronic version of a system, which faithfully represents its physical version, considering logic inputs and outputs, analog signals, physical sensors, subroutines in micro-controllers, among others. The project designed for integration must provide information for the development and validation of the system as a whole before any manufacturing process is started. (WINDHEIM, 2020) (Figure 14).

A second aspect to consider is the design for optimization (DFTOp).

Optimizing a project or process is different from improving it (JONGEN; JONKER; TWILT, 2013). Improvement means that any response could be accepted, if the provided result is to some extent better than the input. The optimization process, in turn, aims to achieve the best result of all possible answers.

In general, we can divide the optimization process into two main categories, discrete or parametric optimization, where the optimum condition is sought in some specific

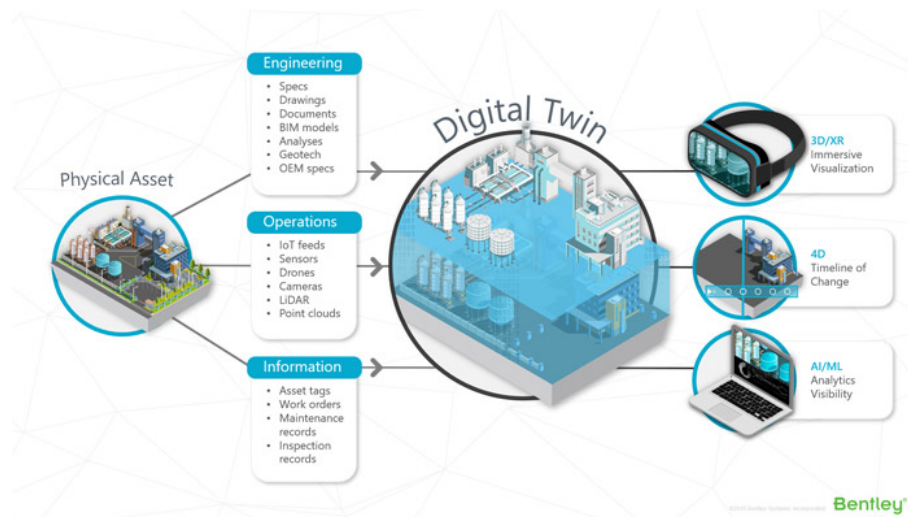
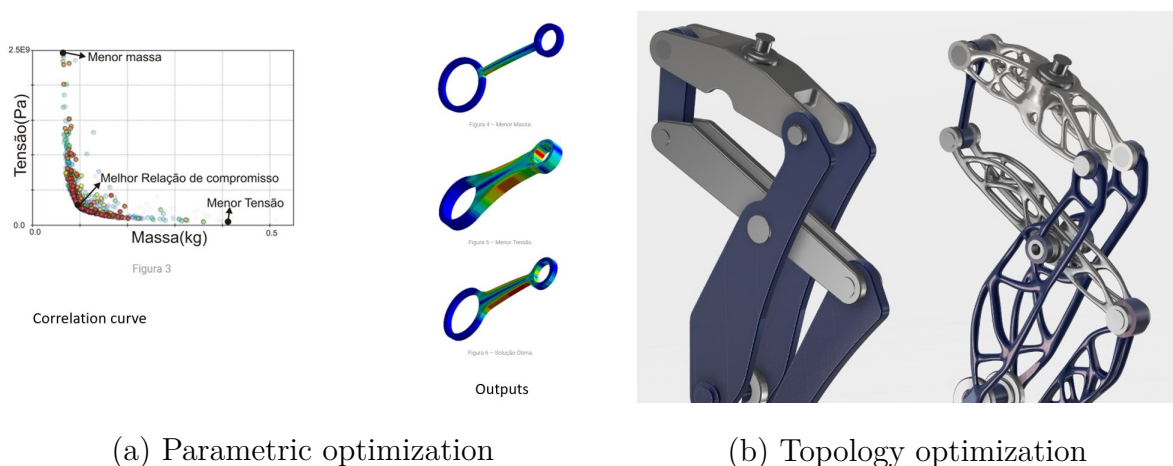


Figura 14 – Digital Twins workflow

Source: <https://www.arcweb.com/blog/digital-twins-advancing-infrastructure>

parameters, as shown in Figure 15(a) (PORTER; VERSEPUT; CUNNINGHAM, 1997), or topological, Figure 15(b) (XIA et al., 2018), where the optimum is sought for the component as a whole (SOHN, 2009). In both methods, the search for the optimal solution can be performed by gradient-based algorithms or genetic algorithms, both of which have their advantages and disadvantages.



(a) Parametric optimization

(b) Topology optimization

Figura 15 – Example of parametric and Topology Optimization

Source (a): [https://www.esss.co/blog/otimizacao de projetos de engenharia](https://www.esss.co/blog/otimizacao-de-projetos-de-engenharia)

Source (b): [https://grabcad.com/groups/generative design topology optimization](https://grabcad.com/groups/generative-design-topology-optimization)

Complementary to the design concept for topological optimization, we can consider the design concept for additive manufacturing shown in Figure 16(BRACKETT;

ASHCROFT; HAGUE, 2011). While we were thinking about components designed from primitive geometries (square, rectangle, cylinder, etc.) and a group of boolean operation used to combine them, in order to obtain a shape that satisfies the design criteria, the additive manufacturing process did not prove to be an equal competitor when compared to the means of production. The number of materials that can be used is still very limited, and the parts idealized by topological optimization or generative design (Figure 17) may not be possible to produce by conventional means. Additive manufacturing also eliminates the high investment in tooling or fixtures for each product change, which brings it in line with DFCh (Design For Change) as the impact of design changes can be easily absorbed by the manufacturing process.

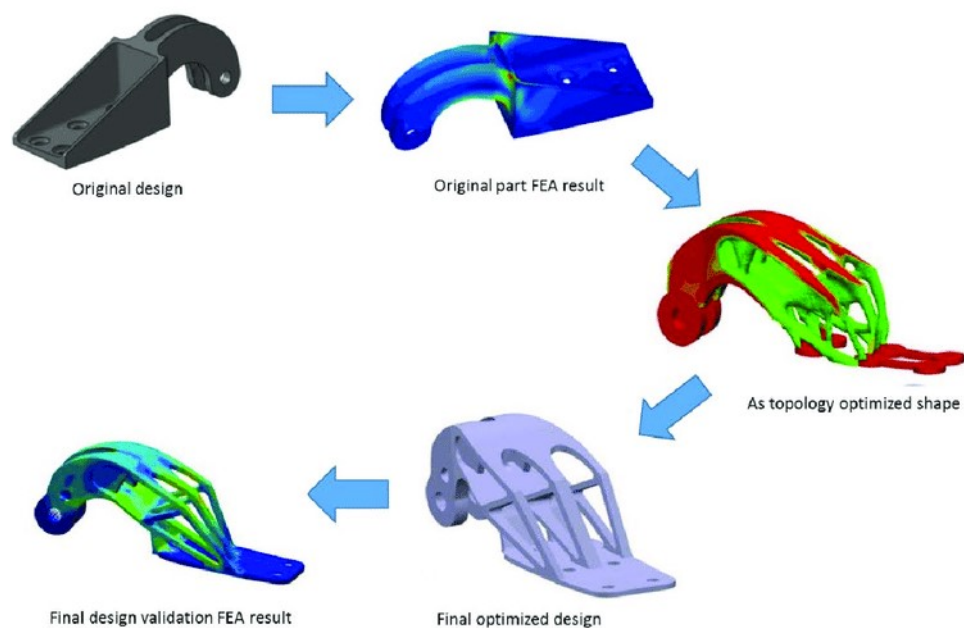


Figura 16 – Topology optimization applied in a component which will be build by addictive manufacturing process

Source: Gebisa e Lemu (2017)

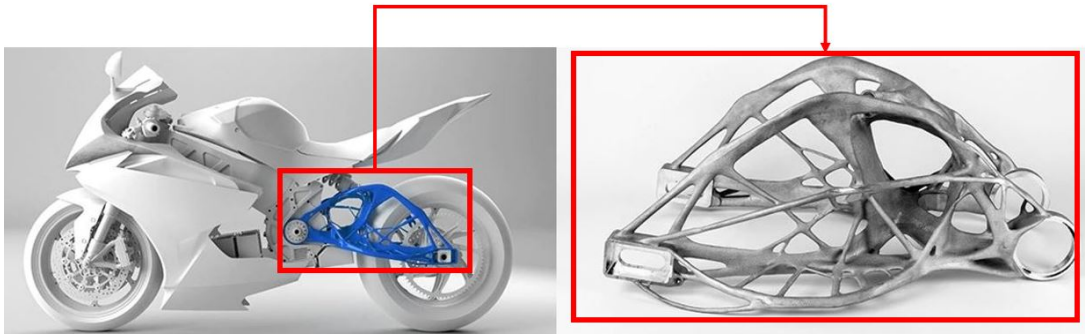


Figura 17 – Example of Generative Design concept

Source: Adapted from <https://www.autodesk.com/campaigns/generative-design/lightning-motorcycles>

2 OBJECTIVES

The objective of this work is to design an electric tricycle for the transportation of goods or people. The result should be a versatile and easy-to-use tricycle for intercity transportation. During the design process, best practices related to new product development and safety aspects will be considered.

3 METHODOLOGIES FOR PRODUCT DEVELOPMENT

3.1 Engineering design

Product development implies the application of a very broad concept in terms of design techniques (BACK et al., 2008). Integrated product development assumes that the process of information acquisition and transformation must be carried out by a multidisciplinary team. The idea of integrated product development can also be seen under the terminology of concurrent engineering.

Magrab Eduard B. (2008) expanded on the concept presented by Back et al. (2008) by emphasizing the idea that manufacturing processes cannot be separated from product development.

In this context, Magrab Eduard B. (2008) proposed IP^2D^2 , which stands for **I**ntegrated **P**roduct and **P**rocess **D**esign and **D**evelopment.

This concept is based on the following pillars:

- IP^2D^2 teams need to interact with customers to understand their needs and preferences and get their feedback on existing products;
- Quality is very important to customers. Therefore, IP^2D^2 teams must ensure that the quality of a product meets customer expectations;
- IP^2D^2 teams must continuously monitor competitors' products through benchmarking;
- IP^2D^2 teams must work with senior management to understand how the current product fits into the company's overall strategy;
- IP^2D^2 teams need to work with suppliers to understand their cost structure and seek advice on manufacturability;

Considering the concepts proposed by Magrab Eduard B. (2008), we can understand the following. Engineering Design as a systematic, creative, and iterative process that applies engineering principles to design and develop components, systems, and processes that meet a specific need. This process is both dynamic and evolutionary and involves four distinct aspects (MAGRAB EDUARD B., 2008):

- Problem definition: the transition from a fuzzy set of facts and myths to a coherent problem statement. This is the phase in which the idea for the product is developed.
- Creative process: a highly subjective means of developing a physical embodiment of the solution that is highly dependent on the specific knowledge of the people involved in the process. In this phase, various concepts are developed to transform the idea into a product.
- Analytical process: this is where it is determined if the proposed solutions are correct and means to evaluate them is provided. In this phase, prototypes are built and evaluated.
- Final inspection: here it is confirmed that the design meets the original requirements. Once the most appropriate solution is selected, the preliminary design of the new products begins. This is a very dynamic process where the parameters of the project must be defined, as well as the impact on the system if one of these parameters is changed.

Once the most viable solution is selected, the preliminary design of the new products begins. This is a very dynamic process where the parameters of the project must be defined, as well as the impact on the system if any of these parameters are changed..

3.1.1 1-D Modeling and Simulation

Implementing the modeling and simulation of a complex and dynamic system requires some skills:([BACK et al., 2008](#)).

- knowledge of systems engineering
- knowledge about the physics in which the problem is involved
- Knowledge about the mathematical models used.
- Ability to interpret the results correctly
- Ability to code the mathematical equation and apply it correctly to the model
- Knowledge to understand the interaction between the model and the numerical algorithms used to solve it.

Once the design team members are qualified, a simulation technique must be selected. 1D simulation is one of the most commonly used procedures in the preliminary

design phase, leading to:

- definition of the synthesis of the mechanism.
- Analysis of the mechanism
- Mechanical analysis
- Fluid analysis (hydraulic or pneumatic system)
- Electromechanical analysis
- Thermal analysis
- Simulation of control systems

Once the project is complete, it moves to the conceptual design phase, where the simulation uses a multi-dimensional environment. The system moves from a schematic drawing to a 3D representation.

In Figure 18, you can see that the cost of change increases throughout the product lifecycle. Changes to the product concept in the first phase are easier to make than in the production phase. Large changes with small impacts at the beginning of the project are possible.

This means that development work must be done in the early phases, where there are more options with less impact.

3.1.2 Problem Definition

The first step of product design is to identify the main idea of the product. This path may allow for some shortcuts or be longer, depending on the structure and strategy of the company. The iterative activities for product realization and their relationship to the four phases of product development proposed by Magrab Eduard B. (2008) can be seen in the figure 19.

At this stage, we can get the following elements as output:

- Clearly understand the customer need
- Determine the market potential (according to the company strategy).

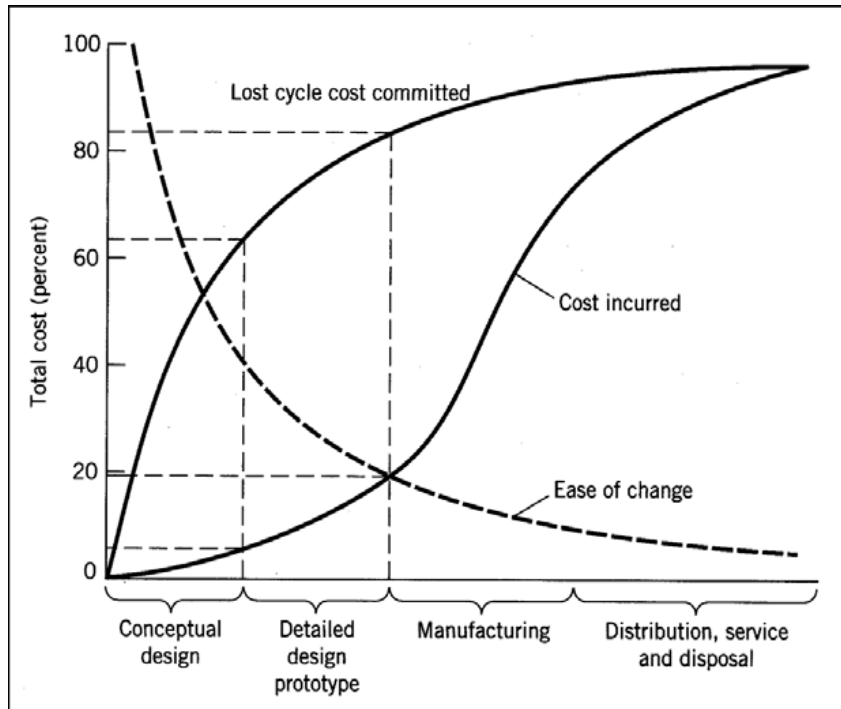


Figura 18 – Cost of a product change

Source: <https://www.immateriell.se/house-of-quality-qfd-quality-function-deployment>

- A business model that shows the company can make a profit from selling the product (according to the corporate strategy)
- Identify and evaluate the risks associated with implementing the project (a SWOT analysis may be of interest for this)
- A determination of whether a sustainable competitive advantage can be achieved
- An estimate of the resources that will be required to develop the product

3.1.3 Product Design Specification

Obtaining the product specification as input to the design is usually not an easy task, first because it involves converting some qualitative criteria into some quantitative criteria.

Considering the tools available for this, we take two that focus on the customer, the **QFD** and the **Design Thinking**. The first strategy aims to get the product specifications and the second helps to keep the customer needs in focus.

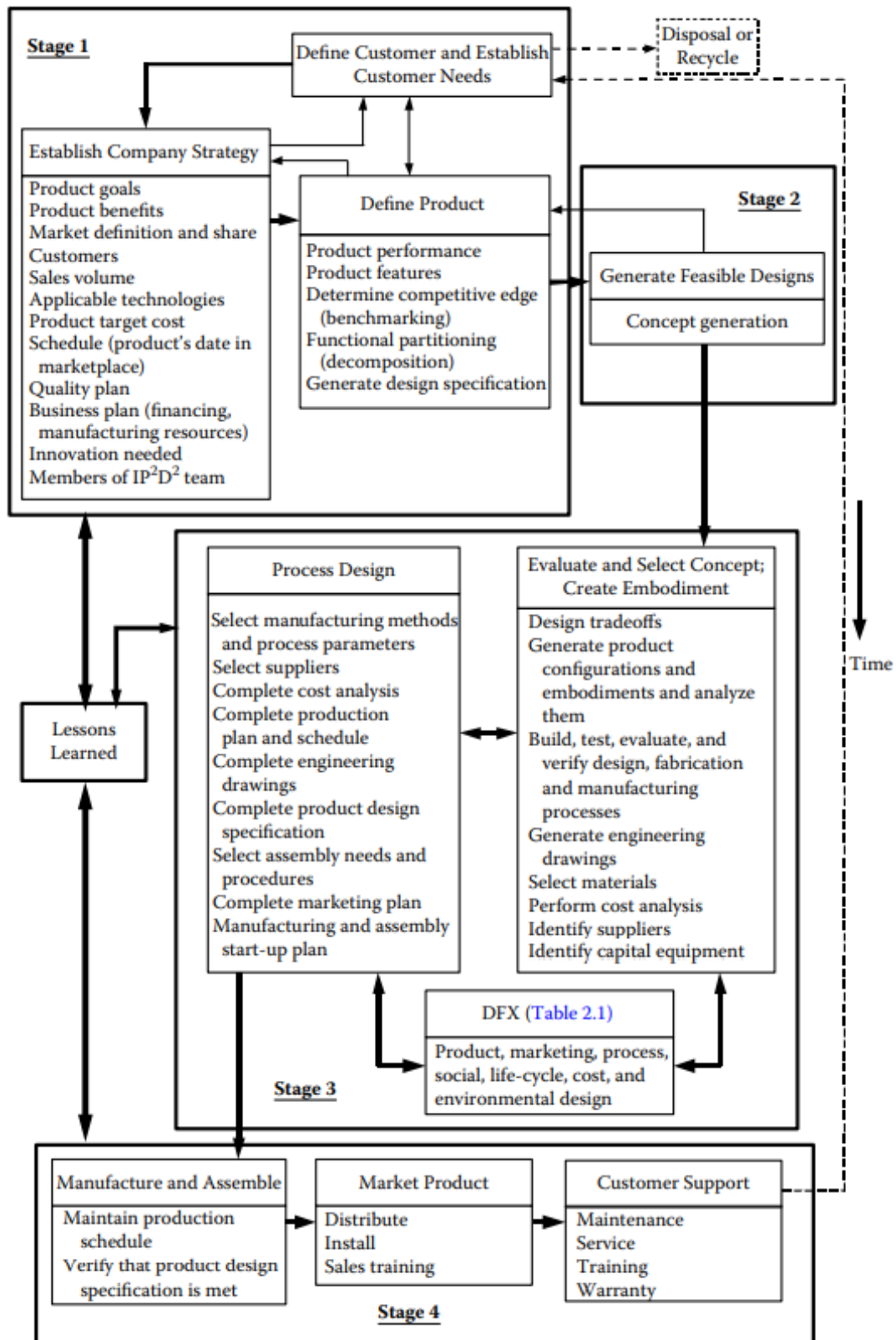


Figura 19 – Stages of IP²D²

Source: Magrab Eduard B. (2008)

3.1.4 Quality Function Deployment

Quality Function Deployment (**QFD**) is a method developed by [Akao \(1994\)](#) that helps transform the voice of the customer into technical characteristics for a product.

[Akao \(1994\)](#) described the QFD matrix as a "method for converting qualitative user requirements into quantitative parameters, deploying the functions that form quality, and using methods to achieve design quality in subsystems and components, and ultimately in specific elements of the manufacturing process."

The House of Quality, a part of QFD, is the basic design tool for developing quality functions ([HAUSER JOHN R.; CLAUSING, 2016](#)). It identifies and classifies the following aspects:

- the customer wishes (What's)
- the importance of these wishes
- the technical features that may be relevant to these desires (How's)
- correlates the two, allows to check these correlations
- assigns goals and priorities for the system requirements

The House of Quality output is typically a matrix with customer requirements on one dimension and correlated non-functional requirements on the other dimension. The cells of the matrix table are filled with the weights assigned to the stakeholder characteristics when those characteristics are affected by the system parameters at the top of the matrix.

At the bottom of the matrix, the column is summed, allowing weighting of system characteristics by stakeholder characteristics. System parameters that are not correlated with stakeholder characteristics may be unnecessary to the system design and are indicated by blank matrix columns, while stakeholder characteristics (indicated by blank rows) that are not correlated with system parameters indicate "characteristics that are not addressed by the design parameters".

System parameters and stakeholder characteristics with weak correlations indicate missing information, while matrices with "too many correlations" indicate that stakeholder needs should be refined. The "House of Quality" can be seen in the figure [20](#)

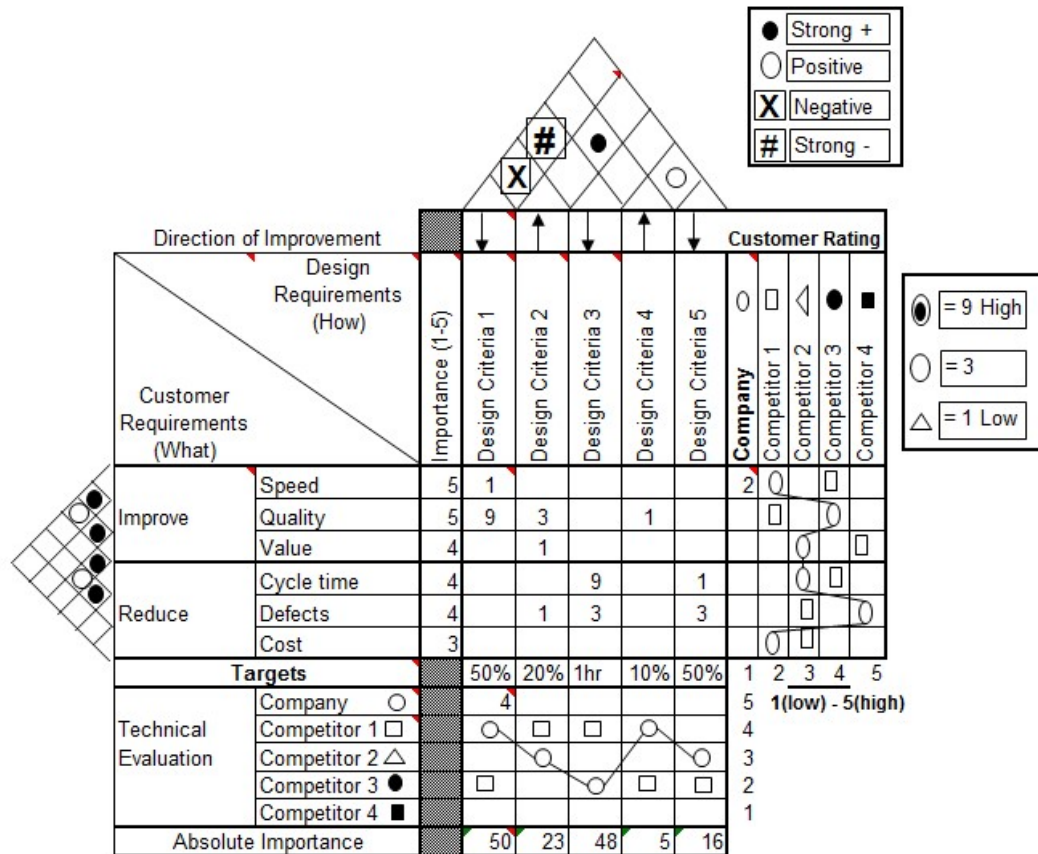


Figure 20 – Example of QFD Matrix

Source: <https://www.immateriell.se/house-of-quality-qfd-quality-function-deployment>

3.2 Design Thinking

According to Przybilla1 Leonard. (2016), design thinking focuses on developing human-centered innovation. An innovation that addresses the needs and desires of the user while ensuring technical feasibility and commercial viability.

A Design Thinking project is divided into work on the problem space and the solution space (Figure 21). Both are first expanded before being merged, resulting in a double-diamond shape. Assigning the same size to the problem space and the solution space means that a lot of time is spent on fostering understanding of the actual problem to be solved.(PRZYBILLA1 LEONARD., 2016)

The formulation of a challenge initiates the divergent part of the problem space through needs identification, which is transferred to the solution space through synthesis. The solution space is opened and converges to a final solution through prototyping and testing activities. A variety of different methods can be used in these phases. For example, interviews or ethnographic observations can be used in the needs assessment, while the

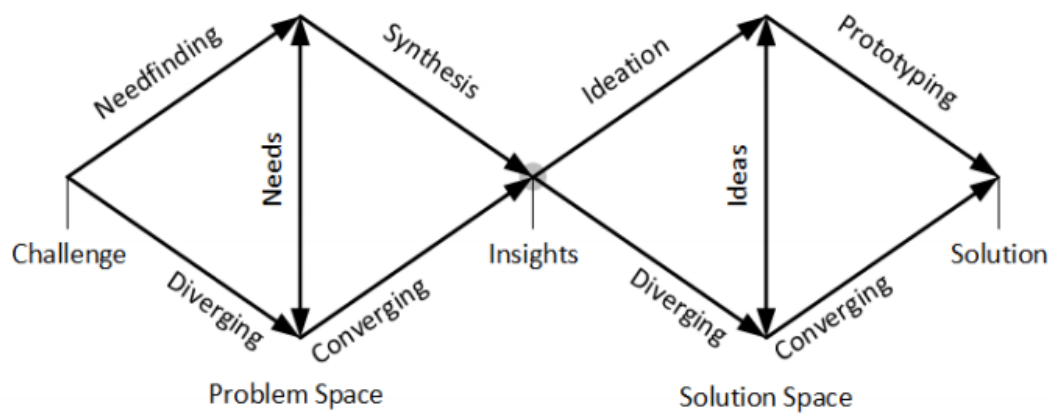


Figura 21 – Design Thinking represented by a double diamond graph

Source: (PRZYBILLA1 LEONARD., 2016)

development of initial rough prototypes and their iterative refinement to a detailed prototype characterize the solution space.

Design thinking methods can be divided into seven phases (SANDINO; MATEY; VÉLEZ, 2013):

- Define
- Explore
- Ideate
- Prototype
- Select
- Implement
- Check

3.3 C-K Design Theory

Concept-knowledge theory (C-K) is both a theory of design and a theory of reasoning in design. It defines reasoning in design as a logic of extension processes. According to Braha D. Maimon (1998):

- Provides a comprehensive formalization of design that is independent of a design domain or object

- Explains invention, creation, and discovery in the same framework and as design processes.

C-K theory was a response to three perceived limitations of existing design theories (HATCHUEL A. WEIL, 2003):

- Design theory is unable to address the innovative aspects of design
- Classical design theories dependent on object domains, machine design, architecture, or industrial design favored design theories tailored to their specific knowledge bases and contexts. Without a unified design theory, these fields have difficulty collaborating in real design situations.
- Design theories and creativity theories were developed as separate areas of research. However, design theory was intended to incorporate the creative, surprising, and accidental aspects of design, while creativity theories were unable to address the intentional invention processes common in the design field (HATCHUEL A., 2003).

C-K theory uses an approach that is domain-independent and that allows acting on unknown objects and changing the definitions of known objects during the process (revising the identities of the objects) (HATCHUEL A., 2003).

The C-K roadmap can be seen in figure 22. The initial concept is created based on the existing knowledge. Additional concepts are created based on the initial concept, resulting in an expansion of the concept space. This new concept may reach the limits of the team's knowledge base, so the knowledge space must be expanded to make some of the new concepts feasible.

As new concepts are created, unexpected ideas may emerge that result in a "crazy concept" for which the knowledge base is not yet defined. These crazy concepts eventually become the starting point for disruptive solutions. This is similar to the concept of mutation used in some optimization algorithms. The interaction between concept and knowledge space can also be seen in Figure 23 and Figure 24.

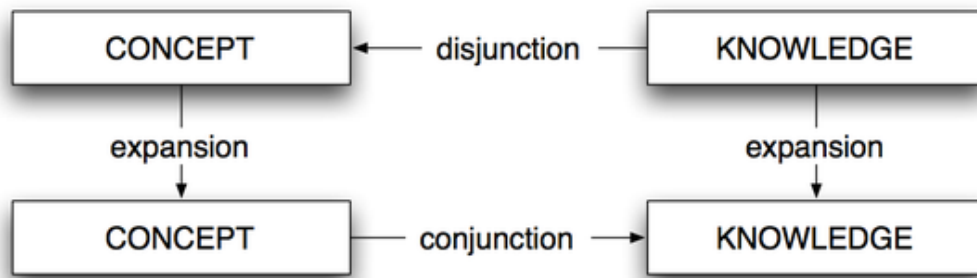


Figura 22 – C-K Road Map

Source: <https://www.immateriell.se/house-of-quality-qfd-quality-function-deployment>

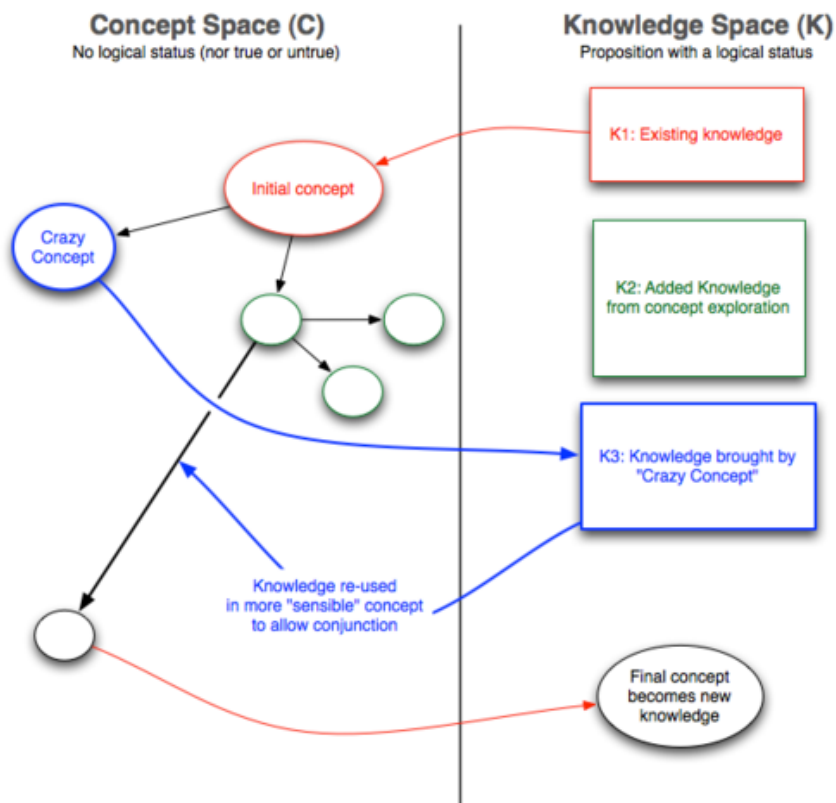


Figura 23 – C-K Theory - Crazy Concept

Source: <https://creativante.com/new/index.php/2013-02-03-19-36-05/2021/499-theories-design-and-implementation-of-strategies-teorias-design-e-implementacao-de-estrategias-parte-3>

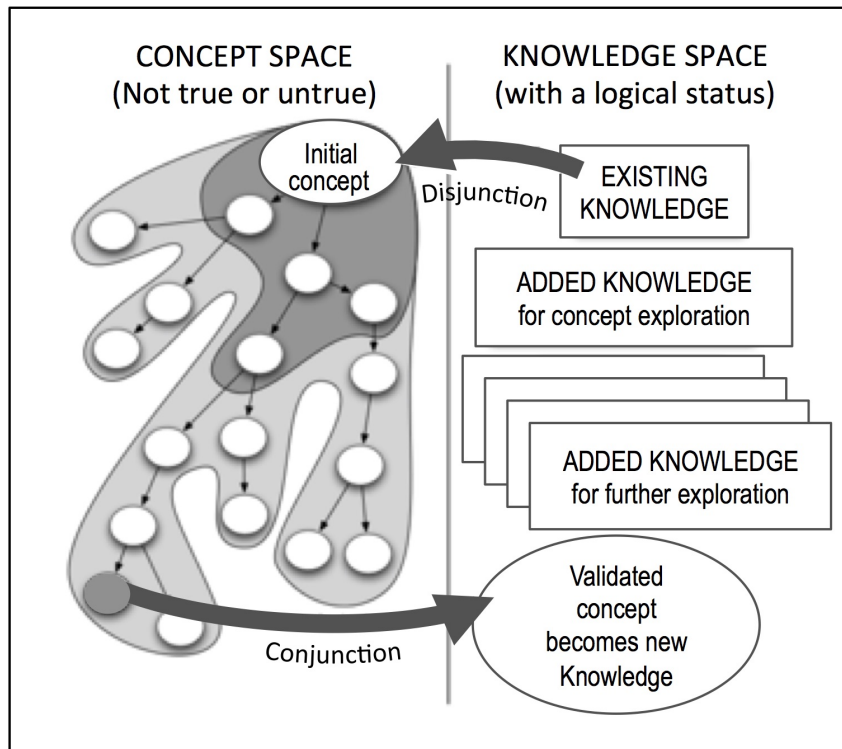


Figura 24 – Concept and Knowledge spaces - C-K Theory

Source: <https://open-organization.com/fr/2016/11/29/knowledge-and-innovation-a-tight-interdependency/>

3.4 Morphological Matrix Method

As a starting point, this method proposes the identification of the functions or operations of the process. This information is expressed in the form of a matrix.

The first column of the matrix is filled with the identified functions, and the other columns are filled with the solution principles for each operation. Once the matrix is completed, the goal is to find the best combination that meets all the requirements of the new product. (RESIN et al., 1989).

The process to get solutions for each function is supported by creative methods like brainstorming or researching some patents or publications.

To combine only feasible answers, this method aims to apply the morphological matrix created in the following steps:

1. Create a list of product demand (functions or operations);
2. Identify / research the solution principle for each function;
3. Research, investigate, and create a graphical representation of the possible combinations for the possible solutions.

Figure 25 shows an example of this matrix. The pictures of the possible solutions are not necessary, but their use makes the understanding clear.

The possible combinations are expressed by the color paths shown in the figure.

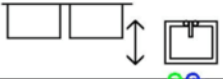
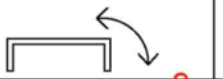
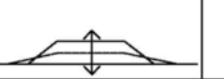


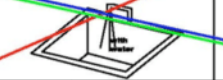
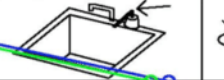
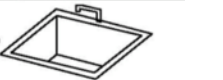

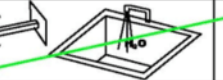
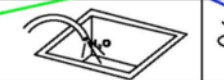
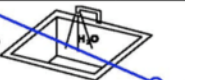


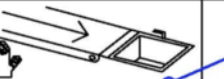
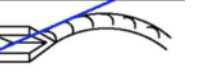
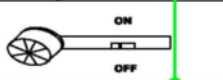





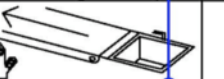

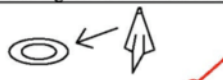
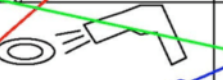

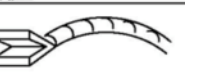
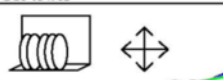

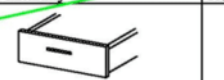

Activity	Working method			
Adjust for height sink				
	Moving sink	Kitchen step	Adjusting floor	Height adjusting shoes
Put detergent in sink				
	Pick up bottle and turn it	Pump directly into sink	Sort of faucet that includes detergent	Button press and detergent gets into sink
Put water in sink				
	Round faucet, directly in sink	Pump - handle directly in sink	Put water in sink using hose	Button to press and water gets into sink
Pick up piece and put in water				
	Rubber gloves with texture	Tongs	Moving belt and rubber gloves	Robot arm
Sweep piece with sponge				
	Electric brush (hand held)	Static brush	Electric brush (part of sink)	Robot arm
Put piece in drying frame				
	Rubber gloves with texture	Tongs	Moving belt and rubber gloves	Robot arm
Dry piece of dish				
	Use towel	Use electric dryer	Dry naturally	Robot arm
Put piece away				
	Adjustable cupboard	Long tongs	Automatic drawer	Robot arm

Figura 25 – Morphological Matrix

Source: <https://www.immateriell.se/house-of-quality-qfd-quality-function-deployment>

3.5 Ranking and selection of the better solution

The steps that should be followed to obtain the best and innovative concept are (ION; LOW, 1998):

1. Decision matrix/grid.
2. Selection matrix/grid
3. Problem matrix
4. Opportunity analysis
5. Criteria evaluation form
6. Criteria-based matrix

The weighting of the criteria is determined as an agreement between the design team members. An example of the Pugh matrix is shown in Figure 26.

Criteria	Optional Importance Weighting	Current Solution	Alternative #1	Alternative #2
Effectiveness	5	0	1	1
Availability of Resources	3	0	0	1
Support from Business	2	0	0	1
Long Term Benefit	2	0	1	0
Time to Implement	4	0	-1	0
Ease to Implement	1	0	0	0
Cost of Implement	5	0	-1	-1
	Totals	0	-2	5

Figura 26 – Sample of Pugh Matrix

Source: <https://www.modernanalyst.com/Careers/InterviewQuestions/tabid/128/ID/2159/What-is-a-Pugh-Matrix.aspx>

With a score for each criterion, the alternatives are ranked as follows:(ULLMAN, 1992)

1. Not feasible (should not be considered as a solution).
2. Possibly feasible (could be considered as a solution under certain conditions)
3. Feasible (should be considered as a possible solution).

After the first step, the Pugh matrix can be reused, but the general criteria must be modified for some specific criteria. It acts like a filter that reduces the number of possibilities.

It is important to note that an alternative with a higher score is not necessarily the best alternative. It is necessary to include some qualitative aspects in the analysis and take them into account when choosing the solution.(MICHELOTTI et al., 2016)

3.6 TRIZ

TRIZ methodology is an inventive problem solving process. It was proposed by Altshuller (1984). Its tools are intended to replace the unsystematic trial-and-error method of finding solutions to problems.

The TRIZ method does not itself provide solutions, but instead suggests various solution

principles to solve the problem.

Domb (1998) pointed out that TRIZ researchers have encapsulated the principles of good inventive practice and put them into a general problem-solving structure. This general problem-solving structure can be seen in Figure 27.

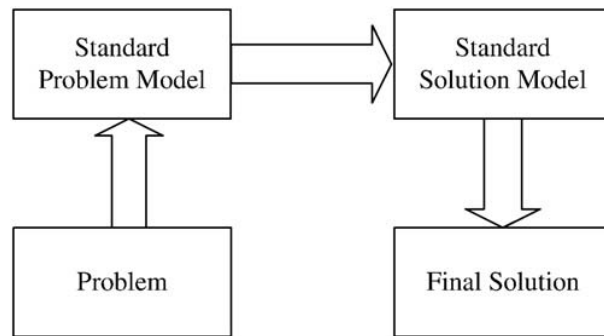


Figure 27 – The general model for TRIZ problem-solving

Source: Lin e Su (2007)

Mann (2009) has depicted the TRIZ methodology with a triangular pyramid in a hierarchical perspective (Figure 28), suggesting that TRIZ at the top of the pyramid can be seen as a systematic study of excellence. Then some other concepts are presented, such as the elimination of inconsistencies and the preservation of functionality. At the bottom of the TRIZ hierarchy, there are a number of tools and techniques for problem solving.

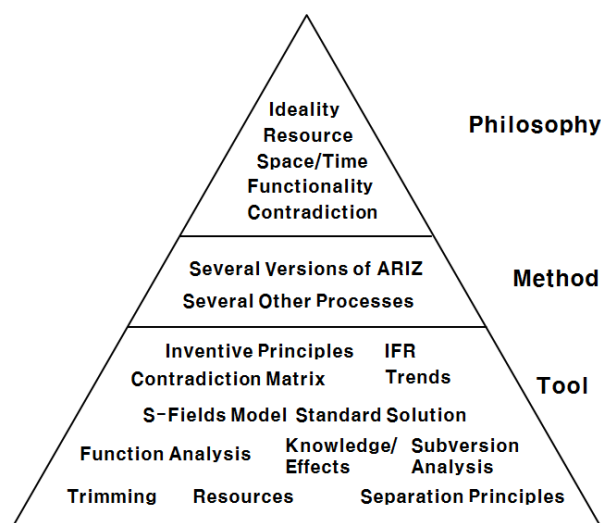


Figure 28 – The hierarchical view of TRIZ

Source: Mann (2009)

3.7 CORA

Although the Component-Oriented Requirements Analysis (CORA) method is most commonly used in software development (RANKY et al., 2012), it can also be applied in general development (RANKY; CHAMYVELUMANI, 2003). It is a systematic, customizable method for analyzing product and process requirements. It is a matrix-based method, similar to QFD practices, developed for user requirements analysis and integrated in four modules, namely (PROCHAZKA et al., 2008):

- User Requirements;
- Technical Solutions;
- Parameter Calculations;
- benchmark

The basic units of CORA are the unified checklist, requirements information management, specification drivers, functional and non-functional analysis, and criteria analysis (Figure 29).

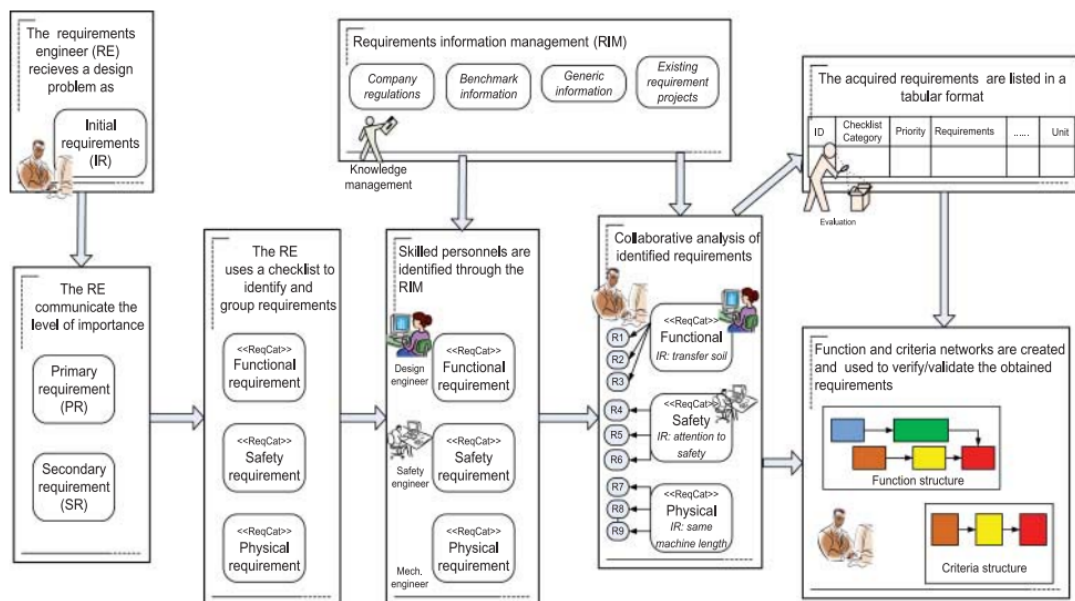


Figura 29 – A CORA road-map

Source: Brace e Cheutet (2012)

3.8 Strategy Frameworks

Different methods may be used for the same project. The arrangement of tools for a particular project is called a framework.

Cross (2021) points out the importance of having a well-defined design framework where it is clear which tool is used at each stage. An example of a framework can be seen in the table30.

	<i>Stage in the desing process</i>	<i>Appropriate method</i>
1	Identify opportunities	User scenarios
2	Clarifying objectives	Objectives tree
3	Establishing functions	Function analysis
4	Setting requirements	Performance specification
5	Determine characteristics	Quality function deployment
6	Generating alternatives	Morphological chart
7	Evaluating alternatives	Weighted objectives
8	Improving details	Value engineering

Figura 30 – Framework Strategy

Source: [Brace e Cheutet \(2012\)](#)

Both phases and methods vary from one project to another.

4 TRICYCLE DESIGN BASED ON DFSS

Design for Six Sigma (DFSS) is a methodology that applies the principles of Six Sigma to design and develop new products and processes that meet or exceed customer requirements while minimizing defects and variability. The goal of DFSS is to get the design "right the first time," reducing the need for rework and improving overall efficiency.

There are several key elements to DFSS, including the use of a structured approach and the use of data-driven decision making. The structured approach includes a series of phases, including Define, Measure, Analyze, Design, and Verify (DMAIC). In each phase, the techniques presented in Chapter Three can be applied.

Frizziero, Liverani e Nannini (2019) shows how DFSS can be applied to the development of a motorcycle. The same approach is used for the tricycle project.

4.0.1 Define stage

According to PRODIP methodology, propose by Back et al. (2008), this is the first stage of a project.

Planning a project requires identifying the activities to be developed, its sequence or simultaneity, define time and resources required, responsibility for the tasks. The time-frame must be clear, considering the beginning, the development and the conclusion of the project.

In this stage (planning), a project chart was created (Figure 31).

The application of a methodology or tool is important to get the definitions clear, mainly in complex projects. In the development of the Tricycle, the tool applied in the planning phase was 5W2H.(BACK et al., 2008)

The answer of 5W2H questions pointed for the main design is shown in the table 4.0.1.

4.0.1.1 Customer needs

The customer needs was defined based in three main lines. The experience of the author with motorcycles and vehicle design, research in internet forums, like GrabCAD

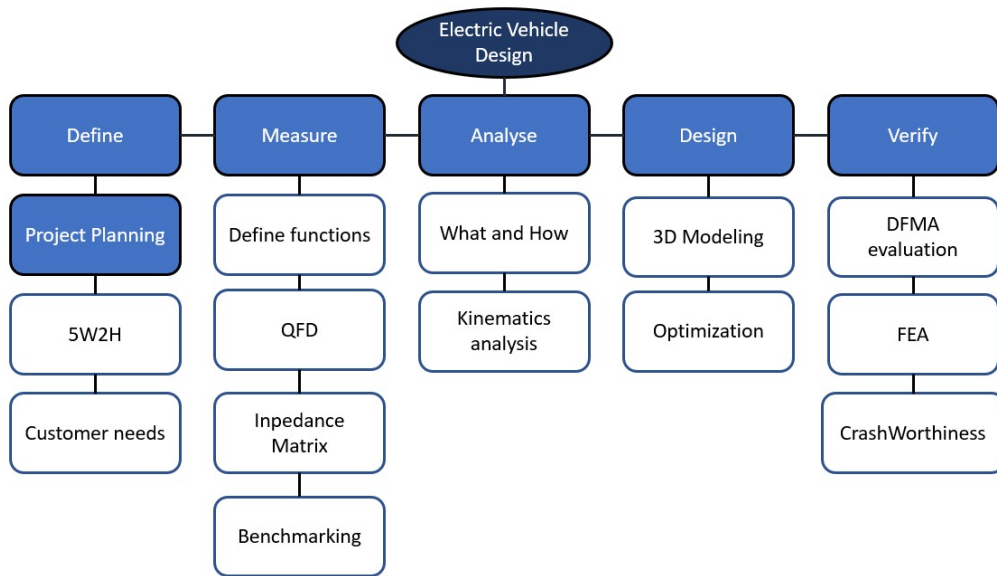


Figura 31 – Project Chart

Source: Author

and a couple of questions done for autonomous workers, who deliver food using platforms like iFood and Uber Eats. The questions were:

- What is more important characteristic for you, in a motorcycle?
- What would make you take a decision of buy or not buy a vehicle?
- Is there any characteristic that could make your day easier?

The question above were made in a informal way, like a brainstorm.

The customer needs obtained by the transcription of the Autor's experience, website research and user answer is:

- High Autonomy - As there's no so much places to recharge the vehicle in the Brazilians cities, autonomy may play a crucial role
- Lightness - It's not only contributes with the Autonomy aspect, as well make the vehicle easier to drive or it would allow the transport of a higher cargo using the same power, when compared with a heaviest vehicle
- Comfort - As the vehicle is designed for professional scenarios, it should be considered the driver will spend the whole day in it.

What	What are the uses of the product? A transport for cargo or people under short and medium routes
Why	Why was the product chosen? It could be chosen due the environment impact, energy consuming, flexibility, stability and safety performance
Who	Who uses the product? Autonomous who works for iFood, Uber, etc Companies focused in delivery good Small producers Technologist enthusiasts
When	When is it used? Along all year, but it will be easier to use it in a favorable weather
Where	Where is the product used? It is mainly used along urban roads
How	How is the product used? The product is driven directly by the end user and mainly used for work, as goods and people transportation. It also can be used inside companies for logistical needs.
How Much	Target undefined, but should be as cheap as possible

Tabela 2 – 5W2H applied to Main Project

- Low price - It should be accessible to every one who works with logistics
- Easy to recharge - As there are no many recharges points in most of Brazilian cities, the vehicle should be able to be recharged using residencial sockets (low / medium voltage and low / medium current)
- Safety - None of the riders mentions safety as an important characteristics, even though it was added by the author.

4.0.2 Measure stage

Once the customer's requirements are known, the importance of these parameters and the degree of independence between them must be determined. To achieve this, the QFD matrix was used.

The relative importance matrix (table 3) was used to determine which parameter has greater importance than the others. In particular, one wonders whether the element of the row is more important than that of the column.

According to the QFD methodology as defined by its inventors ((AKAO, 1994)), the following values are used:

1 = The element of the row has the same importance as the element of the column.

0 = The element of the row has less importance than the element of the column.

Tabela 3 – Relative Importance Matrix

Importance Matrix	High Autonomy	Lightness	Comfort	Low price	Easy to recharge	Safety	Total
High Autonomy	1	1	2	1	1	1	7
Lightness	1	1	2	0	0	0	4
Comfort	0	0	1	0	0	0	1
Low price	1	2	2	1	2	1	9
Easy to recharge	1	2	2	1	1	1	8
Safety	1	2	2	1	1	1	8

Tabela 4 – Correlation Matrix

Correlation Matrix	High Autonomy	Lightness	Comfort	Low price	Easy to recharge	Safety	Dependencies (Total)
High Autonomy		9		3			12
Lightness			1	9	3	3	16
Comfort		3		3			6
Low price	9	9	1		9	3	31
Easy to recharge	9			3			12
Safety		9		3			12
Independence (Total)	18	30	2	21	12	6	

2 = The row element has more importance than the column element.

The most important parameters are in bold and are used for the following analyzes.

Summarizing the results of the relative importance analysis related to the matrix of relative importance, it can be seen that the first objectives for the designer to consider: low price, low time for recharging and safety.

Thus, the above characteristics are the starting point for the design.

It is used to identify the possible dependency relationships between the different characteristics to be analyzed (Table 4).

To proceed with the compilation, the following question is proposed:

How does the element in the rows depend on the elements in the columns?

Therefore, we indicate through the values a weak, medium and strong dependence, quantified by the values 1, 3 and 9. If there is no relationship between them, the field remains empty, corresponding to a value of 0.

Also in this table, the sum value is calculated along the rows and columns to determine which parameters are more independent.

In particular, the sum of the rows defines how much a feature depends on the others, while the sum of the columns identifies the most independent parameters.

As in the case of the relative importance matrix, the authors also summarize the results of the second QFD analysis related to the independence matrix (table 4). It is confirmed that the second objectives for the designer are price, lightness and high

autonomy, because they are considered the most independent requirements.

It is important to select the most independent requirements because they are characteristics that are not derived from others, so if there is no focus on them, they would not be present in the project.

In contrast, the dependent requirements were not relevant to be selected; in fact, they became available in the project because they depended on the independent requirements.

In this case, the analysis of the relative importance matrix and the analysis of the independence matrix do not lead to the same results. Thus, these characteristics are not only the starting point, but they should be tracked along the design looping in order to ensure none of them will be lost.

4.0.2.1 Benchmarking

When developing an innovative electric vehicle, it is necessary to know the current market offer in order to analyze and compare the different technical specifications and create a product that can improve the current landscape.

For this purpose, the top-flop analysis tool was used, which allows a quick qualitative comparison between a set of objects based on a fixed number of parameters for evaluation. In this way, it was possible to indicate the best and worst values among the different brands and models for each specification and to determine what is innovative and what is not. In this way, it was possible to identify the parameters that could improve the current selection and bring an innovative product to the market.

The motorcycles presented in the comparison correspond to existing models, although the market in this category is still developing. A brief analysis of the main brands and their products follows.

Since there are not many competitors in this field, the comparison is mainly made considering the motorcycle brands, including all the main groups, such as scooters, naked bikes and sportive bikes.

Once the analysis of the various competitors was completed, the available data was analyzed with the technical specifications of each model. In this way, it was possible to proceed with the compilation of the table for the top-flop analysis (Table 3) [3]. The comparison between the different motorcycles took place based on the following parameters:

Tabela 5 – Top Flop Matrix

Brand Model	Energica Ego	Zero SR ZF	Brammo Empulse	Volt Lacama	Lito Sora	Lightning LS-218	Johammer J1	BMW CE 04
Wheelbase (mm)	1465	1410	1473	1482	1498		1455	2225
Width (mm)	870		807	830			814	855
Seat Height (mm)	810	807	800	830	800	810	650	780
Weight (kg)	258	188	213	250	260	225	178	231
Power (kW)	107	52	40	70	42.5	150	16	31
Torque (Nm)	200	146	83	208	90	168	220	62
Max Speed (km/h)	240	164	161	180	190	350	120	120
Acceleration 0-100 km/h	2.8	3.3	4.8	4.6	4.3	1.8	8	2.6
Autonomy (km)	200	217	200	180	200	175	200	130
Battery (kWh)	11.7	14.4	10.4	11.7	12	12	12.7	
Charging times (min)	210	150	240	180	210	120	210	65
Price (\$)	31040	19286	16225	35046	70092	35046	24933	11795
Number of Top	0	2	0	0	0	3	3	3
Number of Flop	2	1	1	1	2	0	3	3
Delta	-2	1	-1	-1	-2	3	0	0

- Wheelbase, width, seat height and weight, related to the dimensional characteristics
- Power, torque, top speed, acceleration, which characterize the performance of the motorcycle
- Autonomy, battery and charging time, to highlight the characteristics of an electric vehicle
- Price, as one of the determining factors for the diffusion of this market.

The best values for each characteristic were highlighted in green, while the worst values were shown in red. Then, a balance was made to calculate the delta, i.e., the difference, between the positive results, tops, and the negative ones, flops, to determine which model represented the best innovation.

Based on these results, the most innovative model, i.e., the model with the highest delta, could be determined. The reference is the Lightning Ls-218 model with a delta of 3. To develop an innovative motorcycle, one must overcome or compensate for this delta by improving 4 or 5 characteristics without worsening other values. Taking the best results of each specification as a reference, it is possible to create a table showing how to work to improve (Table 4).

In the specific case of this project, the final product will be used for freight transportation. For this reason, aspects such as maximum speed will be neglected. Obviously, the weight must be as low as possible to favor autonomy and handling (safety), while all parameters related to the lightness of the bicycle must be as high as possible to

Tabela 6 – Innovation Table

Characteristic	Target Value
WheelBase	>1500mm
Width	<870 mm
Seat Height	<800 mm
Weight	<178 kg
Power	>150 kW
Torque	>220Nm
Max Speed	>350km/h
Acceleration 0-100 km/h	<1.8 seg
Autonomy	>217km
Battery	>14.4 kWh
Charging time	<120 min
Price (\$)	<16.200
Delta	>3

compete in the competitive market.

In order to compete with gasoline vehicles, a high level of autonomy is required. To ensure this, the capacity of the battery must also be as large as possible to allow for longer run times.

However, one of the main drawbacks in affirming mobility through electric vehicles is certainly the duration of recharging, which is why the system with the lowest possible value will be chosen.

The manufacturing cost will be the most difficult parameter to determine. However, an estimate will be made.

4.0.3 Analyse stage

Once the Define, Measure, Benchmark, and Top-Flop Analysis phases are completed, the process defined by the QFD can be concluded with the Analysis phase, in which the "WHAT /HOW relationship matrix" is created.

4.0.3.1 WHAT /HOW Relationship Matrix

The "what", i.e. the needs of the product from the customer's point of view, is compared with the "how", i.e. the technical requirements for the realization of the product, as it is used in the top-flop analysis. In this phase, the parameters that have emerged most clearly from the previous tables, indicated by yellow colored cells, are used. Numerical ratings for the type of relationship are also used in this case: Nothing (empty field, equivalent to 0),

Tabela 7 – What and How table

What / How Matrix	WheelBase	Width	Seat Height	Weight	Power	Torque	Max Speed	Acceleration 0-100 km/h	Autonomy	Battery	Charging time	Price (\$)	Total
High Autonomy	0	0	0	9	3	0	0	3	9	9	0	3	36
Lightness	1	1	0	9	1	0	0	3	9	3	0	3	30
Low price	0	0	0	3	3	1	1	1	3	3	3	9	27
Easy to recharge	0	0	0	0	3	0	0	0	0	9	9	0	21
Safety	3	0	0	9	0	0	3	0	1	0	0	3	19
Total	4	1	0	30	10	1	4	7	22	24	12	18	

Weak (1), Medium (3), Strong (9). Finally, the sums for rows and columns are performed for these numbers. So, from reading this "WHAT /HOW matrix"(Table 7), it can be seen which are the most important values to be improved for the innovative design of an electric vehicle.

Summing:

- The sum of the row values indicates which requirement is most affected by the technical specifications
- The sum of the column values indicates the priority of the actions that must be taken to achieve the maximum impact on the requirements of the row

Based on the values obtained, it can be assumed that the priority in the development of an innovative electric vehicle is mainly related to the highest ranked specifications, such as vehicle weight, autonomy, battery capacity and price.

This means that the designer should emphasize the above features (weight, autonomy, battery capacity, and selling price) during the design process to satisfy the customer.

As the most important feature where defined, It is possible to create the morphological matrix (Figure 32, which will be used to determine the solution applied in the earlier design.

For the each feature, a group of possibilities was evaluated and one was choose as starting point for the design stage. They are numbered in the morphological matrix and related following

High Autonomy: For the high autonomy aims, the battery's technology plays an important role. The chosen model was Lithium based.

In the morphological matrix there are three different kinds, which are indicated bellow:

- 1 - Lithium battery
- 2 - Lead battery

















Morphological Matrix				
Main function	Elementary function	Possible solutions		
High Autonomy	High battery power			
	Multiple battery module			
	Source of energy			
Lightness	Small steering radius			
	Easy to park			
	Lighter materials			
Low price	Few manufacturing steps			
	Easy to assembly			
	Low cost components			
	Possibility of customization			
Easy to recharge	Battery bank recharging			
	Battery bank replacement			
Safety	Low speed balance			
	Easy to park			
	Stability while loading / unloading			
	Passive safety systems			

Figura 32 – Morphological Matrix

Source: Author

- 3 - Nickel Metal Hydrate battery (NiMH)

Lightness: For achieve this goal, some different strategies of body frame was considered. The choice was the model based in addictive manufacturing, with the concern of looking for a lighter, and less expensive material. The options shown in the morphological matrix are:

- 1 - Double beam frame
- 2 - Backbone frame
- 3 - Tubular frame (truss)
- 4 - Mono-block frame
- 5 - Addictive manufactured frame

Low price: For this objective, two conditions for motor mounting was considered, for one of them would be necessary to include a chain or belt transmission system. For the second option it is not necessary. In order to keep the number of components as smaller as possible, the second option was selected.

- 1 - Electric motor centered in the frame + transmission from electric motor to rear wheel
- Electric motor centered on the rear wheel

Easy to recharge: For the recharging strategy three possibilities where take into account, a plug and play connection, what make it possible to be done at home, an

inductive system and a battery swapping using a battery batch. For that feature, the first option was took.

- 1 - Manual plug
- 2 - Inductive recharge system 3 - Swapping battery

Safety: The safety feature could be subdivided in some sub-functions, which have some possible solutions each. In order to keep the matrix readable, only the selected options for the sub-system is chosen.

- 1 - Inverted tricycle - To allow the load and unload goods, without destabilizing the vehicle, a the three wheel solutions was taken. It also make the parking easy, even while loaded and in irregular floor.
- 2 - To avoid or reduce injuries to the rider in case of rollover of the vehicle, a ROPS (Rollover Protective Structure) will be designed.
- 3 / 4 - Although a car design it is not what is being dealing with, some of the passive safety systems commonly used in automobile will be added to this vehicle design, such as front airbags, curtain airbags and seat-belts.

As mentioned early, the design phase will start from the solutions pointed-out in the morphological matrix.

4.0.4 Design stage

Once the main feature are defined and the possible solutions were selected, the design phase may begin.

Along the project, some models were done, in the first time, a street motorcycle were considered, them a scooter model took place and lastly a tricycle. This sketches was used as inspiring for the final design.

4.0.5 Verify stage

Considering the definition and exploration of the possibilities, the first concept of the vehicle was **ideated**. For it the software Fusion 360 was used (Figure 33 and Figure 43).

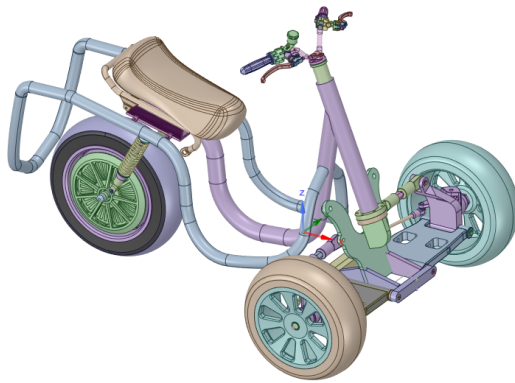


Figura 33 – Initial Trike Design



Figura 34 – Ideated Trike

Source: Author

The trike was designed to be convenient for the driver and also to carry the load. Its main dimensions, such as the distance between the axles, the caster angle and the position of the mass, were first specified in the table 6 and then adjusted based on the author's experience. Some characteristics of this tables was not considered due the natural difference between motorcycle and tricycle, likewise the width. It can be seen in figure 35.

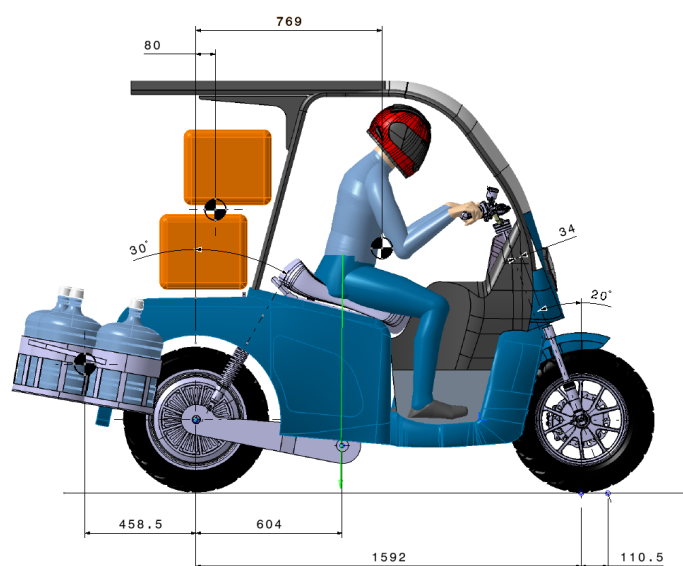


Figura 35 – Load Position

Source: Author

Tabela 8 – Use cases

[HTML]C0C0C0 Case	Path	Velocity (m/s)	Acceleration (m/s ²)	Cargo (kg)	DownHill	UpperHill	Obstacle
1	Linear	Variable	2	140	No	No	No
2	Curvilinear	16	140	140	No	No	No
3	Linear	Variable	2	140	Yes	Yes	Yes

The rider was assumed to be a man, for which the main dimensions can be seen in Figures 36 and 37

This first sketch was used in the first looping of the dynamics analysis, which was done with the MSC Adams Software. As first input, the weight of the motorcycle considered was 192 kg (Figure 38).

From the dynamic analysis the load applied in the optimization phase was obtained. It was done in done according to the cases shown in table 8:

From this analysis, the resulting forces in each suspension on each of the modeled lanes were determined (see Figures 45, 46 and 47).

These values were used in the finite element model to develop the frame and rear arm.

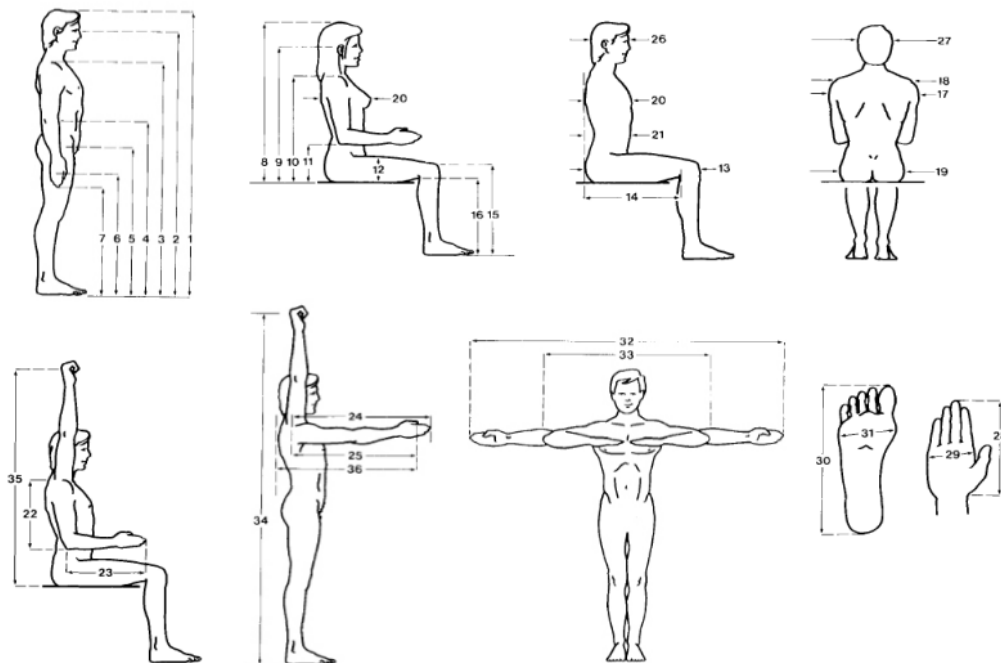


Figura 36 – Rider's dimension scheme

Source: © 2020 The Ergonomics Center

Anthropometric Data for U.S. Adults (all dimensions in inches)



Dimension	Men				Women			
	5th %ile	50th %ile	95th %ile	SD	5th %ile	50th %ile	95th %ile	SD
1 Stature	64.88	69.09	73.62	2.70	60.04	64.02	68.50	2.53
2 Eye height	60.47	64.57	69.02	2.62	55.94	59.72	64.02	2.43
3 Shoulder height	52.72	56.65	60.87	2.49	48.90	52.44	56.46	2.29
4 Elbow height	39.53	42.64	45.94	1.97	36.69	39.45	42.68	1.79
5 Hip height	32.44	35.39	38.78	1.94	30.47	33.23	36.18	1.76
6 Knuckle height	26.50	28.78	30.51	1.39	24.88	27.01	28.50	1.27
7 Fingertip height	23.35	25.75	28.23	1.47	21.89	24.13	26.46	1.37
8 Sitting height	33.86	36.14	38.46	1.41	31.61	33.74	35.91	1.37
9 Sitting eye height	29.53	31.65	33.86	1.31	27.48	29.45	31.46	1.20
10 Sitting shoulder height	21.73	23.74	25.71	1.21	20.28	22.20	23.98	1.10
11 Sitting elbow height	7.76	9.69	11.46	1.13	7.44	9.17	10.87	1.03
12 Thigh clearance	6.18	7.09	8.15	0.61	5.71	6.57	7.52	0.55
13 Buttock-knee length	22.40	24.29	26.34	1.20	21.30	23.19	25.43	1.28
14 Buttock-popliteal length	18.07	19.76	21.57	1.08	17.36	19.02	21.06	1.13
15 Sitting knee height	20.04	21.77	23.70	1.10	18.46	20.08	21.93	1.07
16 Popliteal height	15.35	16.93	18.54	0.98	13.78	15.24	16.85	0.93
17 Shoulder breadth (bideltoid)	18.07	20.04	22.32	1.28	15.98	17.72	19.65	1.13
18 Shoulder breadth (biacromial)	15.12	16.34	17.60	0.75	13.19	14.37	15.59	0.72
19 Hip breadth	12.13	13.54	15.24	0.95	12.24	13.90	15.75	1.05
20 Chest (bust) depth	8.31	9.96	11.73	1.03	8.07	9.65	11.65	1.08
21 Abdominal depth	7.87	9.88	12.60	1.47	7.24	8.94	11.22	1.24
22 Shoulder-elbow length	13.15	14.29	15.51	0.72	12.09	13.15	14.29	0.68
23 Elbow-fingertip length	17.48	18.90	20.47	0.92	15.91	17.24	18.90	0.92
24 Upper limb length	28.50	30.94	33.58	1.53	26.10	28.35	30.91	1.47
25 Shoulder-grip length	25.75	27.99	30.43	1.43	23.51	25.59	28.07	1.39
26 Head length	7.40	7.87	8.31	0.28	7.01	7.48	7.95	0.29
27 Head breadth	5.75	6.06	6.42	0.22	5.51	5.79	6.14	0.20
28 Hand length	6.97	7.60	8.27	0.39	6.50	7.09	7.83	0.40
29 Hand breadth	3.19	3.46	3.78	0.17	2.83	3.07	3.35	0.15
30 Foot length	9.84	10.67	11.54	0.52	8.90	9.59	10.55	0.49
31 Foot breadth	3.70	4.02	4.37	0.21	3.35	3.66	3.98	0.19
32 Span	66.14	71.34	77.05	3.33	60.20	65.24	70.98	3.27
33 Elbow span	31.18	33.54	36.11	1.49	28.38	30.76	33.18	1.43
34 Vertical grip reach (standing)	77.68	84.21	91.90	3.87	71.34	77.32	84.21	4.11
35 Vertical grip reach (sitting)	46.93	51.26	55.75	2.46	43.03	47.05	51.14	2.67
36 Forward grip reach	27.05	29.76	32.72	1.72	24.53	27.20	30.12	1.68

References: References: Gordon, Claire C. et. al (2014). 2012 Anthropometric Survey of U.S. Army Personnel: Methods and Summary Statistics.

Figura 37 – Rider's dimension table

Source: © 2020 The Ergonomics Center



Figura 38 – Center of mass (Unload motorcycle)

Source: Author

The setups of the dynamic analysis performed on Adams software can be seen in the Figures 39,40, 41, 42. To perform the analysis, the front and rear suspensions were

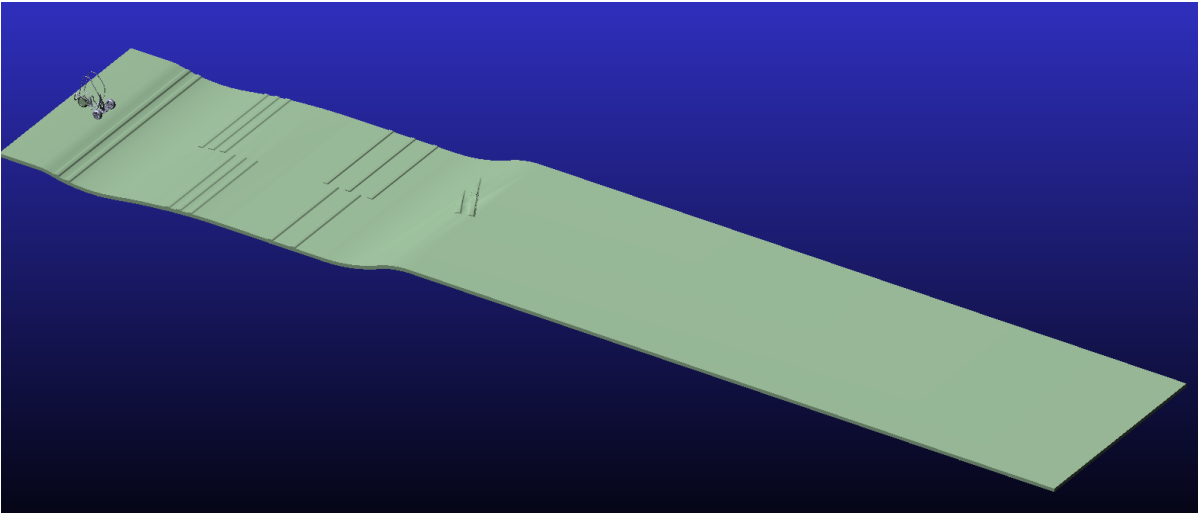


Figura 39 – Trike - First road used on dynamic simulation

Source: Author



Figura 40 – Trike - First road used on dynamic simulation

Source: Author

first defined in BikeSim software ((LEE; POLAK; BELL, 2008)). Later, the front and rear suspension attributes were used on Adams to perform dynamics simulation (Figures 43 and 44).

One more scenario was considered in the dynamic analysis. The second simulation aimed to determine the limiting speed and maximum roll angle of the motorcycle to validate or identify changes for urban/freight traffic.

In this context, the analysis was performed assuming that the scooter is in a curve and the speed and roll angle are continuously increased. In Figure 48 you can see the limiting speed of 125km/h and in Figure 49 the maximum roll angle of 40°. Despite the fact that the scooter became unstable and tipped over after exceeding the speed limit, 125km/h can be considered sufficient for urban use.

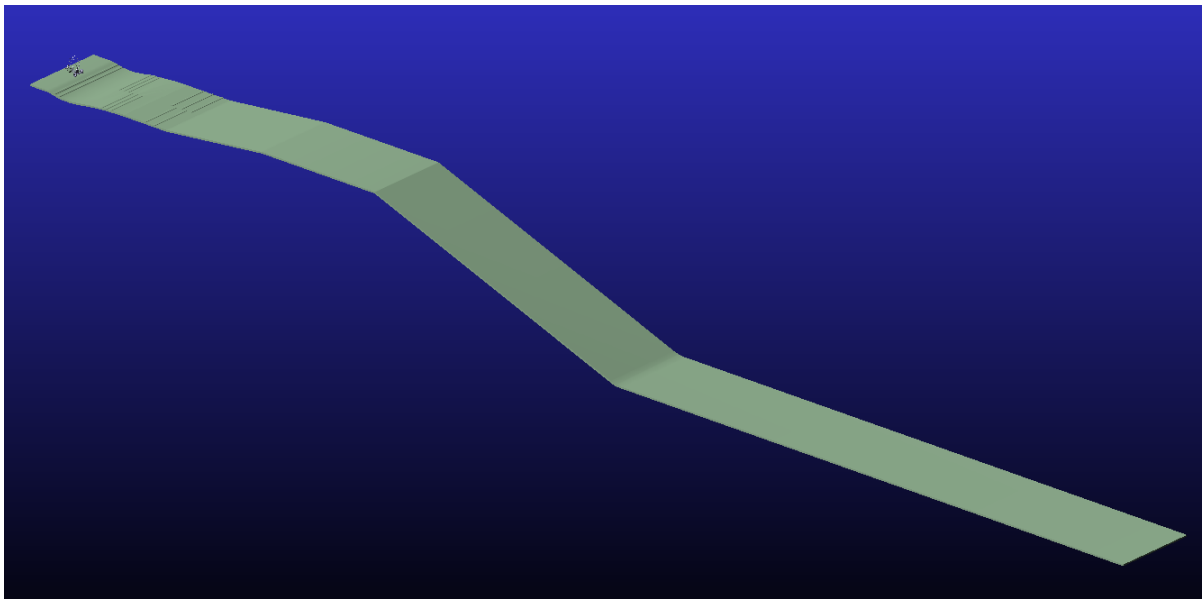


Figure 41 – Trike - Second road used on dynamic simulation

Source: Author

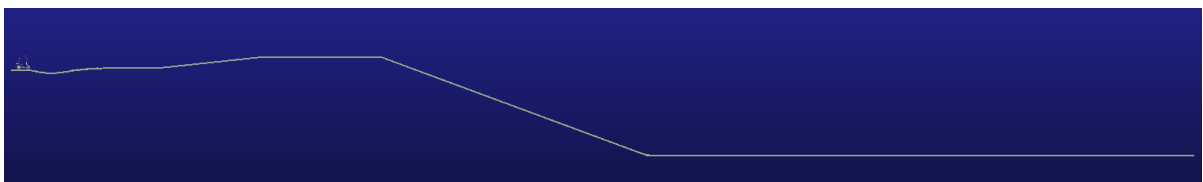


Figure 42 – Trike - Second road used on dynamic simulation

Source: Author

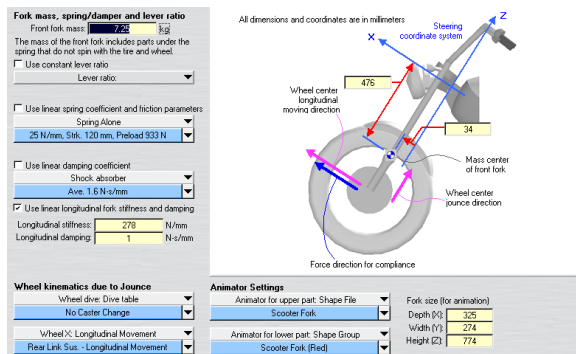


Figure 43 – Properties: Front Suspension

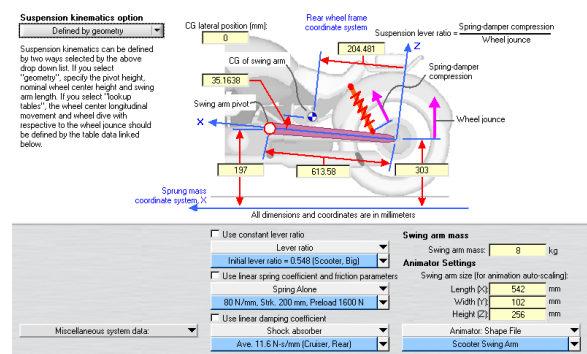


Figure 44 – Properties: Rear Arm

Source: Author

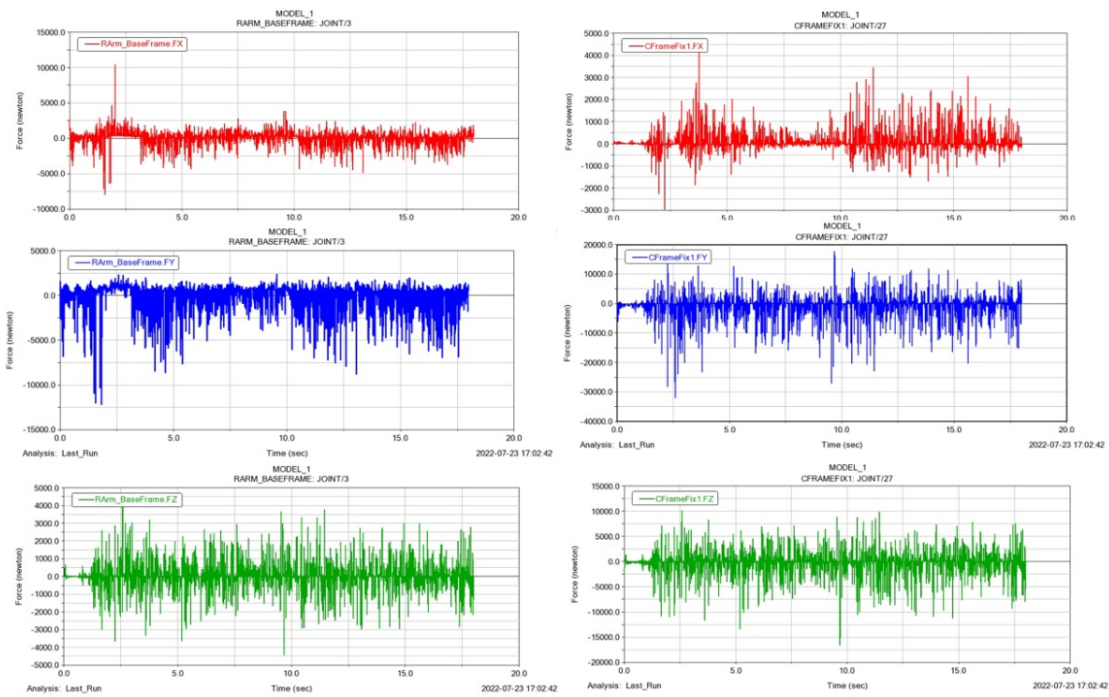


Figure 45 – Adams Results for path 1 - In the left, forces of rear suspension (FX, FY and FZ), in the right Force of front suspension (FX, FY and FZ)

Source: Author

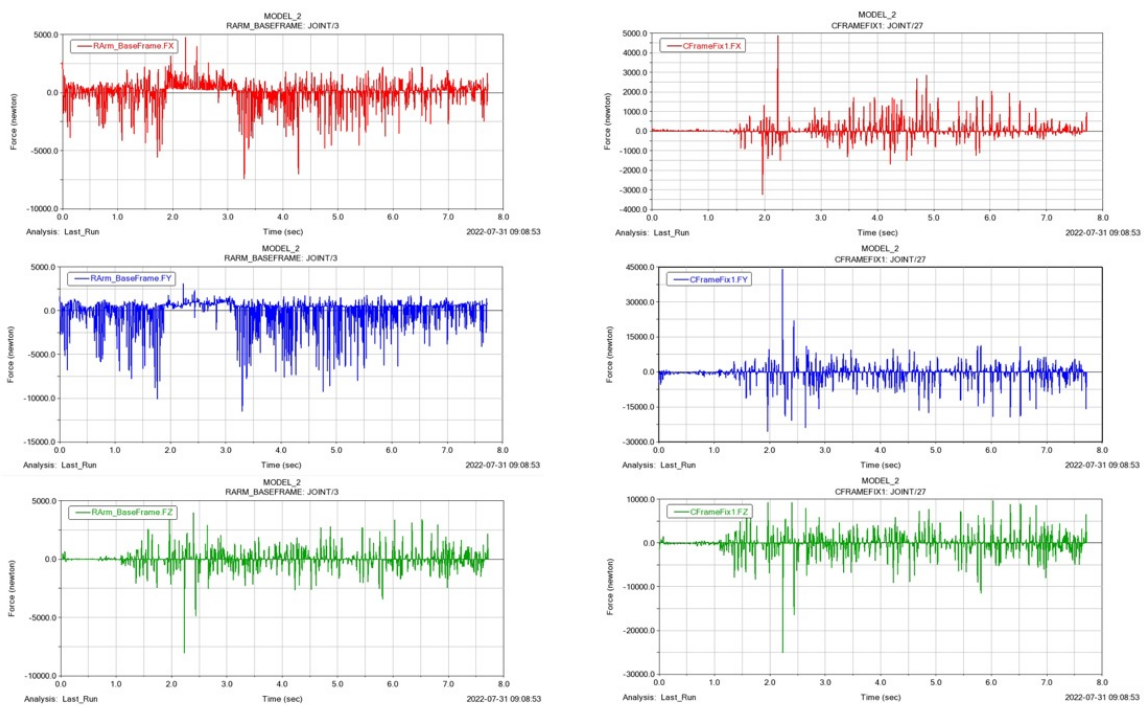


Figure 46 – Adams Results for path 2 - In the left, forces of rear suspension (FX, FY and FZ), in the right Force of front suspension (FX, FY and FZ)

Source: Author

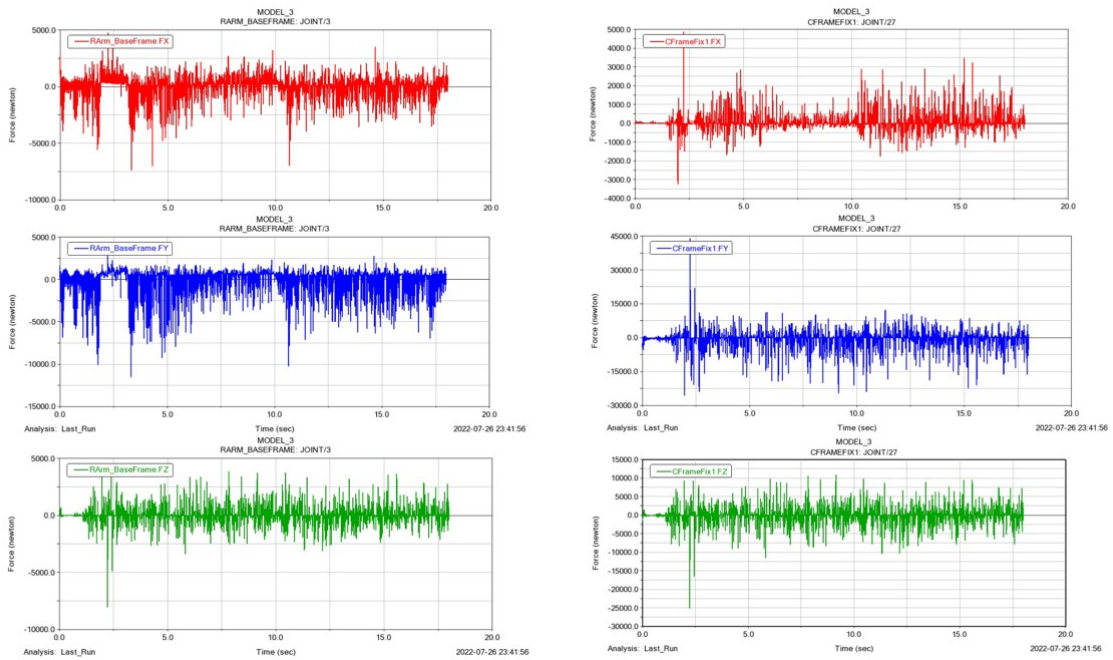


Figure 47 – Adams Results for path 3 - In the left, forces of rear suspension (FX, FY and FZ), in the right Force of front suspension (FX, FY and FZ)

Source: Author

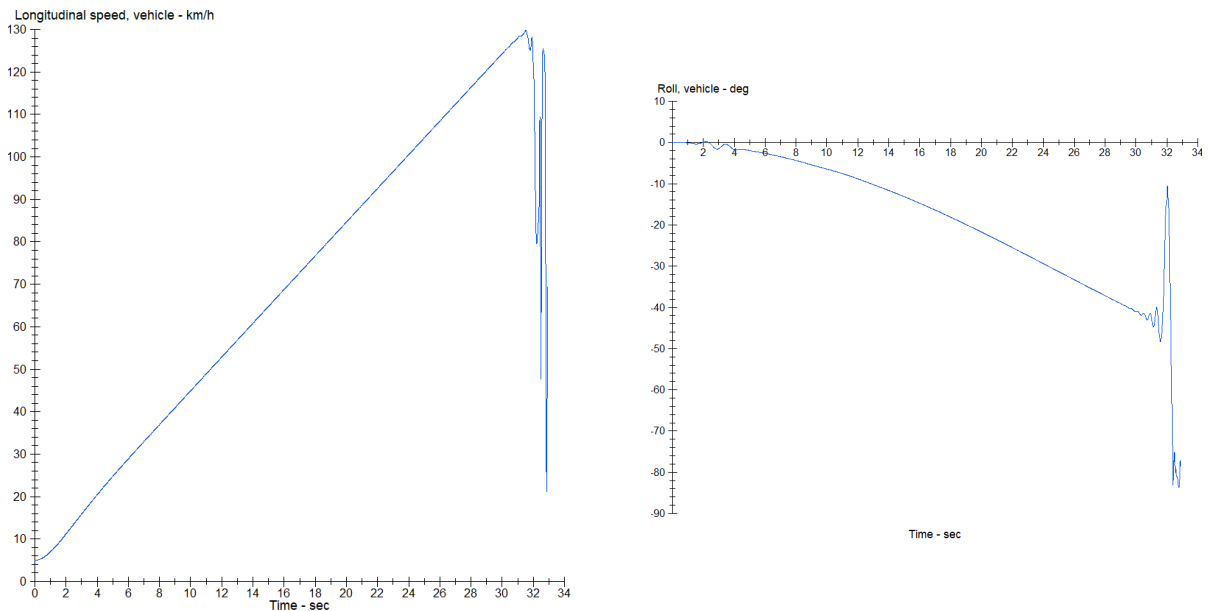


Figure 48 – Longitudinal Speed in constant radius, with longitudinal acceleration

Figure 49 – Roll Angle in constant radius, with longitudinal acceleration

Source: Author

4.0.5.1 Generative Designing

Both the loads (Figure 58) and the constrains (Figure 51) of the preliminary design were used as input in a generative model to define the frame, the rear arm and the front console concepts.

As a premise, the material considered was polyetherketone ketone HT -23 (PEKK) (Figure 52) reinforced with carbon fibers to enable the manufacturing process through additive manufacturing, also through the EOS P 700 3D printer (Figure 53).

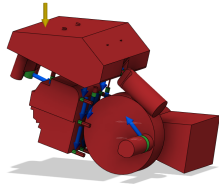
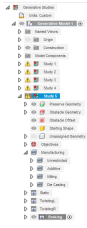


Figura 50 – Load Case 1 - Frame

Source: Author

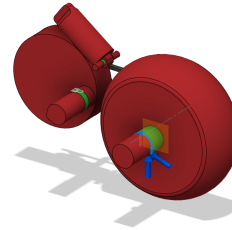
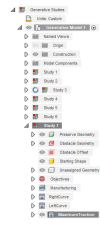


Figura 51 – Load Case 2 - Rear Arm

Source: Author

The maximum components of the load determined in the dynamic analysis for each user case were included in the generative model. These forces can be seen in the table 9.

The results from the combination of material and manufacturing process can be seen in Figures 54 to 59.

4.1 Design result


The final result was a tricycle suitable for carrying both goods and passengers (Figure 61). The preliminary design can be found in the Appendix section. A simple

Tabela 9 – Maximum components of forces per user case

Load Case	Loads from Front Suspension (N)			Loads from Rear Suspension (N)		
	F _x	F _y	F _z	F _x	F _y	F _z
1	4500	-30000	-16000	10200	-14000	4500
2	5000	45000	-25000	-7500	-12000	-8000
3	-3000	-3000	-25000	-7500	-12500	-7500

Physical Properties	Metric
Density	1.36 - 1.62 g/cc
Filler Content	20 - 40 %
Water Absorption	0.040 %
Linear Mold Shrinkage	0.00050 - 0.0030 cm/cm
Melt Flow	5.0 - 18 g/10 min
Mechanical Properties	Metric
Tensile Strength, Ultimate	134 - 324 MPa
Elongation at Break	1.2 - 2.5 %
Modulus of Elasticity	8.96 - 48.0 GPa
Flexural Yield Strength	214 - 448 MPa
Flexural Modulus	7.58 - 31.0 GPa
Izod Impact, Notched	0.534 - 1.07 J/cm
Izod Impact, Unnotched	4.81 - 9.40 J/cm
Charpy Impact Unnotched	3.40 - 4.00 J/cm ²
Charpy Impact, Notched	0.500 - 0.600 J/cm ²
Coefficient of Friction	0.16 - 0.17
Coefficient of Friction, Static	0.218 - 0.25
Thermal Properties	Metric
CTE, linear	9.00 - 45.0 $\mu\text{m}/\text{m}\cdot\text{°C}$
Melting Point	340 - 360 °C
Deflection Temperature at 1.8 MPa (264 psi)	260 - 327 °C
Glass Transition Temp, Tg	160 °C
Flammability, UL94	V-0
Processing Properties	Metric
Melt Temperature	377 - 382 °C
Mold Temperature	149 - 232 °C
Drying Temperature	149 °C
Moisture Content	0.10 %
Dew Point	-28.9 °C
Injection Pressure	103 - 138 MPa

Figura 52 – PEKK Properties

Source: <https://matweb.com>


Additive Manufacturing of Series Parts
Up to 1 Meter in Length

EOS P 770

EOS P 770

Technical Data
EOS P 770

Download FactSheet | pdf | 216.3 KB

Construction Volume	700 x 380 x 580 mm (27.6 x 15 x 22.9 in)
Laser Type	CO ₂ 2 x 70 W
Precision Optics	F-theta lens, surface module, high-speed scanner
Scan Speed	up to 2 x 10 mm (32.8 ft/min)
Power Supply	32 A
Power Consumption	typical 3.1 kW; maximum 12 kW
Machine Dimensions (W x D x H)	2,250 x 1,550 x 2,100 mm (88.6 x 61 x 82.7 in)
Recommended Installation Space	min. 4.8 x 4.8 x 3.0 m (159 x 159 x 118 in)
Weight	approx. 2,300 kg (5,071 lb)
Software	EOS ParameterEditor, EOSCAM, EOS RP Tool, EOSCONNECT Core, EOSCONNECT MachinePark, PSW 3.8

Figura 53 – EOS P 700 3D Printer

Source: EOS web page - <https://www.eos.info/en>



Figura 54 – Generative Design Result -
Frame

Source: Author



Figura 55 – Generative Design Result -
Frame

Source: Author



Figura 56 – Generative Design Result -
Rear Arm

Source: Author



Figura 57 – Generative Design Result -
Rear Arm

Source: Author

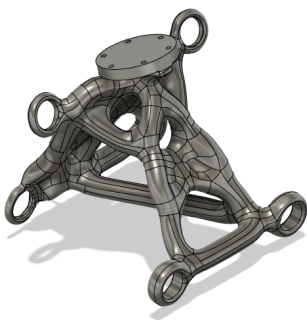


Figura 58 – Generative Design Result -
Front suspension support

Source: Author

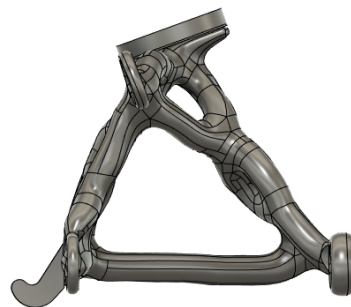


Figura 59 – Generative Design Result -
Front suspension support

Source: Author

indexing system, similar to the ISOFIX used in cars ((NO, 2014)) was provided so that the transport devices could be easily interchanged. The dimensions of the ISOFIX Hooke's can be found in the figure 60. For passenger transport, the ISOFix system should be used to secure a seat, backwards towards the rider's seat, as shown in figures 63 and 64.

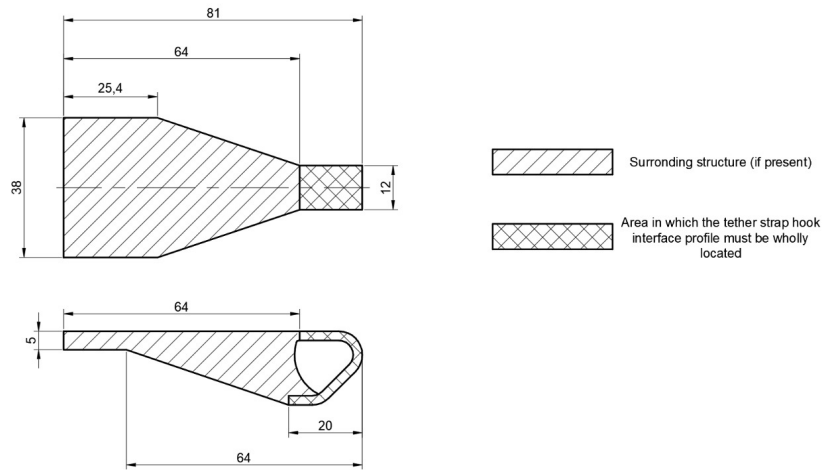


Figura 60 – ISOFIX Dimensions

Source: Adapted from [Lowne et al. \(2002\)](#)

Because of the flexible fastening system, any other device can also be used. This depends on the needs of the end user, as well as a backpack or gallon transport (Figure 62).



Figura 61 – Final tricycle design

Source: Author

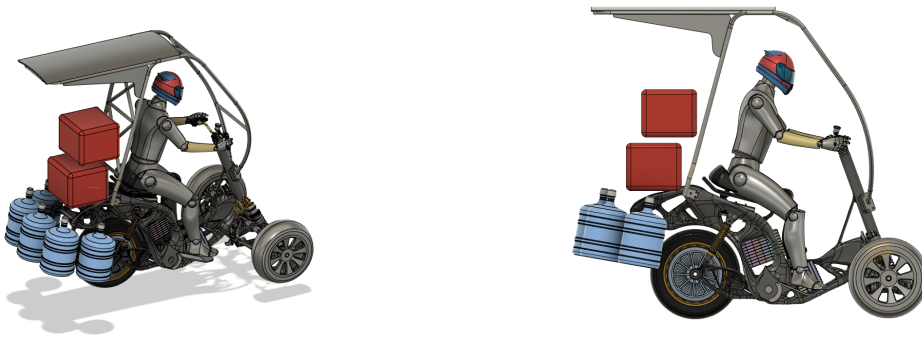


Figura 62 – Final trike design for goods transportation

Source: Author

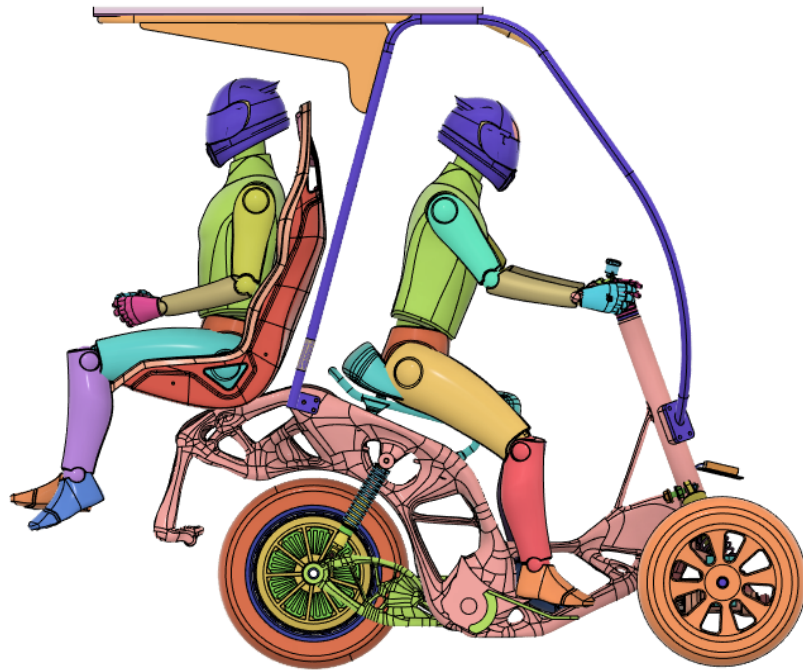


Figura 63 – Final trike design with passenger transportation - Side view

Source: Author

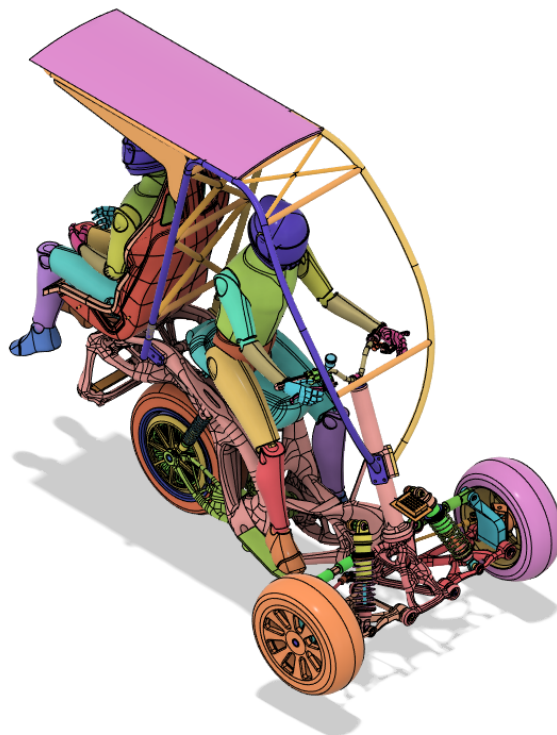


Figura 64 – Final trike design with passenger transportation - Isometric view

Source: Author

5 SAFETY ANALYSIS

5.1 THUMS Overview

Neither the development nor the improvement of the human body model was the subject of this project, but since it has a great impact on the analysis, not only in terms of results, but also in terms of debugging the whole model, some details are given about the THUMS project.

The THUMS used in this work is a model of the human body of an adult male of the 50th percentile (AM50). The height and weight are 175 cm and 77 kg, version 5. The Figure 65 shows the developed FE model, which includes a head/brain model, the internal organs, and the skeleton, which includes the major bones such as the skull, ribs, spine, femur, tibia, pelvis, humerus, ulna, and radius, and the major anatomical joints such as the ankle, knee, hip, shoulder, elbow, and hand.

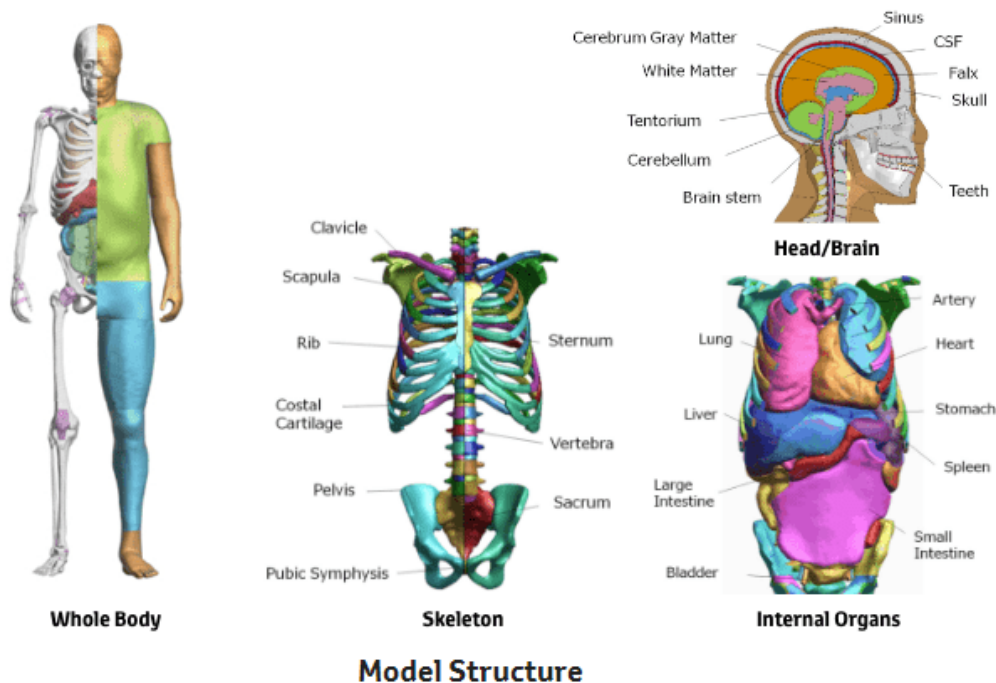


Figura 65 – Thums model

Toyota webpage www.toyota.co.jp/thums/about/

The model was developed by Toyota Motor Corporation and is freely available for

download from their website.

THUMS version 5 has been validated using 36 test sets of postmortem human surrogates (PMHS) and volunteer tests in frontal, side, and rear impacts. The validation sets are also available on the Toyota Motor Corporation website.

5.1.1 Materials used in human models

5.1.1.1 Hard Materials

The behavior of human bone is like a brittle material whose properties are recorded in mechanical tests.

Li et al. (2010) show in their paper how a test was performed to describe the material properties of a rib. They took ribs 2, 4, and 10 from men between the ages of 31 and 62 and tested them for tension, compression, and shear. They also examined different velocities to determine the relationship between response and velocity. The experimental test matrix can be seen in Figure 66, and the model setup as in Figure 67.

Subject ID/gender	Ribs 2-10	Age	Aspect L/R	Loading rate (m/s)		x_0 (mm)	z_0 (mm)	Cortical thickness	
				Static	Dynamic			Range (mm)	Mean \pm STD (mm)
419/m	2	31	R	0.002	1.0	25	107.1	0.23 – 2.55	0.7 ± 0.27
413/m	4	54	L	0.002	0.5	69	149.9	0.21 – 2.96	0.86 ± 0.4
412/m	10	62	L	0.002	0.5	72	171.5	0.28 – 2.87	0.89 ± 0.39

Figure 66 – Experimental test matrix

Source: Li et al. (2010)

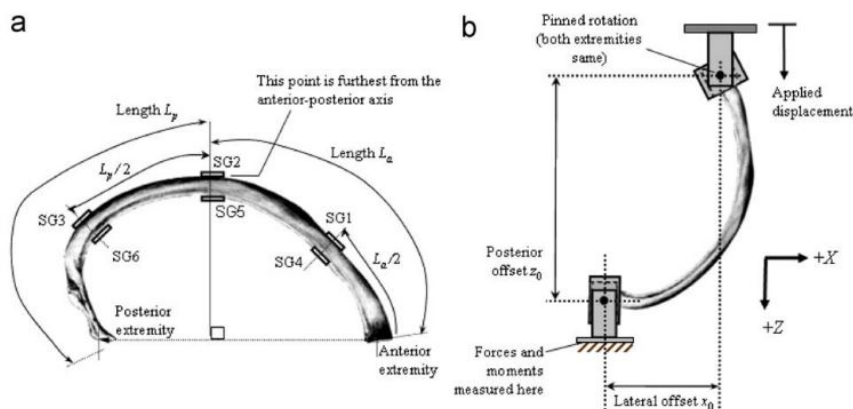


Figure 67 – Model Setup

Source: Li et al. (2010)

The problem was also modeled using a finite element method to validate a material curve. The results obtained are available in the figure 68.

Subject	Model	Static data		Dynamic data				Number of rib elements	
		Displacement (mm)	Resultant reaction force (N)	Fracture time (ms)	Fracture displacement (mm)	Resultant reaction force (N)	Initial run time step (ms)	Hex	Shell
419m-Rib 2R	Exp	10	57.1	18.9	18.9	90.7	-	-	-
	Hex	10	52	18.5	18.5	96.7	9.5e-5	36,807	-
	HS1	10	62.7	19	19	104.7	1.2e-4	6429	2208
	HS2	10	61	19.5	19.5	109.9	1.5e-4	3280	1798
	HS3	10	54.1	18.5	18.5	91.9	1.4e-4	3280	1798
413m-Rib 4L	Exp	14	51.9	82	41	123.4	-	-	-
	Hex	14	59.9	76	38	120	1.2e-5	42,318	-
	HS1	14	55.1	72	36	122	1.0e-5	6397	2837
	HS2	14	57.3	83	41.5	131	1.1e-4	3347	1948
	HS3	14	50	88	44	120	1.3e-4	3347	1948
412m-Rib 10L	Exp	16	46.7	104	52	126.8	1.3e-4	3347	1948
	Hex	16	41.2	122	61	87.4	-	-	-
	HS1	16	44.4	82	41	76.5	8.1e-5	48,350	-
	HS2	16	52.6	66	33	84.9	9.3e-5	6494	2660
	HS3	16	50.4	72	36	84.1	1.5e-4	3164	1968
HS4	HS3	16	45.1	82	41	80	1.2e-4	3164	1968
	HS4	16	44.5	104	52	82.2	1.2e-4	3164	1968

Figura 68 – Experimental test results

Source: Li et al. (2010)

5.1.1.2 Soft Materials

Material models used to represent organ response are much more complex than those used for bone. Because of the high degree of nonlinearity present in the model. Budday et al. (2017) show that an experiment could be performed on a human brain to obtain the correct parameters to model it correctly.

It is possible to see that a certain damping system is applied to the material model (Figure 69), which itself introduces a high degree of complexity to optimize the curves.

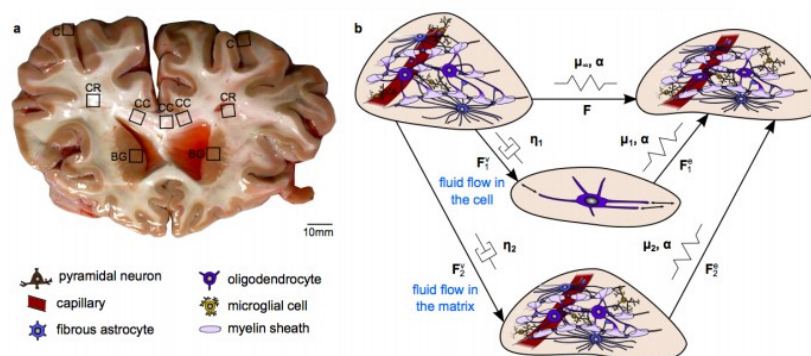
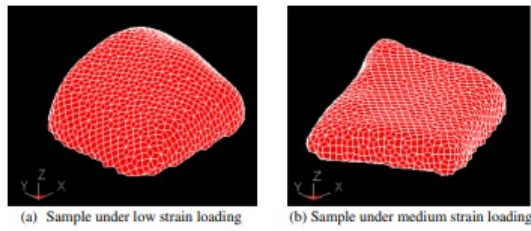


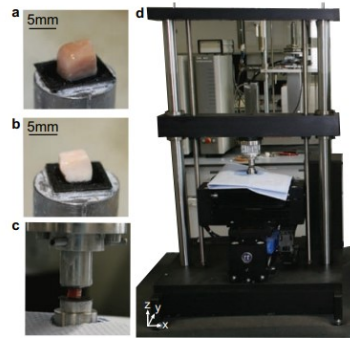
Figura 69 – Brain Model

Source: Budday et al. (2017)

As usual, an experiment was performed with a small part of the organ. In the specific case of the brain, both the white and gray matter were used. Then a finite element model was created to validate the material model, and finally the model was extrapolated

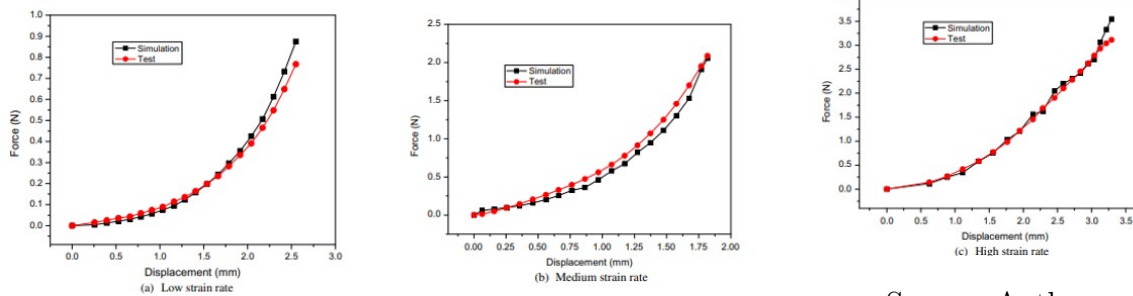


Experimental and numerical curve for brain



Experimental and numerical curve for Rib4

Source: [Budday et al. \(2017\)](#)



Source: Author

Figura 70 – From left to right: Low strain rate, Medium strain rate and High strain rate

Source: [Budday et al. \(2017\)](#)

to a higher-level problem.

The curves are obtained considering different rates, as is shown in the picture 70.

There are many other important aspects to consider, such as the behavior of joints ([Yue, Shin e Untaroiu \(2011\)](#)), shown in Figure 71, or the contribution of tissue and ligaments ([Fice, Cronin e Panzer \(2011\)](#)), see Figure 72. The tissue and ligaments play an important role when tensile loads are applied, but they can usually be neglected when compressive loads are applied.

Depending on the analysis and the desired target, spinal posture prediction may be considered (Figure 73).

To use the Piper application to position the THUMS in the preprocessing phase of a finite element analysis, a metafile must be created.

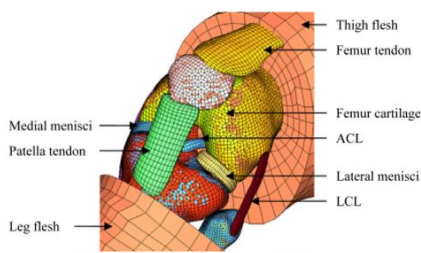


Figure 5. Knee joint isometric view with soft tissues.

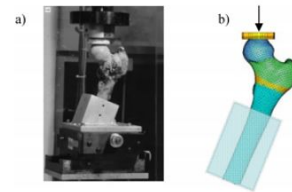


Figure 7. a) Femur head compression test setup (Keyak et al. 1998), b) FE model setup.

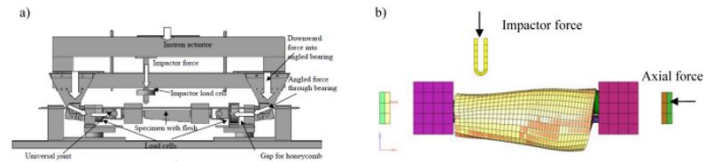


Figure 8. a) Leg combined loading test setup (Untaroiu et al. 2008), b) FE model setup.

Figure 71 – Knee Joint experiment

Source: Yue, Shin e Untaroiu (2011)

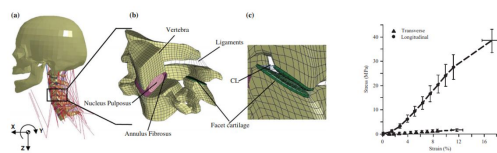


Figure 72 – Neck Ligaments

Source: Fice, Cronin e Panzer (2011)

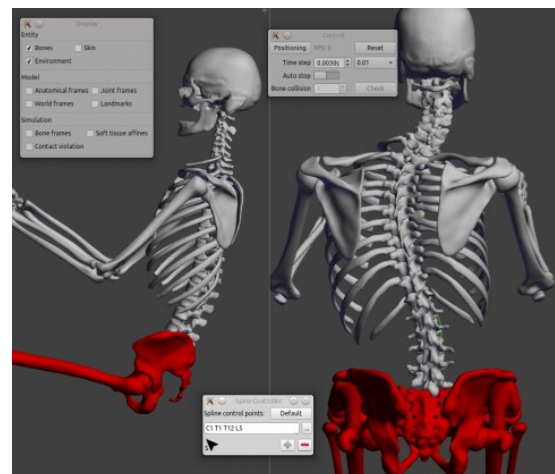


Figure 73 – Spine Posture prediction

Source: Claude, Lyon e Projets (2017)

Of course, however, the full model of the human body is much more complex than presented here, as are the material models, since they not only determine the outcome of the analysis, but also imply relevant properties such as time step or failure mode, which are important to understand in order to properly handle safety simulations.

5.1.2 Modeling and Pre-Processing

The trike model was developed entirely by the author. Given the complexity of the mesh of the optimized model, which would have small solid elements, which in turn would significantly reduce the time step and make the analysis infeasible, the tube frame version was chosen for the simulation, which is simpler and

allows the analysis (Figure 74).

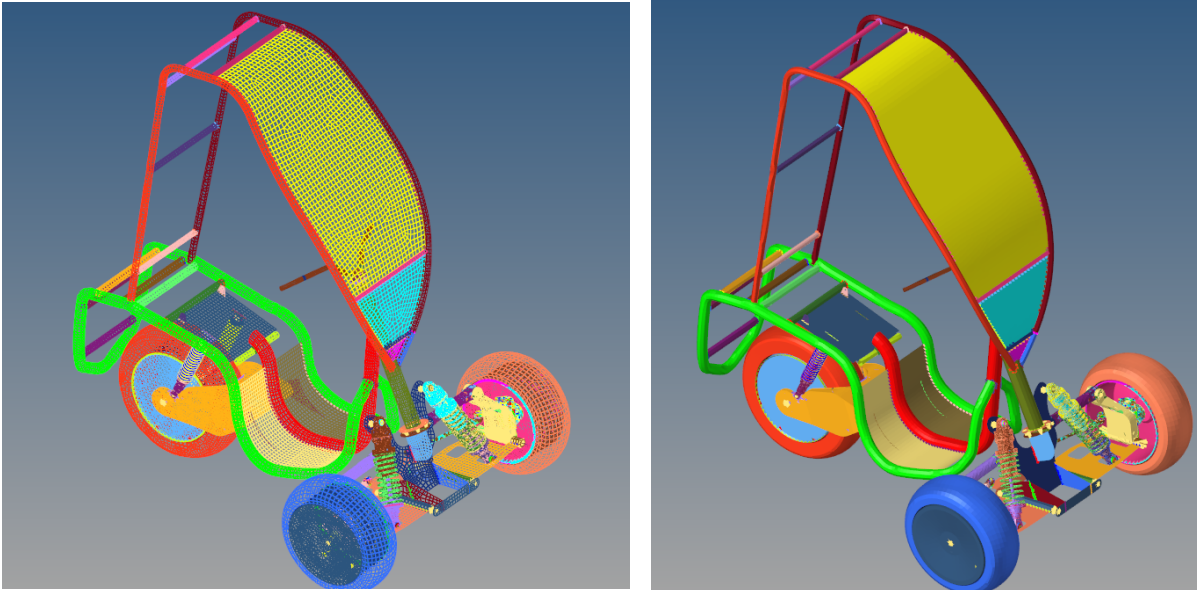


Figura 74 – Pre-processing in Hypermesh

Source: Author

After preprocessing the trike model, the helmet was modeled. The 3D CAD was created based on the public references available in the GrabCAD platform. The outer shape was simplified to reduce the number of components and to obtain a patterned mesh. The inner shape was adapted to the thum's head size to position the helmet without interference (Figure 75).

A belt model without the 1D slip rings was added to the helmet to keep it in the THUMS head during analysis.

The material properties of the helmet, both for the outer skin and the inner foam, were taken from the GMSIE team that had previously worked with the helmet.

Then the tricycle, the helmet, and the Total Human Model for Safety - THUMS V5 were imported together. The positioning of Thums on the tricycle was done with the software Piper (Figure 76).

The final pre-processing result can be found in the Figure 77.

Since the Federal Motor Vehicle Safety Standard FMVSS 581 and ECE-R42 only

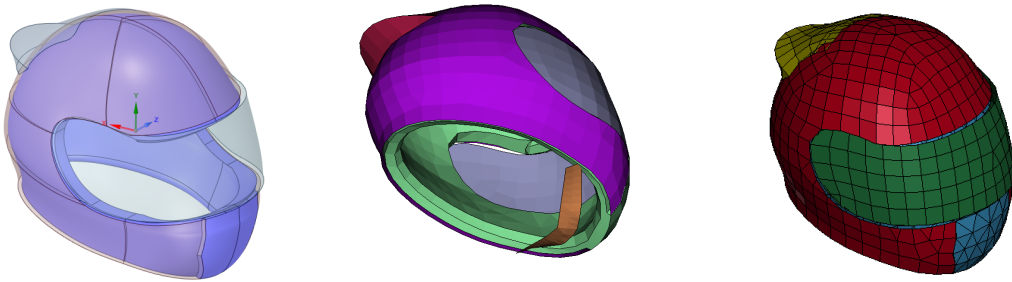


Figura 75 – In the left, helmet model, in the middle, the helmet with the lower belt and in the right helmet meshed

Source: Author

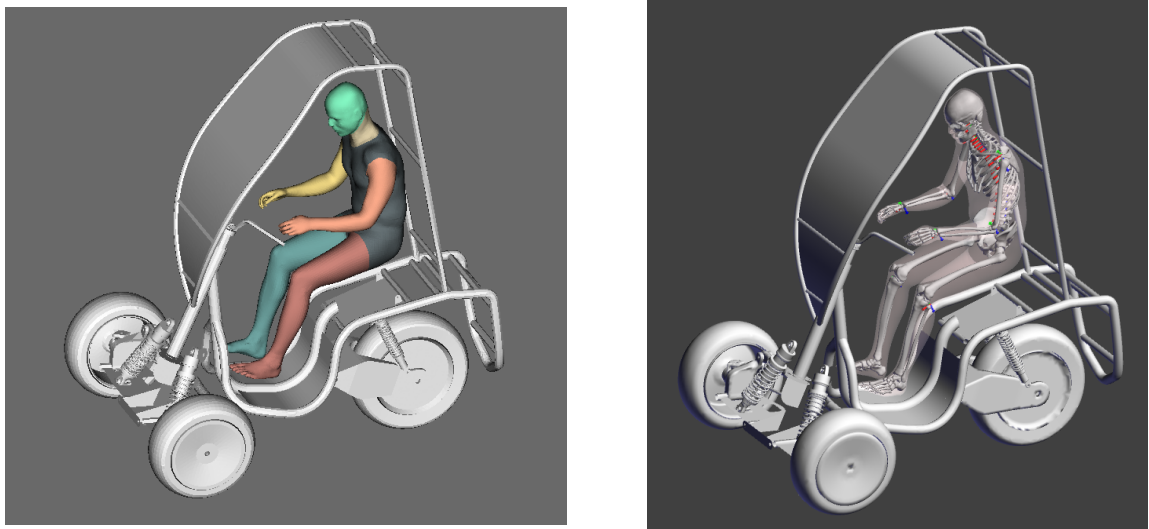


Figura 76 – Thums model positioning with Piper's software

Source: Author

specify requirements for vehicle parts (such as bumpers) in low-speed front and side impacts, the (UNECE, 1958) criterion chosen for driver evaluation was that the head must not exceed 80g for 3 ms.

5.2 THUMS Evaluation

The response of THUMS was evaluated under two different conditions, frontal impact and side impact.

For this analysis, a numerical model of the tricycle was used to simulate the impact against a rigid wall or a rigid vertical post with a diameter of 273 mm. The initial velocity applied was 8 m/s (29 km/h), which closely matched Federal Motor Vehicle Safety Standard 214 (FMVSS214) - Figures 78 and 79.

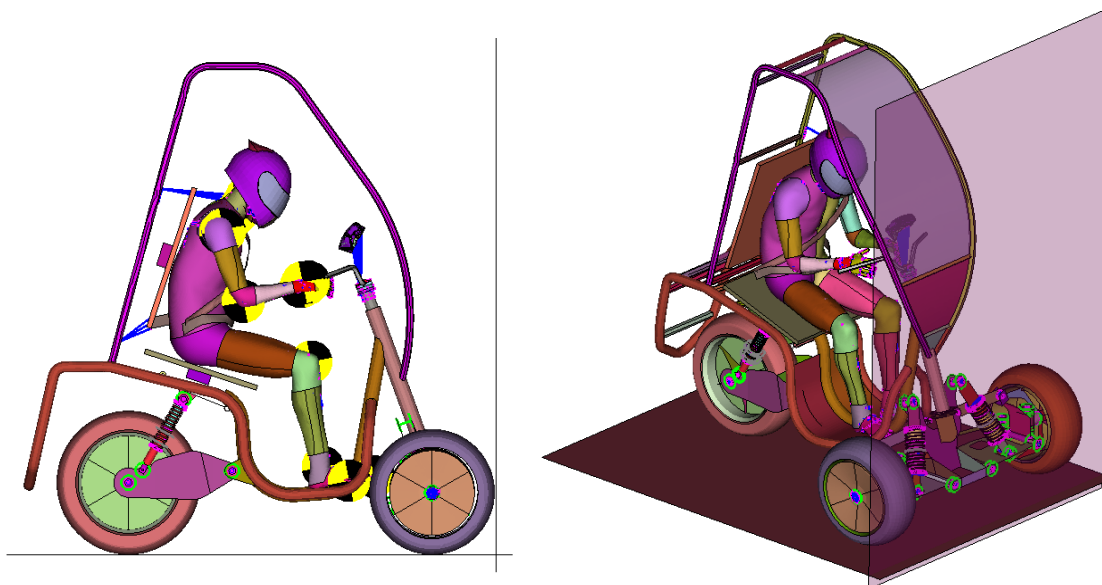


Figura 77 – Complete model pre-processed - Trike, THUMS and Helmet

Source: Author



Figura 78 – Frontal Crash simulation - Trike, Thums, Helment and Frontal Airbag

Source: Author

The side impact was performed with curtain airbags, but they did not function as expected and extended above the rider's head (Figure 79). Nevertheless, it could be retained in the final design, as it should provide additional protection at least in rollovers - which were not simulated in this work.

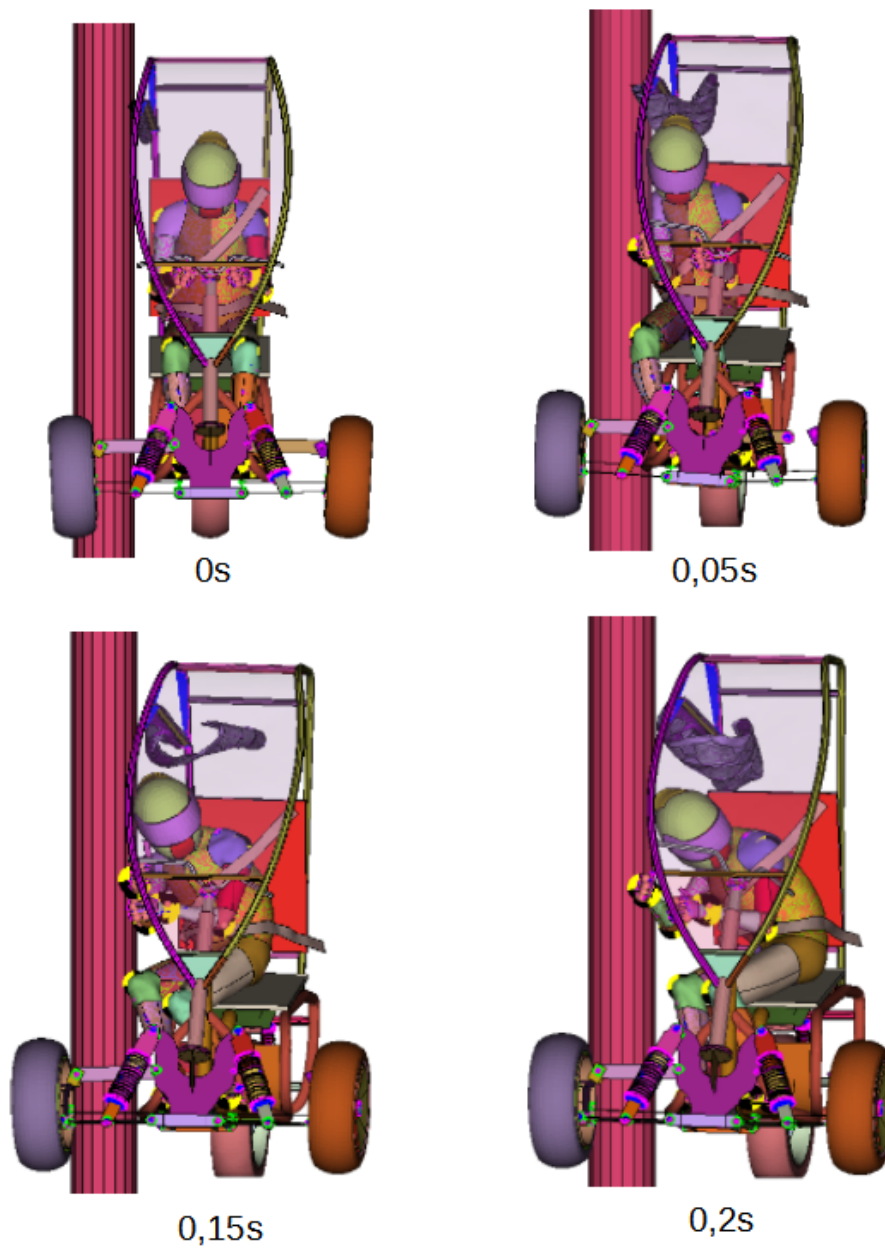


Figura 79 – Side Impact simulation - Trike, Thums, Helment and Frontal Airbag

Source: Author

The first feature analyzed was the energy balance. For this purpose the following components were considered:

- Total energy
- Kinetic energy
- Internal energy

- External work
- Hourglass energy

The energies are a first indicator of the success of a simulation. As can be seen in the figure 80, the total energy increases slightly over the course of the analysis, but the magnitude of the increase is considered acceptable.

The trend in kinetic and internal energy is correct. The hourglass energy, a parameter considered non-physical, should be below 10% of the total energy according to the LS -dyna guidelines, and as can be seen, this constraint is met.

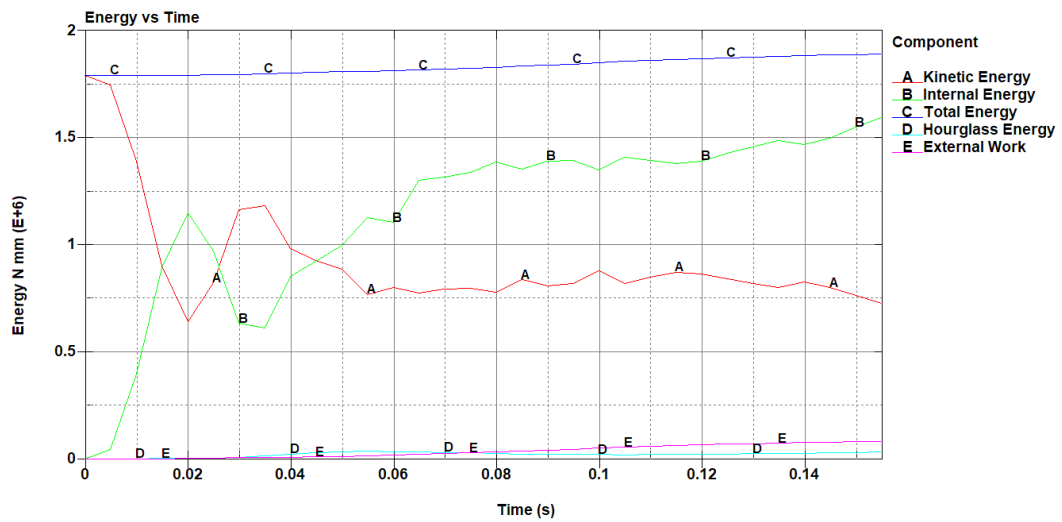


Figure 80 – Energy balance

Source: Author

6 RESULTS AND DISCUSSION

6.1 Product design

In the development of a project, it is widely recognized that using a well-defined methodology is crucial for effectively organizing activities at each stage. In the tricycle project, the DFSS methodology was employed, incorporating a combination of different tools.

The TRIZ tool, utilized during the Benchmarking phase, facilitated the discovery of an innovative solution, given that the trike's design is based on a polymer. This allows the structure to be adapted according to the application, if necessary. Moreover, the ISO-Fix system was adapted for the vehicle, offering a variety of accessories that can be installed, such as elements for transporting food, goods, and even passengers.

In contrast to commercial motorcycles and tricycles, this design includes seat belts, front and curtain airbags, and a rollover protective structure (RoPS). Although the simulation with the curtain airbag was unsuccessful, it was retained in the project due to its potential to reduce damage to the motorcyclist in the event of a trike rollover.

A solar panel was incorporated to minimize energy consumption and power the displays and lighting system. The conceptual design features a 475 mm x 1 m solar panel, and the daily energy generation can be calculated using the following formula:

$$\text{Energy (Wh)} = \text{Power (W)} \times \text{Sunlight hours per day (h)}$$

Replacing the area value, it is possible to estimate to generate around 85.5 watts of power under ideal sunlight conditions, assuming an average efficiency of 18% and an irradiance of 1000 W/m² (KALOGIROU, 2014).

It should be noted that these are only estimations at this stage of the project. During the detailed design phase, the solar panel's characteristics and available sunlight in the specific location should be thoroughly investigated to provide a more accurate assessment of the solar panel's performance and energy generation capacity.

Regarding the tricycle development objectives, it is possible to mention the following:

1. **High autonomy:** The battery capacity was estimated to achieve a 220 km autonomy. A lithium battery package was assumed, and some simplifications were made for the conceptual phase (DOE, 2020):

To estimate the power required to overcome forces and the battery capacity, we will use the following equations, considering a vehicle mass of 118 kg and lithium battery. Other variables were assumed in the conceptual phase based on the author's experience:

Calculate the rolling resistance force $F_{(rr)}$:

$$F_{rr} = C_{rr} \times m \times g$$

Assuming a rolling resistance coefficient $C_{(rr)}$ of 0.015, and the gravitational acceleration g as $9.81m/s^2$, we have:

$$F_{rr} = 0.015 \times 118 \times 9.81 = 17.36 \text{ N}$$

Calculate the aerodynamic drag force $F_{(drag)}$:

$$F_{drag} = 0.5 \times C_d \times A \times \rho \times V^2$$

Assuming a drag coefficient C_d of 0.7, a frontal area A of $0.8m^2$, an air density of $1.225kg/m^3$, and a vehicle speed V of $20m/s$, we have:

$$F_{drag} = 0.5 \times 0.7 \times 0.8 \times 1.225 \times 20^2 = 112.28 \text{ N}$$

Calculate the total force $F_{(total)}$:

$$F_{total} = F_{rr} + F_{drag}$$

$$F_{total} = 17.36 + 112.28 = 129.64 \text{ N}$$

Calculate the power P required to overcome the forces:

$$P = F_{total} \times V$$

$$P = 129.64 \times 20 = 2592.8 \text{ W}$$

Calculate the energy required for the trip:

$$\text{Energy (Wh)} = P \text{ (W)} \times \frac{\text{Trip Distance (km)}}{\text{Average Speed (km/h)}}$$

Assuming an average speed of $60km/h$ and a trip distance of $220km$, we have:

$$\text{Energy (Wh)} = 2592.8 \times \frac{220}{60} = 9,520 \text{ Wh}$$

Calculate the required battery capacity:

$$\text{Battery Capacity (Wh)} = \frac{\text{Energy (Wh)}}{\eta_{\text{battery}} \times \eta_{\text{motor}}}$$

Assuming a battery efficiency η_{battery} of 0.95 and a motor efficiency η_{motor} of 0.9, we have:

$$\text{Battery Capacity (Wh)} = \frac{9,520}{0.95 \times 0.9} = 11,162.81 \text{ Wh}$$

2. **Lightness:** The use of polymers and generative design techniques reduced the mass from 192kg to 118kg.
3. **Comfort:** The front windshield and riding position offer greater comfort than current motorcycles and tricycles.
4. **Low Price:** While a detailed cost analysis was not conducted during the preliminary design phase, the structure's minimal components should contribute to reduced assembly and maintenance costs.
5. **Easy to recharge:** Batteries were positioned to enable quick recharging and easy replacement.
6. **Safety:** Significant advancements were achieved. The results will be discussed in the following sections

6.1.1 Process Planing

As in the other phases of the project, computer-aided tools were used in process planning to optimize the workflow.

Typically, the process planner combines information from 2D drawings with data from the model CAD, to define the best sequence of machines for manufacturing.

In the tricycle project, several parts were developed using the generative design method, resulting in complex surfaces that can be produced by additive manufacturing or injection molding.

However, the components may require post-processing, such as machining to improve the surface or to reach the assembly areas, inserting Ensat bushings for threaded holes, and more.

As diverse 3D software were used in the Trike development, like Catia V5, Fusion 360 and SpaceClaim, and the manufacturing attributes are lost in translation, to facilitate the understanding and minimize process errors, it is proposed to use a color pattern in the 3D design in addition to the part information in the 2D design to help the process engineer

define the best manufacturing strategy for the product. A proposed pattern can be seen in Figure 81





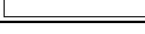







Condition	Surface roughness	Colors
Regular shape (Flat or Cylindrical)	$\sqrt{\text{12.5}}$ (\sim)	 (Dark Green)
	$\sqrt{\text{3.2}}$ (∇)	 (Blue)
	$\sqrt{\text{0.8}}$ ($\nabla\nabla$)	 (Magenta)
	$\sqrt{\text{x}}$ ($\nabla\nabla\nabla$)	 (Yellow)
	$\sqrt{\text{x}}$ (specific)	 (White)
Irregular shape (3D milling required)	$\sqrt{\text{3.2}}$ ($\nabla\nabla$)	 (Cyan)
Threats	Metric STD	 (Green)
	Others	 (Purple)
Symetric components	-----	 (Violet)
Standards components (Bearings, Bushings, etc)	-----	 (Grey-28%)
Skeletons (Geometry of reference)	-----	 (Dark Blue)
Components shown in more than one position	-----	 (Black)** <small>** Apply 75% of transparency</small>

Figura 81 – Color Pattern

Source: Author

Different colors for each features are proposed because they are kept in the most comom standard extension, like .step and .igs

An application of the standard color can be seen in the figure 82

6.1.1.1 Manufacturing

The Tricycle project involves the use of additive manufacturing for several components. Although it is an innovative technology, it is not yet accessible for all sizes of components. Especially not for large parts.

One way to get around this limitation is to split a large part into two or more parts

, manufacture the parts separately, and then join them together using screws, high-strength adhesives, or ultrasonic welding.

These methods were not considered in this work.

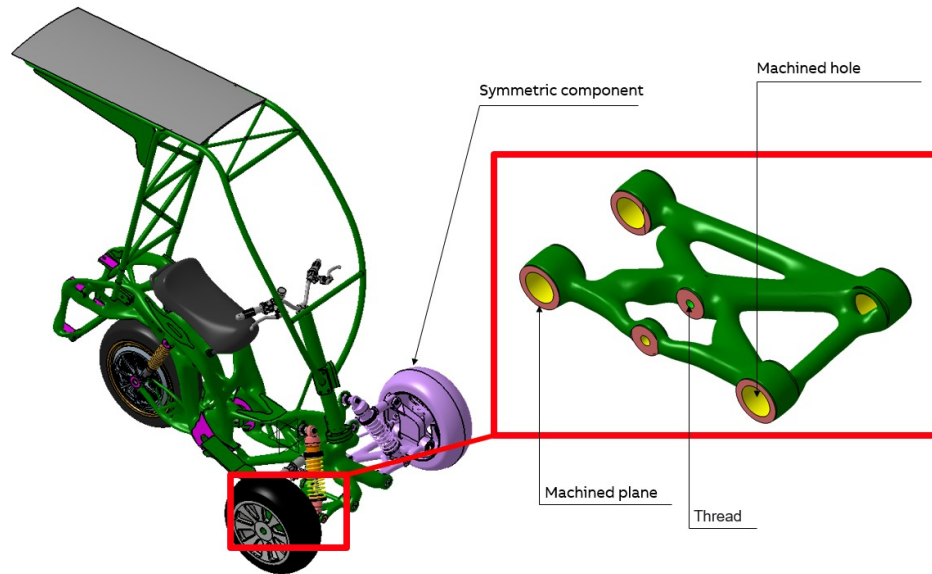


Figura 82 – Application Color Pattern

Source: Author

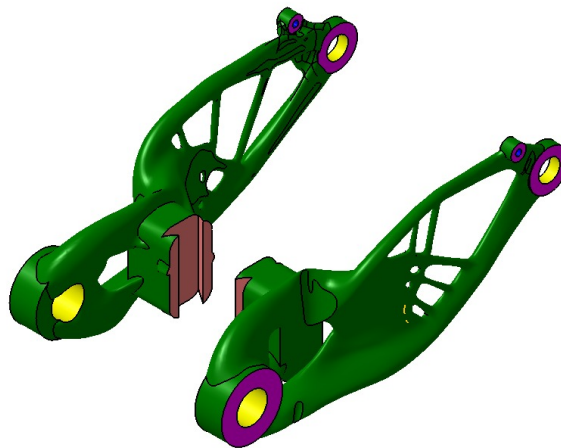


Figura 83 – Example of divided component in two parts

Source: Author

6.2 Safety analysis

6.2.1 Injuries evaluation

6.2.1.1 Head and Neck

According to (UNECE, 1958), the head injury criterion (HIC36) must not exceed 1000 and the head acceleration must not exceed 80g for 3 ms with respect to the neck, the bending moment must not exceed 57 Nm and the tensile and shear criteria should be below the curves in the figure 84.

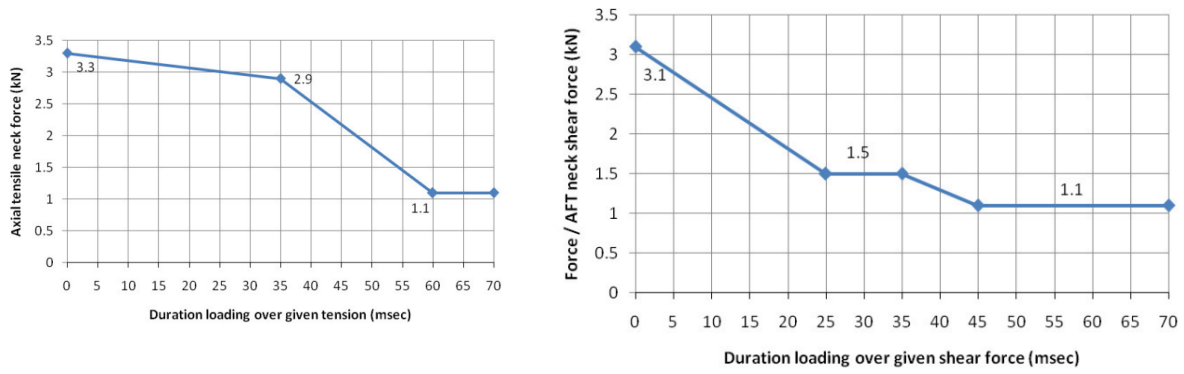


Figura 84 – Neck Injury Criteria

Source: UNECE 2017b

Head acceleration was assessed in both frontal and side impacts (Figures 85 and 86). In both cases, the critical value is reached.

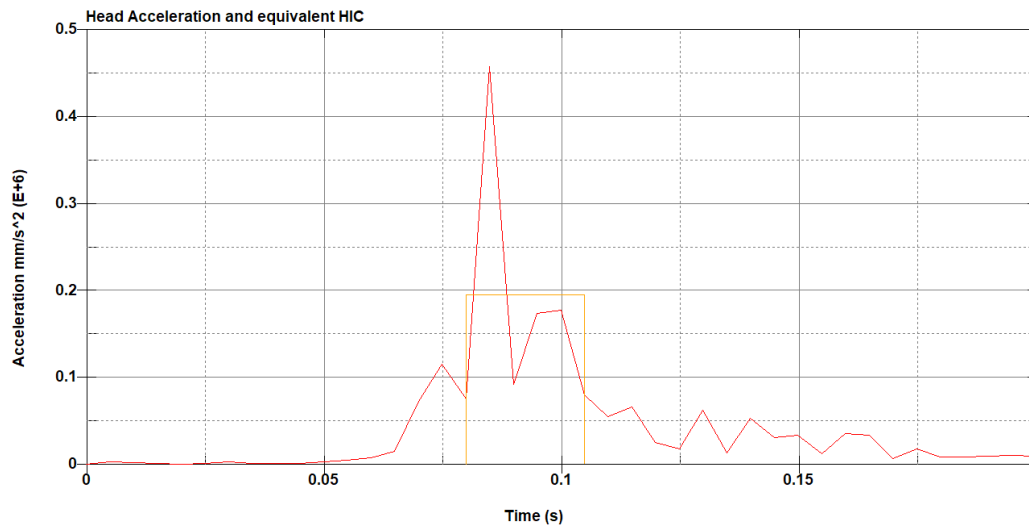


Figura 85 – Head Acceleration and equivalent HIC36 - Frontal Impact

Source: Author

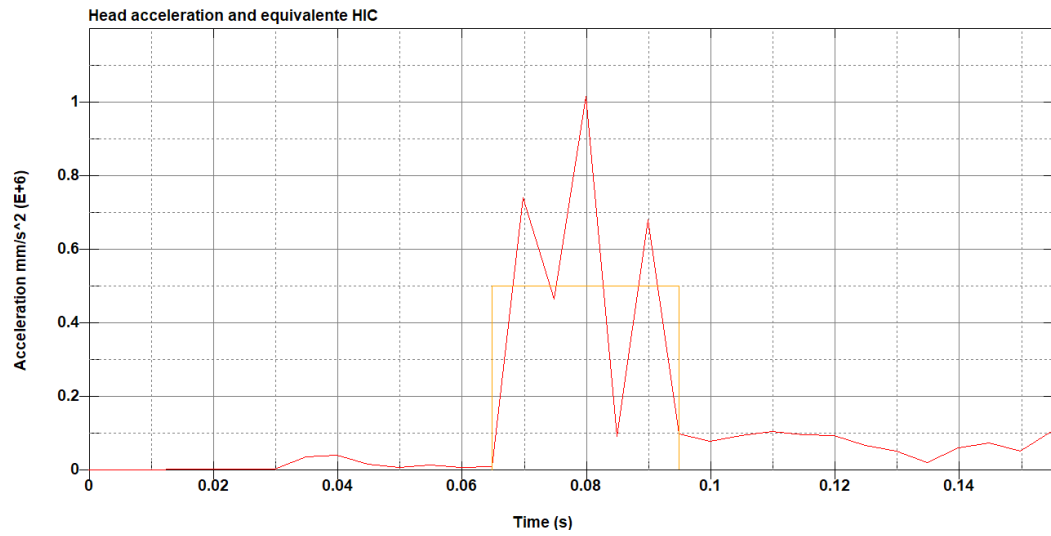


Figura 86 – Head Acceleration and equivalent HIC36 - Side Impact

Source: Author

With respect to the neck, the shear and tensile forces were extracted for the upper and lower vertebrae, C1 and C7, respectively (87).

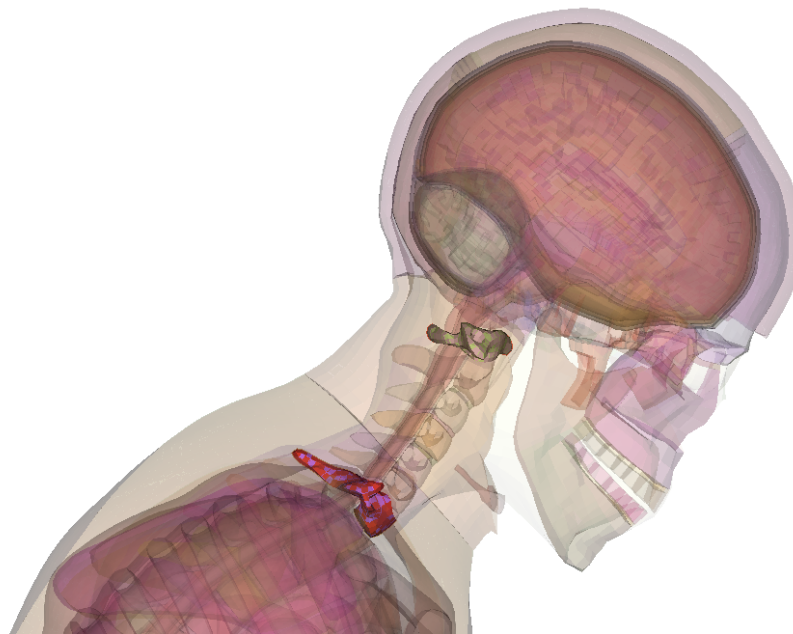


Figura 87 – Vertebrae C1 and C7

Source: Author

The results of the frontal impact are shown in 88 and 89, and those of the side

impact are shown in 90 and 91.

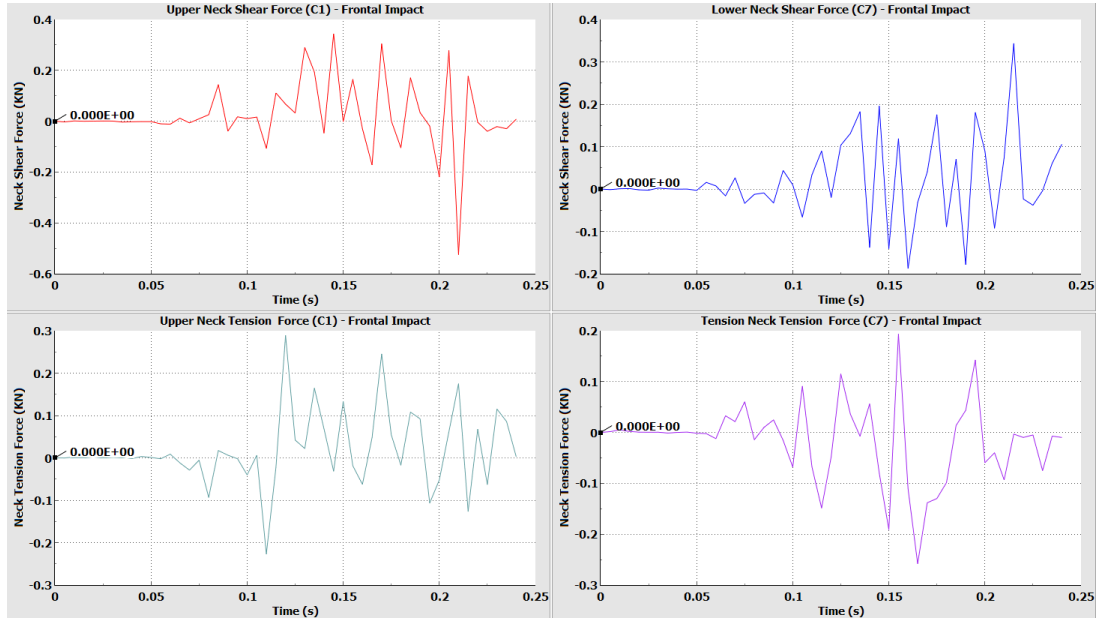


Figura 88 – Neck Shear and Tension Force - Frontal Impact

Source: Author

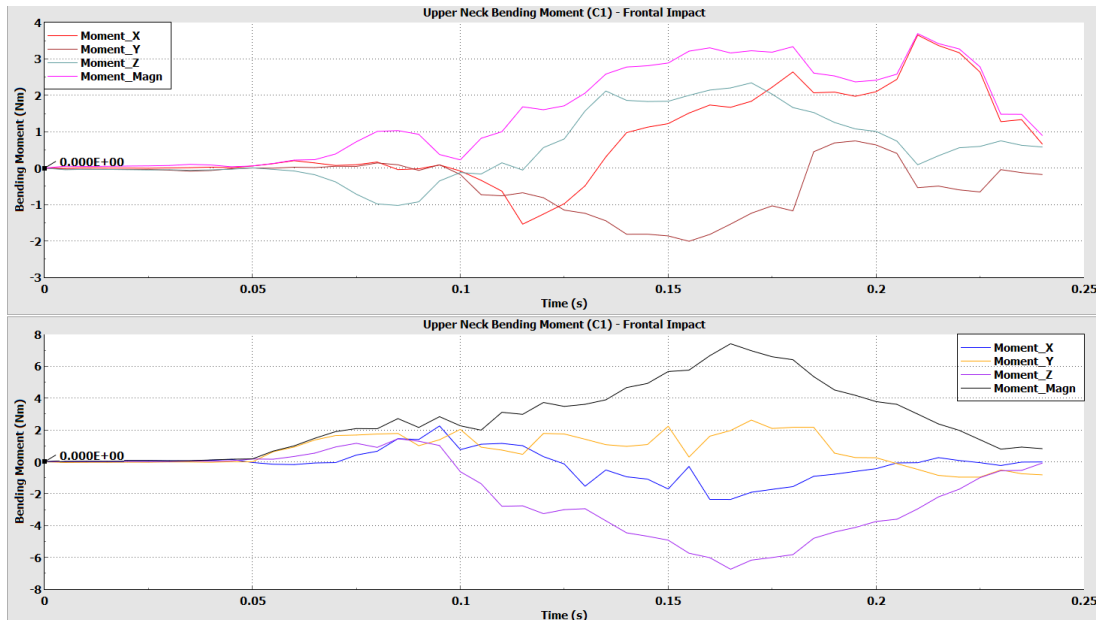


Figura 89 – Neck Bending Moment - Frontal Impact

Source: Author

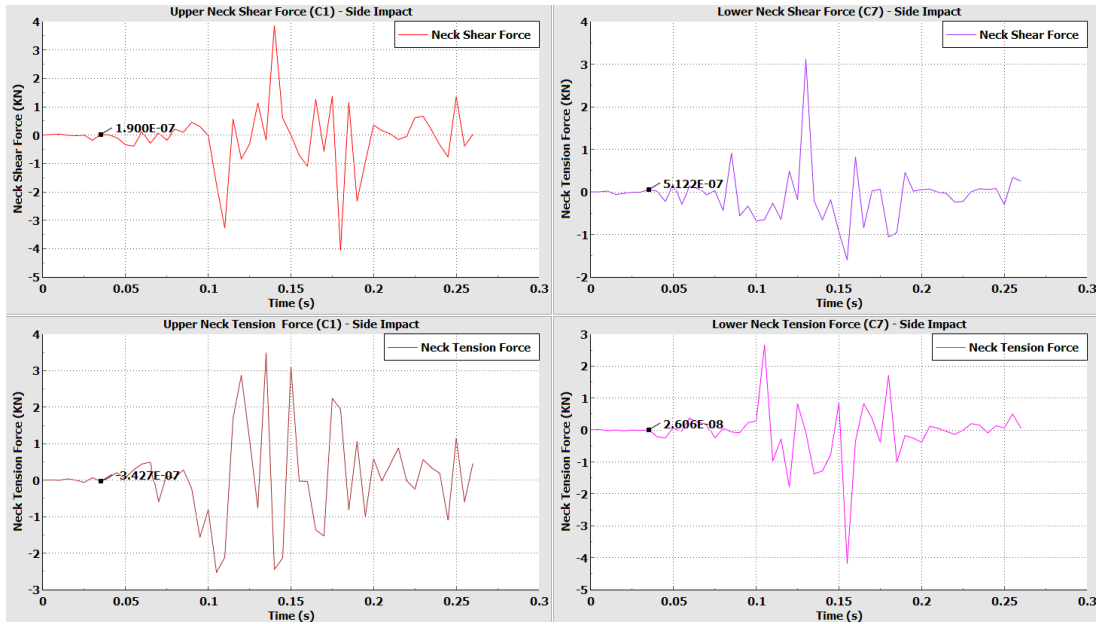


Figura 90 – Neck Shear and Tension Force - Side Impact

Source: Author

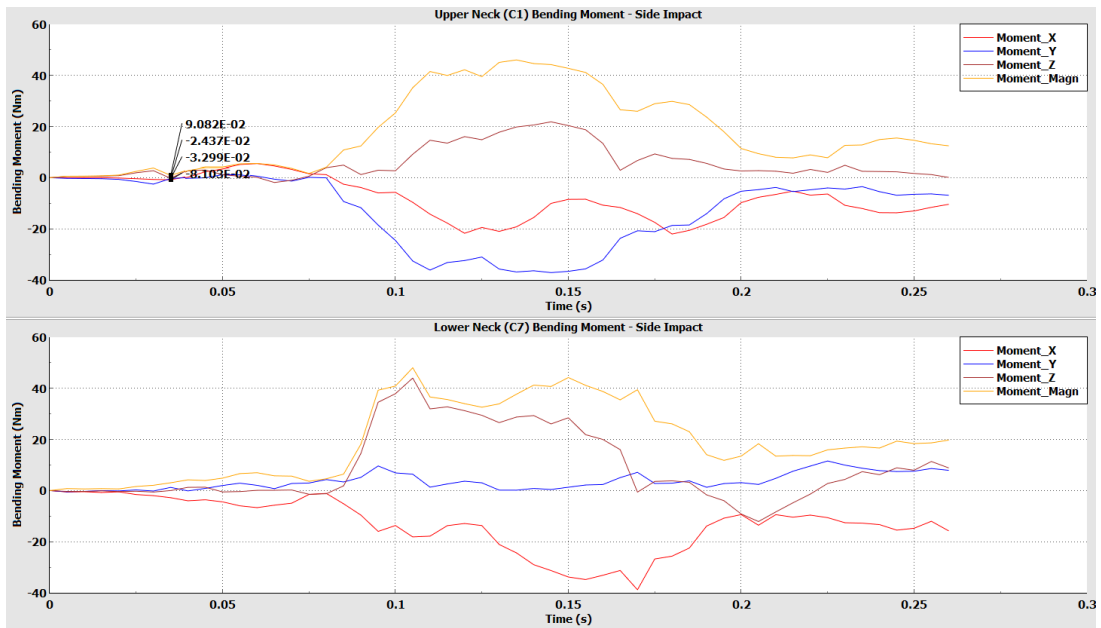


Figura 91 – Neck Bending Moment - Side Impact

Source: Author

In a frontal impact, the rider’s head does not contact any component of the tricycle or the rigid barrier, so both the bending moment and the shear force are much lower than in a side impact.

The side impact meets the criteria, but it is noticeable that the risk of injury to the rider is significantly higher because the helmet collides directly with the rigid pole.

Compared to the frontal crash model, the model differs only with regard to the airbags. The front airbag was eliminated, and a curtain airbag was added. The other conditions, such as helmet and safety for the occupant, were kept.

However, the curtain airbags were not effective in mitigating the impact, since they opened to the sides, not downwards. Even so, they could kept in the design, as they certainly reduce the damage to the driver in the event of a rollover.

6.2.2 Skull and Brain

The development of complete human body models, such as the THUMS used in this project or the HBM developed by Elemance, sets a precedent for establishing other criteria for evaluating damage, such as criteria based on stress, strain, energy, or volume change.

Germanetti summarized the study of several authors who proposed methods for estimating injuries other than those presented by [UNECE \(1958\)](#).

The summary of this study for the assessment of injuries to the skull and brain can be found in [Figure 92](#)

	Damage	Metric	Threshold	Reference	
Skull	Cortical bone fracture	Maximum Principal Strain	0.6%	Mattos et al. [47]	
	Cortical bone fracture (50% risk)	Strain Energy	865 mJ	Deck and Willinger [51]	
		Strain Energy (SUFHEM-based IC)	439 mJ	Willinger et al. [32]	
		Intracranial Pressure (ICP)	>235 kPa	Ward et al. [52]	
	Contusion	Intracranial Pressure (ICP)	>300 kPa	Newman et al. [53]	
Brain	Mild Traumatic Brain Injury (mTBI)	(RIC) Cumulative Strain Damage Measurement (CSDM)	<15%	Kimpara and Iwamoto [56]	
		More severe Traumatic Brain Injury (TBI)	(PRHIC) Cumulative Strain Damage Measurement (CSDM)		>20%
	Diffuse Axonal Injury (DAI) 50% risk	Von Mises Strain	25% (mild) to 35% (severe)	Deck and Willinger [51]	
		First Principal Strain	31% (mild) to 40% (severe)		
		Von Mises Stress	26 kPa (mild) to 33 kPa (severe)		
		Maximum Principal Strain (MPS)	87%		Takhounts et al. [41]
		Von Mises Stress (SUFHEM-based IC)	27 kPa		Willinger et al. [32]
	Diffuse Axonal Injury (DAI)	Angular acceleration—duration time	10,000 rad/s ² 4 ms	Davidsson et al. [61]	
		Angular velocity change	19 rad/s		
	Brain White Matter contusion	Maximum Principal Strain (MPS)	21%	Bain and Meaney [55]	
Subdural Hematomas (SDH) (50% risk)	Minimum of Cerebrospinal Fluid Pressure (MCSFP)	-135 kPa	Deck and Willinger [51]		
	Cerebrospinal Fluid (CSF) Internal Energy (SUFHEM-based IC)	-135 kPa	Willinger et al. [32]		

Figure 92 – Summary of proposed injuries criteria for skull and brain

Source: ([GERMANETTI F.; FIUMARELLA, 2022](#))

Some results were taken for the frontal and side impacts, and they can be seen at [figures 93, 94, 95 and 96](#).

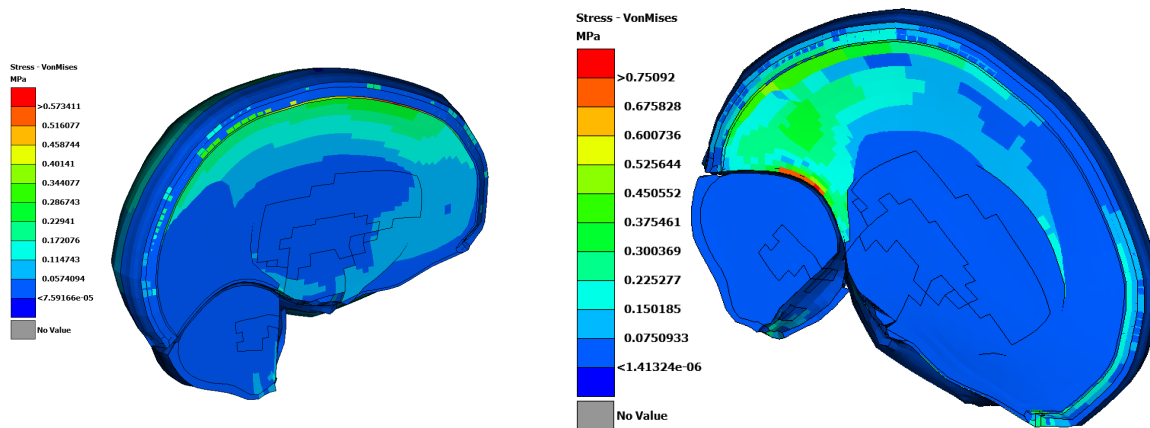


Figure 93 – In the left, Brain First Principal Strain and in the right Brain VonMises Stress for the Frontal Impact

Source: Author

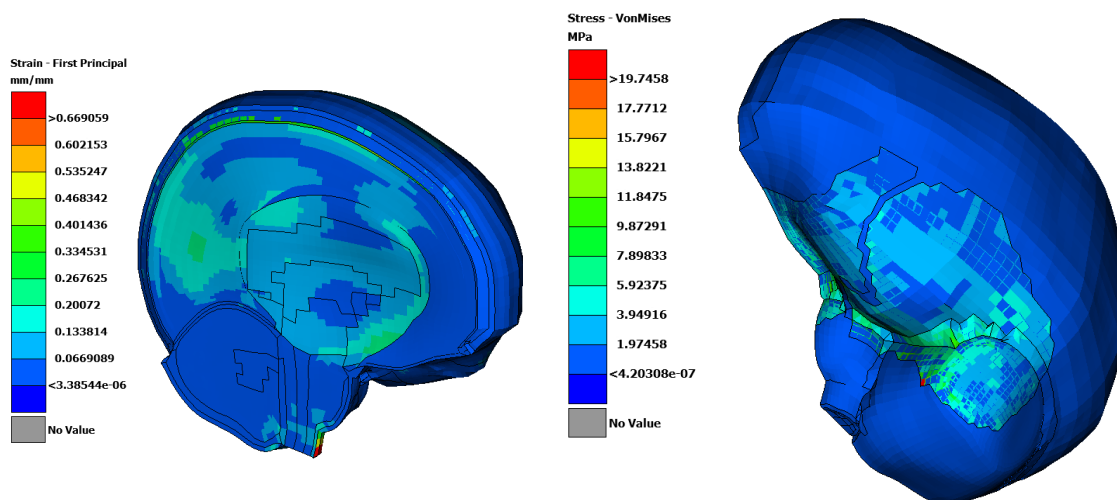


Figure 94 – In the left, Brain First Principal Strain and in the right Brain VonMises Stress for the Side Impact

Source: Author

It can be found that the first principal strain over 31% can lead to moderate and over 40% to severe damage to the brain. For the VonMises stress criterion, the same rule applies: up to 26KPa moderate damage and over 33KPa severe damage.

Looking at the results for both the frontal impact and the side impact, there is one location that significantly exceeds these limits, but since it is a very concentrated region, it could be a numerical singularity problem. However, there is a large region of the

brain that has a high probability of severe damage under both criteria in both accident simulations.

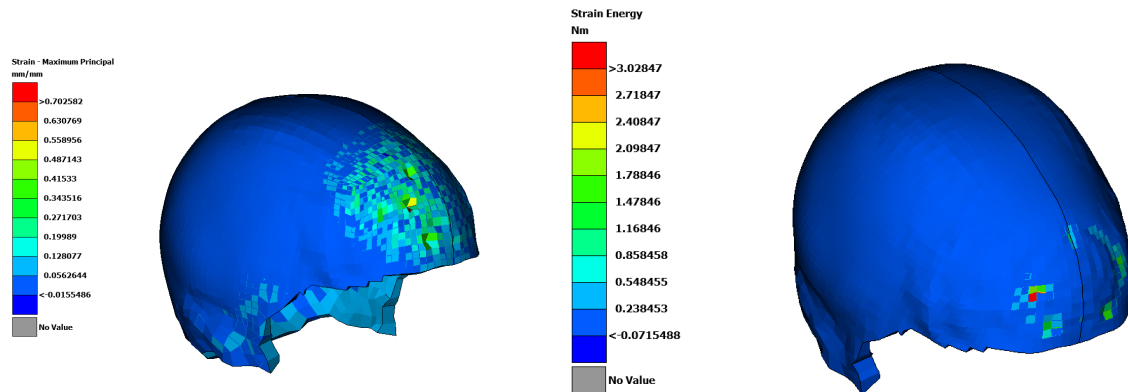


Figura 95 – In the left, Skull Maximum Principal Strain and in the right Skull strain energy for the Frontal Impact

Source: Author

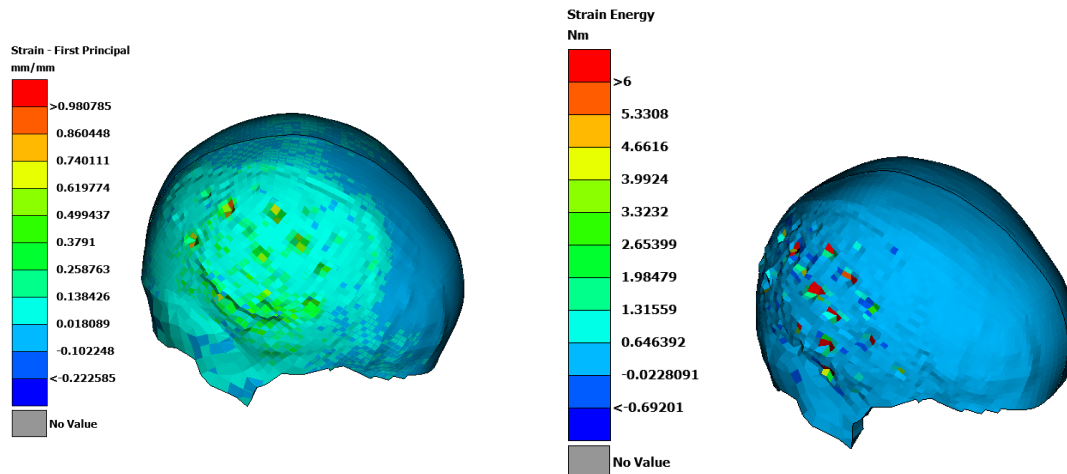


Figura 96 – In the left, Skull Maximum Principal Strain and in the right Skull strain energy for the Side Impact

Source: Author

It is important to note that even if the criteria for head acceleration are met, the skull is well above the limits given by Geovane. One possible reason for this could be related to two aspects of the simulation rather than the actual physical conditions. The first is the use of mass scaling, which causes some nodes to protrude from the model due to the concentrated increase in mass. The second is the hourglass effect, where we have a

large displacement of nodes subjected to a relatively small force.

6.2.2.1 Internal Organs

Concerning internal organs, (GERMANETTI F.; FIUMARELLA, 2022) also summarizes the criterion of several studies. This summary can be seen in the figure 97

	Damage	Metric	Threshold	Reference
Lungs	Pulmonary Contusion (PC)	Maximum Principal Strain (MPS)	34.3%	Gaewsky et al. [74]
			35%	Han et al. [72]
		Nominal strain	15%	Arun et al. [76]
Heart	Contusion	Maximum strain	30%	Shigeta et al. [4]
		Ultimate Tensile Strain (UTS)	30%	
	Damage to myocardial tissue	Ultimate Tensile Strain (UTS)	63%	Han et al. [72]
Spleen	Contusion	Nominal strain	30%	
Kidney	Contusion	Nominal strain	30%	Arun et al. [76]
		Nominal strain	30%	
Liver	Contusion	Maximum Compressive Stress (MCS)	0.127-0.192 MPa	Han et al. [72]
Stomach	Contusion	Maximum strain	1.2%	
Small and Large Intestine	Contusion	Maximum strain	1.2%	Shigeta et al. [4]

Figura 97 – Summary of proposed injuries criteria for internal organs

Source: (GERMANETTI F.; FIUMARELLA, 2022)

From the lung and heart results, profiles were extracted for both frontal and side impact. These results can be seen in figures 98 and 99 As in the case of the brain, the result

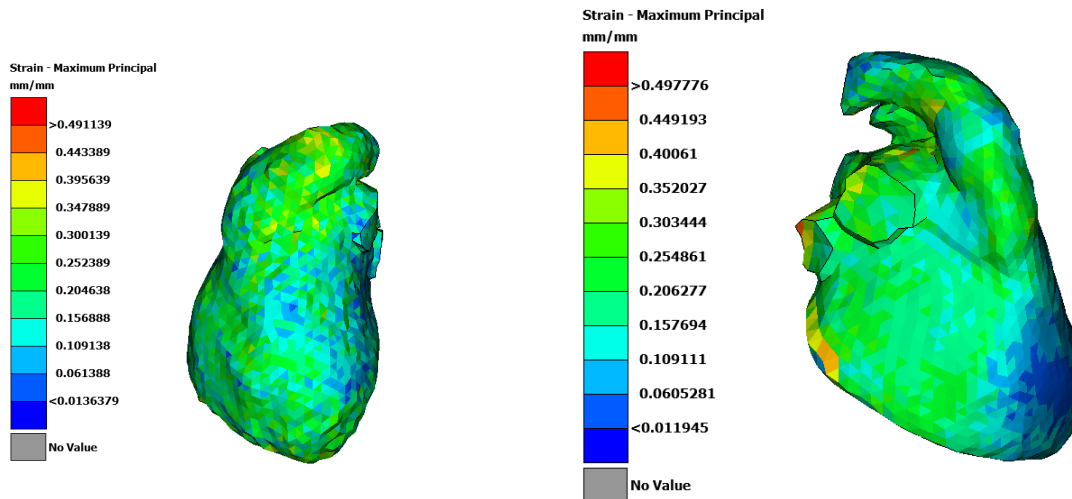


Figura 98 – In the left, Heart Maximum Principal Strain for Frontal Impact and in the right Heart Maximum Principal Strain for the Side Impact

Source: Author

for the heart shows a high strain point, well above the threshold, but very concentrated. Nevertheless, we see a large area of strain greater than 30%, indicating a high risk of

contusion.

The possibility of lung injury is greater in the area under the seat belt, especially in

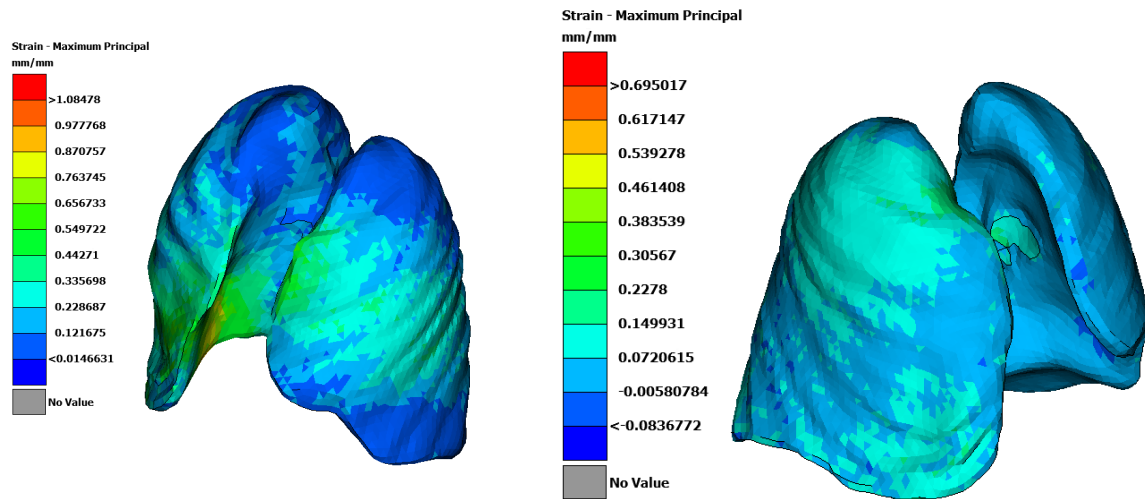


Figura 99 – In the left, Lung Maximum Principal Strain for Frontal Impact and in the right Lung Maximum Principal Strain for the Side Impact

Source: Author

frontal collisions. The maximum principal strain is up to 0.76

6.2.2.2 Thorax

For a summary of the injury criteria that can be used for the thoracic skeleton and organs, see 100 ((GERMANETTI F.; FIUMARELLA, 2022)).

As in the previous case, some criteria were selected and the results were extracted for both frontal and side impact.

The risk of fracture was evaluated according to the criteria of first principal strain and VonMises stress (Figures 101 and 102).

In a frontal impact, the VonMises stresses and the first principal strain found are quite low, even if the ribs have a high deformation that compresses the lung. The main focus is on the cervical spine, where a high stress level is found - about 135 MPa according to the VonMises criteria.

As for the side impact, the first principal strain is low overall, but the VonMises stress in the rib area is close to the fracture limit - 119MPa.

	Damage	Metric	Threshold	Reference	
Thorax	Chest deflection	Change in length (11 locations)	-	Bostrom et al. [65]	
	Thoracic deformation	Chest bands (at 4th, 6th, and 8th rib)	-	Hayes et al. [66]	
	Contusion	Ultimate Plastic Strain (UPS)	3%–0.8%	Poulard et al. [69]	
		Viscous Criterion (VC) max	-	Miller et al. [70]	
	Rib fracture	First Principal Strain	0–25% 25–50% 50–75% >75%	Injury risk groups	Xiao et al. [71]
		Local strain > UTS (rib cortical bone)	Several adjacent elements > threshold		Foreman et al. [64]
		Von Mises stress (stress limit before fracture)	130 MPa		Kemper et al. [73]
		Cortical bone plastic failure strain	0.89%		Golman et al. [68]
		Trabecular bone ultimate failure strain	13%		

Figura 100 – Summary of proposed injuries criteria for thorax

Source: (GERMANETTI F.; FIUMARELLA, 2022)

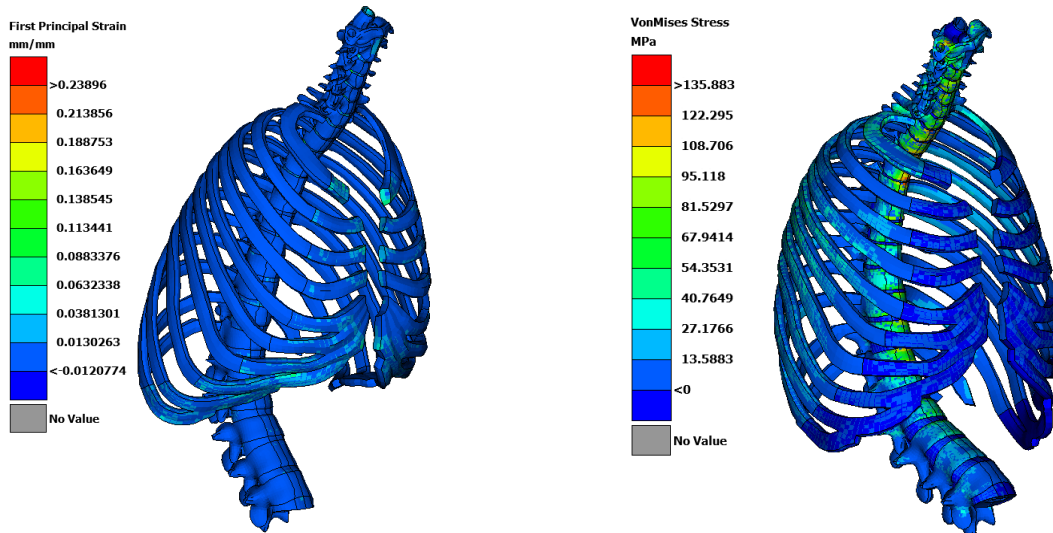


Figura 101 – In the left, Thorax First Principal Strain, and in the right Thorax VonMises stress for the Front Impact

Source: Author

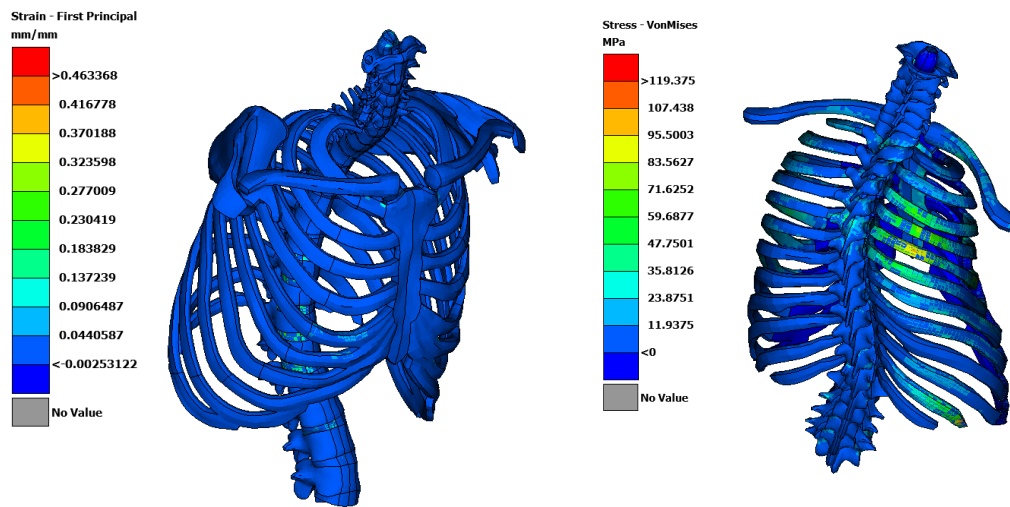


Figura 102 – In the left, Thorax First Principal Strain, and in the right Thorax VonMises stress for the Side Impact

Source: Author

6.3 Model complexity

The model developed for this analysis consists of 2,585 components (including beams, shells, and solids) and more than 2 million elements. This level of complexity makes debugging the analysis difficult, and each loop takes time to run. using THUMS alone, 94 simulations were run, each taking between 20 and 30 hours to complete.

Under these conditions, the use of models with this level of complexity is not justified in all cases.

On the other hand, because the human model is complete, the response of various organs or body parts can be accurately assessed, which can shed light on an area that would likely be neglected in simpler models.

Therefore, the choice of the human model used must be considered as a design criterion.

7 CONCLUSION AND FUTURE WORK

In this dissertation, DFSS design methods were applied with some PRODIP and IP2P tools to develop a tricycle for urban use.

The result was a flexible, manufacturable vehicle that is easy to assemble and provides enhanced safety compared to conventional motorcycles and tricycles. Although significant progress has been made, there is still a certain way to go towards the ultimate goal of achieving zero traffic fatalities.

Defining a framework is important not only because it ensures the achievement of the final result, but also because it minimizes the number of detours in the project phases.

In complex projects, such as the development of a tricycle, it is common to use a group of software to perform CAE or CAM simulations, as well as for the modeling of different areas, such as complex surfaces or the validation of kinematics. Because of this feature, it is important to create a pattern to transfer the attributes from one software to another. In this project a color pattern was used.

Both the design requirements - versatile, innovative and user-friendly, as well the safety requirements were met. However, the manufacturing cost of the solution is not necessarily low, as additive manufacturing was considered and the investment is higher compared to traditional welding/machining processes.

In the validation phase, impact simulations were performed according to FMVSS 581, which specifies parameters for low-speed impact. The THUMS model was used in the tricycle as the rider, and the head acceleration and neck force were determined.

Since the THUMS is a very detailed human model, other criteria can be studied, as mentioned in the discussion chapter, like the based on energy, strain or stress. Some authors have been studied it, and some of their methods applied.

For future work, the evaluation of the criteria could be further explored in relation to the area of the model in which they are applied. As mentioned in the discussion chapter, some authors suggest the application of VonMises stress for the evaluation of bones, such

as the ribs. Since the ribs behave like a brittle material, there is probably a different stress criterion to evaluate them, since the VonMises criterion is generally used for ductile materials.

The effects of hourglass and mass scaling on energy and strain based results could also be analyzed. It was possible to identify non-physical deformations in areas of interest, such as the brain and skull, and in these areas the results were divergent compared to traditional methods, such as head acceleration. This does not mean that the application of mechanical criteria should not be performed, but the consistency of the analysis for their application needs to be verified.

Due to the complexity and size of the model, the impact analysis was performed using a simplified structure of the tricycle. For future work, the full model of the tricycle with the polymer structure should be used instead of the reduced model.

It is also possible to modify the lower structure and implement a bumper on the tricycle. This should improve energy dissipation in the event of a collision.

A rear impact, with a passenger and against other vehicles could also be considered to confirm that the vehicle is safe for daily use.

REFERÊNCIAS

- AKAO, Y. Development history of quality function deployment. **The Customer Driven Approach to Quality Planning and Deployment**, Asian Productivity Organization Minato, Japan, v. 339, p. 90, 1994.
- ALTSHULLER, G. S. **Creativity as an exact science: the theory of the solution of inventive problems**. [S.l.]: Gordon and Breach Science Publishers, 1984.
- ANDERL, R. et al. Digital twin technology—an approach for industrie 4.0 vertical and horizontal lifecycle integration. **it-Information Technology**, De Gruyter Oldenbourg, v. 60, n. 3, p. 125–132, 2018.
- BACK, N. et al. Projeto integrado de produtos: planejamento, concepção e modelagem. Barueri: Manole, 2008.
- BLUNDELL, M.; HARTY, D. **Multibody systems approach to vehicle dynamics**. [S.l.]: Elsevier, 2004.
- BOOTHROYD, G.; DEWHURST, P.; KNIGHT, W. A. **Product design for manufacture and assembly**. [S.l.]: CRC press, 2010.
- BRACE, W.; CHEUTET, V. A framework to support requirements analysis in engineering design. **Journal of Engineering Design**, Taylor & Francis, v. 23, n. 12, p. 876–904, 2012.
- BRACKETT, D.; ASHCROFT, I.; HAGUE, R. Topology optimization for additive manufacturing. In: **Proceedings of the solid freeform fabrication symposium, Austin, TX**. [S.l.: s.n.], 2011. v. 1, p. 348–362.
- BRAHA D. MAIMON, O. A mathematical theory of design: Foundations, algorithms, and applications. 1998.
- BUDDAY, S. et al. Viscoelastic parameter identification of human brain tissue. **Journal of the Mechanical Behavior of Biomedical Materials**, Elsevier Ltd, v. 74, p. 463–476, 2017. ISSN 18780180. Disponível em: <<http://dx.doi.org/10.1016/j.jmbbm.2017.07.014>>.
- CLAUDE, U.; LYON, B.; PROJETS, L. I. PIPER Software Framework and Application : User guide. 2017.
- COCCO, G. **Motorcycle design and technology: how and why**. [S.l.]: Giorgio Nada Vimodrone, Italy, 2013.
- COSSALTER, V. **Motorcycle dynamics**. [S.l.]: Lulu. com, 2006.
- COSSALTER, V. et al. Motorcycle steering torque decomposition. In: **Proceedings of the World Congress on Engineering**. [S.l.: s.n.], 2010. v. 2.
- COSSALTER, V.; LOT, R.; PERETTO, M. Steady turning of motorcycles. **Proceedings of the Institution of Mechanical Engineers, Part D: Journal of Automobile Engineering**, Sage Publications Sage UK: London, England, v. 221, n. 11, p. 1343–1356, 2007.

CROSS, N. **Engineering design methods: strategies for product design**. [S.l.]: John Wiley & Sons, 2021.

DOE, J. **Electric Motor and Battery Design for Electric Vehicles**. [S.l.]: Electric Vehicle Publishers, 2020. ISBN 1234567890123.

DOMB, E. Qfd and tips/triz. **The TRIZ Journal**, 1998.

DONG, O. et al. The bricycle: a bicycle in zero gravity can be balanced or steered but not both. **Vehicle system dynamics**, Taylor & Francis, v. 52, n. 12, p. 1681–1694, 2014.

DORIA, A.; TOGNAZZO, M. The influence of the dynamic response of the rider's body on the open-loop stability of a bicycle. **Proceedings of the Institution of Mechanical Engineers, Part C: Journal of Mechanical Engineering Science**, SAGE Publications Sage UK: London, England, v. 228, n. 17, p. 3116–3132, 2014.

EASTMAN, C. M. **Design for X: concurrent engineering imperatives**. [S.l.]: Springer Science & Business Media, 2012.

EVANGELOU, S. **Control and stability analysis of two-wheeled road vehicles**. 2004. Tese (Doutorado) — University of London London, 2004.

FAJANS, J. Steering in bicycles and motorcycles. **American Journal of Physics**, American Association of Physics Teachers, v. 68, n. 7, p. 654–659, 2000.

FICE, J. B.; CRONIN, D. S.; PANZER, M. B. Cervical spine model to predict capsular ligament response in rear impact. **Annals of Biomedical Engineering**, v. 39, n. 8, p. 2152–2162, 2011. ISSN 00906964.

FILIPOZZI, L. et al. Estimation of tire normal forces including suspension dynamics. **Energies**, Multidisciplinary Digital Publishing Institute, v. 14, n. 9, p. 2378, 2021.

FOALE, T. **Motorcycle handling and chassis design: the art and science**. [S.l.]: Tony Foale, 2006.

FRIZZIERO, L.; LIVERANI, A.; NANNINI, L. Design for six sigma (dfss) applied to a new eco-motorbike. **Machines**, v. 7, n. 3, 2019. ISSN 2075-1702. Disponível em: <https://www.mdpi.com/2075-1702/7/3/52>.

GEBISA, A. W.; LEMU, H. G. A case study on topology optimized design for additive manufacturing. In: IOP PUBLISHING. **IOP conference series: materials science and engineering**. [S.l.], 2017. v. 276, n. 1, p. 012026.

GERMANETTI F.; FIUMARELLA, D. B. G. S. A. Injury Criteria for Vehicle Safety Assessment: A Review with a Focus Using Human Body Models. **Vehicles**. 2022.

HATCHUEL A. WEIL, B. A new approach of innovative design: an introduction to c-k theory. **Proceedings of the international conference on engineering design (ICED'03)**, Stockholm, Sweden,, p. 109–124, 2003.

HATCHUEL A., L. M. P. . W. B. Studying creative design: the contribution of c-k theory. **Studying design creativity: Design Science, Computer Science, Cognitive Science and Neuroscience Approaches**, Aix-en-Provence, France, p. 109–124, 2003.

- HAUSER JOHN R.; CLAUSING, D. The house of quality. 2016.
- HUNT, E. C.; SPROAT, S. B.; KITZMILLER, R. R. Product customization. In: **The Nursing Informatics Implementation Guide**. [S.l.]: Springer, 2004. p. 146–169.
- ION, B.; LOW, B. **Pughs Total Design: Integrated Methods for Successful Product Design**. [S.l.]: Addison Wesley Publishing Company, 1998.
- JONGEN, H. T.; JONKER, P.; TWILT, F. **Nonlinear optimization in finite dimensions: Morse theory, Chebyshev approximation, transversality, flows, parametric aspects**. [S.l.]: Springer Science & Business Media, 2013. v. 47.
- KALOGIROU, S. A. **Solar Energy Engineering: Processes and Systems**. [S.l.]: Academic Press, 2014.
- LEE, T.-C.; POLAK, J. W.; BELL, M. G. **BikeSim user manual version 1.0**. [S.l.], 2008.
- LI, Z. et al. Rib fractures under anterior-posterior dynamic loads: Experimental and finite-element study. **Journal of Biomechanics**, Elsevier, v. 43, n. 2, p. 228–234, 2010. ISSN 00219290. Disponível em: <<http://dx.doi.org/10.1016/j.jbiomech.2009.08.040>>.
- LIEH, J. Closed-form method to evaluate bike braking performance. **Human Power eJournal**, v. 19, n. 7, 2013.
- LIN, C.-S.; SU, C.-T. An innovative way to create new services: Applying the triz methodology. **Journal of the Chinese Institute of Industrial Engineers**, Taylor & Francis, v. 24, n. 2, p. 142–152, 2007.
- LOWNE, R. et al. Dedicated child attachment system (isofix). **Traffic Injury Prevention**, Taylor & Francis, v. 3, n. 1, p. 19–29, 2002.
- MAGRAB EDUARD B., G. S. K. M. F. P. . S. P. A. Integrated product and process design and development: The product realization process. 2008.
- MANN, D. **Matrix 2010: Re-updating the TRIZ contradiction matrix**. [S.l.]: Ifr Press Bidefor, UK, 2009.
- MEIJAARD, J. et al. Linearized dynamics equations for the balance and steer of a bicycle: a benchmark and review. **Russian Journal of Nonlinear Dynamics**, Steklov Mathematical Institute of Russian Academy of Sciences, v. 9, n. 2, p. 343–376, 2013.
- MICHELOTTI, A. C. et al. Inovação em sistemas de partida automotivos: interface com acoplamento permanente. 2016.
- NO, R. 129 of the economic commission for europe of the united nations (un/ece)—uniform provisions concerning the approval of enhanced child restraint systems used on board of motor vehicles (ecrs). **European Commission**, 2014.
- PORTER, S. C.; VERSEPUT, R. P.; CUNNINGHAM, C. R. Process optimization using design of experiments. **Pharmaceutical technology**, [Springfield, Or.: sn, 1977]-2000., v. 21, n. 10, p. 60–71, 1997.
- PROCHAZKA, M. et al. A component-oriented framework for spacecraft on-board software. In: CITESEER. **Proceedings of DASIA**. [S.l.], 2008.

PRZYBILLA1 LEONARD., S. M. K. K. P. C. W. M. . K. H. Combining design thinking and agile development to master highly innovative it projects. 2016.

RAMÓN-RAYGOZA, E.; GUERRA-ZUBIAGA, D. A.; TOMOVIC, M. Methodology to support a collaborative dxf process with integration of pdm and expert system tools. In: TRANS TECH PUBL. **Advanced Materials Research**. [S.l.], 2008. v. 44, p. 381–388.

RANKY, P.; CHAMYVELUMANI, S. A method, a tool (cora) and application examples for analysing disassembly user interface design criteria. **International Journal of Computer Integrated Manufacturing**, Taylor & Francis, v. 16, n. 4-5, p. 317–325, 2003.

RANKY, P. G. et al. **ADAM: R&D Article**. [S.l.]: ADAM. Web, 2012.

RESIN, P. R. S. et al. Desenvolvimento do prototipo de uma maquina desoperculadora de favos de mel. 1989.

SANDINO, D.; MATEY, L. M.; VÉLEZ, G. Design thinking methodology for the design of interactive real-time applications. In: SPRINGER. **International conference of design, user experience, and usability**. [S.l.], 2013. p. 583–592.

SHARP, R. S. The stability and control of motorcycles. **Journal of mechanical engineering science**, SAGE Publications Sage UK: London, England, v. 13, n. 5, p. 316–329, 1971.

SOHN, M. S. **Topics in structural topology optimization**. [S.l.]: University of Illinois at Urbana-Champaign, 2009.

ULLMAN, D. G. **The mechanical design process**. [S.l.]: McGraw-Hill New York, 1992. v. 2.

UNECE. 1958 Agreement - Transport - UNECE. 1958.

WILSON, D. G.; SCHMIDT, T. **Bicycling science**. [S.l.]: MIT press, 2020.

WINDHEIM, M. **Cooperative decision-making in modular product family design**. [S.l.]: Springer, 2020.

XIA, L. et al. Stress-based topology optimization using bi-directional evolutionary structural optimization method. **Computer Methods in Applied Mechanics and Engineering**, Elsevier, v. 333, p. 356–370, 2018.

YUE, N.; SHIN, J.; UNTAROIU, C. D. Development and validation of an occupant lower limb finite element model. **SAE 2011 World Congress and Exhibition**, 2011. ISSN 2688-3627.

ZAWADZKI, P.; ŻYWICKI, K. Smart product design and production control for effective mass customization in the industry 4.0 concept. **Management and production engineering review**, Production Engineering Committee of the Polish Academy of Sciences, Polish . . . , 2016.

ZINN, L. **Zinn's Cycling Primer: Maintenance Tips & Skill Building for Cyclists**. [S.l.]: Velopress, 2004.

ANEXO A – MOTORCYCLE'S CHARACTERISTICS

Although motorcycles consist of complex kinetic systems, we can divide them into four broad groups (COSSALTER, 2006):

- Rear assembly (frame, saddle, tank and motor);
- Front assembly (the fork, the steering head and the handlebar);
- Front wheel;
- Rear wheel;

These rigid bodies are connected by three pivot joints (the steering axle and the two wheel axles) and have ground contact at two wheel/ground contact points.

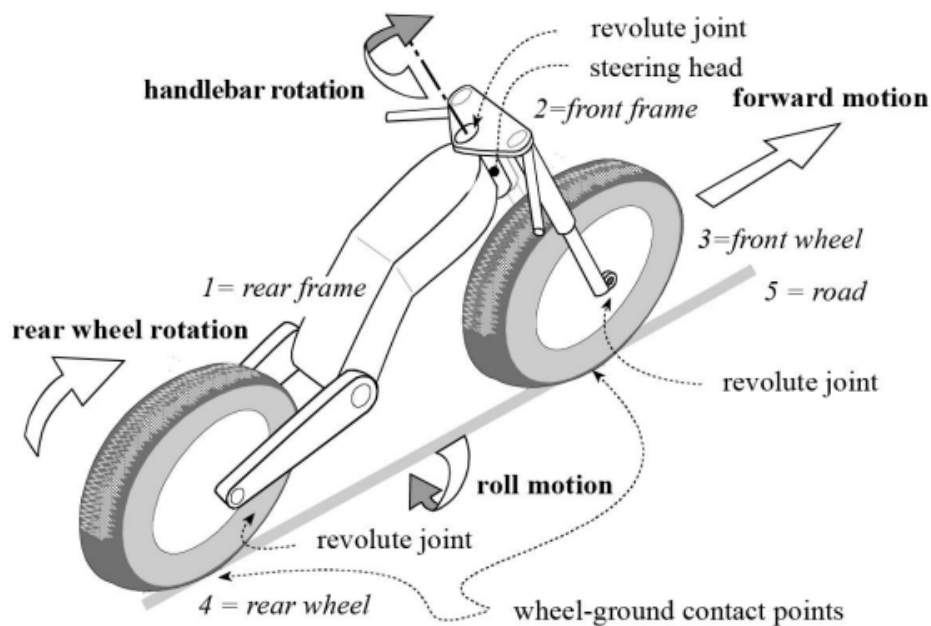


Figura 103 – Kinematic structure of a motorcycle (COSSALTER, 2006)

The main parameters for a motorcycle rigid body are shown in the Figure 104 (COSSALTER, 2006):

- p wheelbase;
- d fork offset: perpendicular distance between the axis of the steering head and the center of the front wheel;

- ϵ caster angle;
- R_r radius of the rear wheel;
- R_f radius of the front wheel;
- t_r radius of the cross section of the rear tire;
- t_f radius of the front tire cross section.

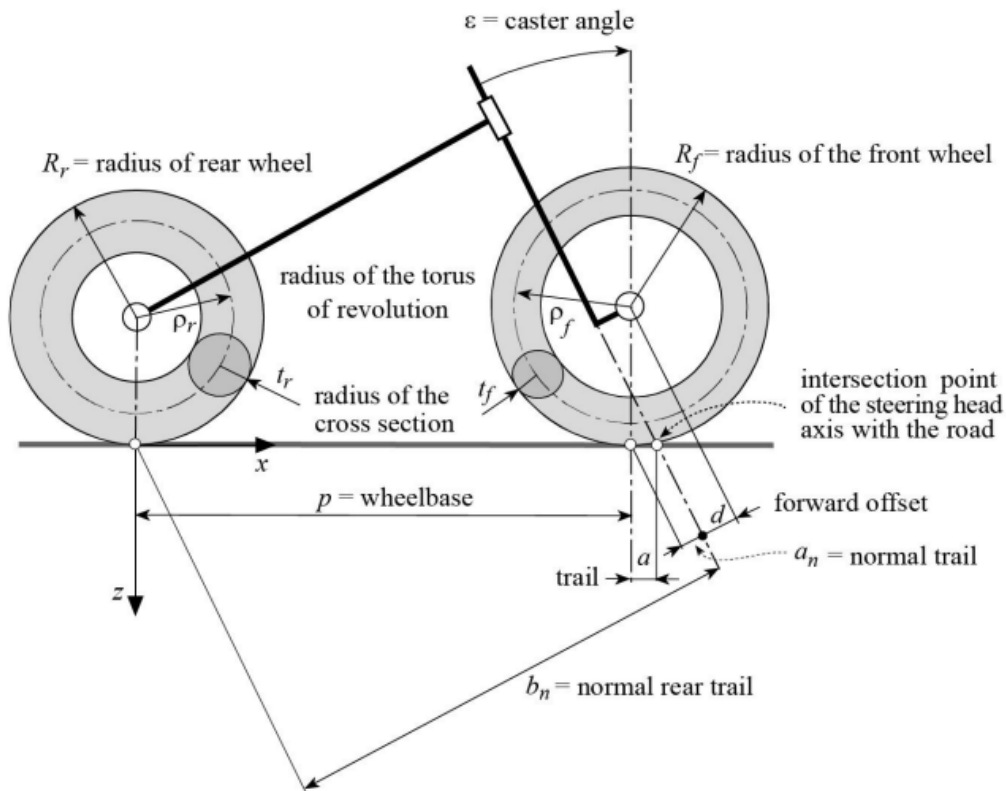


Figura 104 – Geometry of a motorcycle

Source: Cossalter 2014

Some important geometric parameters can be expressed in terms of these variables:

- $r = (R_r - t_r)$ radius of the front torus center circle;
- $f = (R_f - t_f)$ radius of the rear torus center circle;
- $a_n = R_f \sin \epsilon - d$;
- $a = \frac{a_n}{\cos \epsilon} = R_f \tan \epsilon - \frac{d}{\cos \epsilon}$.

The geometric parameters used to describe motorcycles are as follows:

- the wheelbase p ;
- the caster angle ϵ ;
- the normal trail a .
- the real trail d

These parameters are measured when the motorcycle is in a vertical position and the steering angle of the handlebar is set to zero.

A.0.1 Trail

Trail is the distance by which the ground contact point of the front wheel lags behind the ground contact point of the steering axle.

The steering axle is the axis about which the entire steering mechanism (fork, handlebars, front wheel, etc.) pivots. In traditional bike / trike designs with the steering axle tilted rearward from vertical, positive trails tends to steer the front wheel in the direction of a lean, regardless of the speed of travel.([WILSON; SCHMIDT, 2020](#)).

Trail is a function of steering head angle, fork offset or rake, and wheel size. Their relationship can be described by this formula:

$$Trail = \frac{(R_w \cos(A_h) - O_f)}{\sin(A_h)}$$

$$Trail = \frac{(R_w \cos(A_h) - O_f)}{\sin(A_h)}$$

where:

- R_w is the radius of the wheel;
- A_h is the head angle measured clockwise from horizontal;
- O_f is the fork offset or rake.

The more trail a conventional motorcycle has, the more stable it feels, although too much trail can make the motorcycle difficult to steer. Motorcycles with negative trail are reported to feel very unstable([ZINN, 2004](#)).

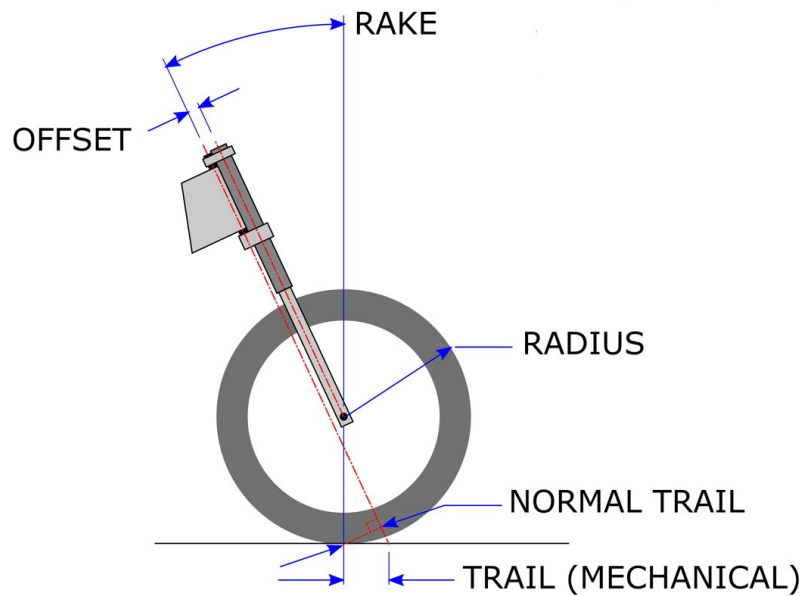


Figura 105 – Dimension of the trail for the electric motorcycle

Source: (COSSALTER, 2006)

A.0.2 Turning

To turn a bicycle, i.e., change the direction of travel, the front wheel must point approximately in the desired direction, as with any front-steered vehicle. The friction between the wheels and the ground then generates the centripetal acceleration necessary to change course from straight ahead, as a combination of cornering force and camber thrust. The turning radius of an upright (not lean) bike can be roughly estimated for small steering angles by (COSSALTER, 2006):

$$r = \frac{w}{\delta \cos(\phi)}$$

where r is the approximate radius, w is the wheelbase, δ is the steering angle, and ϕ is the caster angle of the steering axis.

A.0.3 Leaning

Motorcycles (and bicycles) must also lean during a turn to balance the relevant forces: gravity, inertia, friction, and grip. The angle of inclination, θ , is easily calculated using the laws of circular motion (FAJANS, 2000):

$$\theta = \arctan(v^2/gr)$$

where:

v is the forward velocity

r is the radius of rotation

g is the acceleration due to gravity

This is the idealized case. For motorcycles, a slight increase in lean angle may be required to compensate for the width of the tires at the same forward speed and radius of turn

This lean angle of the motorcycle reduces the actual cornering radius in proportion to the cosine of the lean angle. The resulting radius can be roughly approximated (within 2% of the exact value) by:

$$r = \frac{w \cos(\theta)}{\delta \cos(\phi)}$$

where:

r is the approximate radius

w is the wheelbase

θ is the lean angle

δ is the steering angle

ϕ is the caster angle of the steering axle.

When a bicycle is leaned, the contact patches of the tires shift further to the side and wear.

The limited width of the tires changes the actual lean angle of the rear frame from the ideal lean angle described above. The actual angle of lean between the frame and the vertical axis must increase with tire width and decrease with the height of the center of mass. Bikes with thick tires and low center of mass must lean more than bikes with thinner tires or higher center of mass for the same turn and speed.

The increase in lean angle due to a tire thickness of $2t$ can be calculated as follows:

$$\arcsin\left(t \frac{\sin(\phi)}{h - t}\right)$$

where:

ϕ is the ideal angle of inclination h is the height of the center of mass

It has been shown that the couple generated by gravity and ground reaction forces is necessary for a bicycle to turn. On a custom-built bicycle with suspension outriggers that

precisely cancel this coupling so that the bicycle and rider can assume any lean angle when riding in a straight line, it is impossible for the rider to make a turn. As soon as the wheels deviate from a straight path, the bike and rider begin to lean in the opposite direction, and the only way to correct them is to steer back onto the straight path(DONG et al., 2014).

A.0.4 Countersteering

To initiate a turn and the necessary lean in the direction of the turn, a bicycle must momentarily steer in the opposite direction. This is often referred to as countersteering. Since the front wheel is now at a finite angle to the direction of travel, a lateral force is generated on the tire's contact patch. This force creates a torque around the longitudinal axis (roll axis) of the motorcycle, and this torque causes the motorcycle to lean away from the original steered direction and toward the direction of the desired turn. If there is no external influence, such as a favorable crosswind, that generates the force necessary to tilt the motorcycle, countersteering is necessary to initiate a fast turn(COSSALTER; LOT; PERETTO, 2007).

While the initial steering torque and steering angle are both opposite to the desired direction of the turn, this does not necessarily have to be the case to maintain a smooth turn. The sustained steering angle is usually in the same direction as the curve, but can remain opposite to the direction of the curve, especially at high speeds. The sustained steering torque required to maintain this steering angle is usually opposite to the direction of the curve. The actual magnitude and orientation of both the sustained steering angle and the sustained steering torque of a given bicycle in a given turn will depend on the riding speed, bicycle geometry, tire characteristics, and the combined mass distribution of the bicycle and rider. When you are in a turn, the radius can only be changed by changing the lean angle accordingly. This can be achieved by additional countersteering out of the turn to increase lean angle and decrease radius. To exit the turn, the motorcycle must countersteer again, briefly steering more into the turn to decrease the radius, increasing inertial forces and thereby decreasing the lean angle .(COSSALTER et al., 2010).

A.0.5 Maneuverability

Motorcycle maneuverability and handling are difficult to quantify for several reasons. The geometry of a bicycle, particularly the angle of the steering axis, makes kinematic analysis complicated (MEIJAARD et al., 2013). Under many conditions, bicycles are inherently unstable and must always be under the control of the rider. Finally, the skill of the rider has a major impact on the performance of the bicycle in any maneuver. Bicycle design is

usually about a trade-off between maneuverability and stability(COSSALTER et al., 2010).

Although maneuverability is a difficult parameter to determine, it is generally agreed that the stiffer the structure of the motorcycle, the better it plays its role in this regard, since the entire mechanism tends to respond to calls to change trajectory(COSSALTER; LOT; PERETTO, 2007).

A.0.6 Acceleration

During acceleration, load transfer causes a decrease in the normal force on the front tire and an increase in the normal force on the rear tire (COSSALTER, 2006).

The dynamic load on the front tire (FILIPOZZI et al., 2021)(N_f) is given by:

$$N_f = mg\frac{b}{p} - S\frac{h}{p}$$

The dynamic load on the rear tire (N_r) is given by:

$$N_r = mg\frac{(p-b)}{p} + S\frac{h}{p}$$

The load transfer term in the above equations is the $S\frac{h}{p}$ term(COCCO, 2013)(FOALE, 2006). The driving force (S) multiplied by the ratio of the height to the center of gravity (h) to the wheelbase (p). Acceleration is limited by wheel spin or loss of rear wheel traction, which is a correlation ratio between the distance of the rear wheel contact patch and the height of the *CG*. If the traction coefficient (μ_p) is less than the ratio $\frac{h}{p}$, the acceleration phase is traction limited. If the traction coefficient (μ_p) is larger than the ratio $\frac{h}{p}$, the acceleration is wheel-limited.(COSSALTER, 2006)

Mathematically,

$$\text{if } \frac{b}{h} > \mu_p, a_{\text{traction limited}}$$

$$\text{if } \frac{b}{h} < \mu_p, a_{\text{wheeling limited}}$$

A.0.7 Braking

During braking, the signs of the load transfer term reverse because the \ddot{x} is negative. The dynamic equations become:

$$N_f = mg \frac{b}{p} + S \frac{h}{p}$$

$$N_r = mg \frac{(p-b)}{p} - S \frac{h}{p}$$

Braking is limited by overturning or when the rear wheel lifts off the ground ($N_r = 0$). The maximum deceleration (\ddot{x}) experienced by the best racer is 1.1 to 1.2 g's (LIEH, 2013). The nondimensional equations describe the values of deceleration or force ($m\ddot{x}$) for the entire motorcycle, front tire force (F_f) and rear tire force (F_r), respectively. (COSSALTER, 2006).

$$\frac{\ddot{x}}{g} = \frac{p\mu_r + b(\mu_f - \mu_r)}{p + h(\mu_r - \mu_f)}$$

$$\frac{F_f}{F} = \frac{\mu_f(b + h\mu_r)}{p\mu_r + b(\mu_f - \mu_r)}$$

$$\frac{F_r}{F} = \frac{\mu_f((p-b) - h\mu_f)}{p\mu_r + b(\mu_f - \mu_r)}$$

The deceleration and force equations depend on the geometric values (CG height, wheelbase, distance from CG to rear wheel) of the motorcycle and the coefficient of friction of the tires (μ_r, μ_f) (COSSALTER, 2006).

A.0.8 Tires

Tires affect bicycle dynamics in two different ways: finite crown radius and force generation (COSSALTER et al., 2010) (FOALE, 2006). It has been shown that increasing the crown radius of the front tire results in a reduction in size or elimination of inherent stability. Increasing the crown radius of the rear tire has the opposite effect (SHARP, 1971).

Tires generate the lateral forces necessary for steering and balance through a combination of cornering force and camber thrust. In this context, inflate pressure plays an important role (EVANGELOU, 2004).

A torque generated by a tire, called self-aligning torque, is caused by asymmetries in lateral slip along the length of the contact patch.

Another torque is generated by the limited width of the contact patch and the lean angle of the tire in a corner. The part of the contact patch that is outside the curve moves

rearward with respect to the wheel hub faster than the rest of the contact patch because it is a larger radius away from the hub.

The combination of these two opposing torques creates a yaw moment on the front wheel, the direction of which is a function of the tire's side slip angle, the angle between the tire's actual path and the direction it is pointing, and the tire's camber angle (the angle at which the tire leans from vertical)(WILSON; SCHMIDT, 2020).

A.0.9 Equation of motion

Blundell e Harty (2004) proposes the dynamic analysis of the bicycle based on the multibody approach, which means that the motorcycle is modeled considering rigid subsystems interacting with each other through joints.

The lean equation can be expressed by(MEIJAARD et al., 2013):

$$M_{\theta\theta}\ddot{\theta}_r + K_{\theta\theta}\theta_r + M_{\theta\psi}\ddot{\psi} + C_{\theta\psi}\dot{\psi} + K_{\theta\psi}\psi = M_\theta$$

$$M_{\theta\theta}\ddot{\theta}_r + K_{\theta\theta}\theta_r + M_{\theta\psi}\ddot{\psi} + C_{\theta\psi}\dot{\psi} + K_{\theta\psi}\psi = M_\theta$$

and the steer equation expressed by:

$$M_{\psi\psi}\ddot{\psi} + C_{\psi\psi}\dot{\psi} + K_{\psi\psi}\psi + M_{\psi\theta}\ddot{\theta}_r + C_{\psi\theta}\dot{\theta}_r + K_{\psi\theta}\theta_r = M_\psi$$

$$M_{\psi\psi}\ddot{\psi} + C_{\psi\psi}\dot{\psi} + K_{\psi\psi}\psi + M_{\psi\theta}\ddot{\theta}_r + C_{\psi\theta}\dot{\theta}_r + K_{\psi\theta}\theta_r = M_\psi$$

Where:

- θ_r is the lean angle of the rear assembly;
- ψ is the steer angle of the front assembly relative to the rear assembly;
- M_θ and M_ψ are the moments (torques) applied at the rear assembly and the steering axis, respectively. For the analysis of an uncontrolled bike, both are taken to be zero.

These can be represented in matrix form as:

$$M\ddot{\mathbf{q}} + C\dot{\mathbf{q}} + K\mathbf{q} = \mathbf{f}$$

Where,

- M is the symmetrical mass matrix which contains terms that include only the mass and geometry of the bike;

- C is the so-called damping matrix, even though an idealized bike has no dissipation, which contains terms that include the forward speed v (it is asymmetric);
- K is the so-called stiffness matrix which contains terms that include the gravitational constant;
- \mathbf{q} is a vector of lean angle and steer angle;
- \mathbf{f} is a vector of external forces, the moments mentioned above.

In this idealized and linearized model, there are many geometric parameters (wheel-base, head angle, mass of each body, wheel radius, etc.), but only four significant variables: Inclination angle, inclination rate, steering angle, and steering rate(DORIA; TOGNAZZO, 2014).

The equations show that the bicycle behaves like an inverted pendulum, with the lateral position of its support controlled by terms representing roll acceleration, roll velocity, and roll displacement as a function of steering torque(SHARP, 1971).

ANEXO B – MECHANICAL DRAWINGS

QTY	DESCRIPTION	UNIT	QTY	DESCRIPTION	UNIT
01	01	01	01	01	01
02	02	02	02	02	02
03	03	03	03	03	03
04	04	04	04	04	04
05	05	05	05	05	05
06	06	06	06	06	06
07	07	07	07	07	07
08	08	08	08	08	08
09	09	09	09	09	09
10	10	10	10	10	10
11	11	11	11	11	11
12	12	12	12	12	12
13	13	13	13	13	13
14	14	14	14	14	14
15	15	15	15	15	15
16	16	16	16	16	16
17	17	17	17	17	17
18	18	18	18	18	18
19	19	19	19	19	19

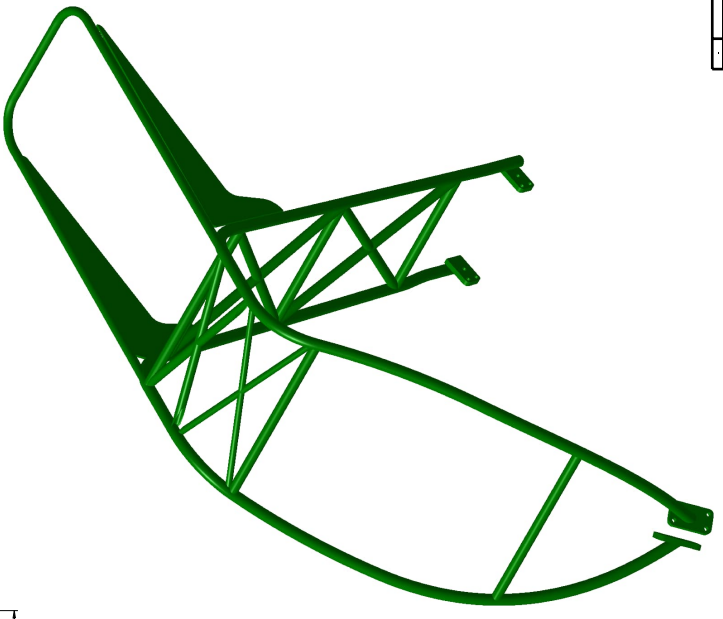
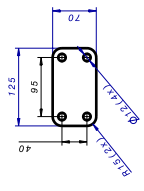
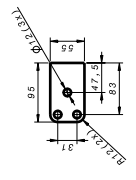
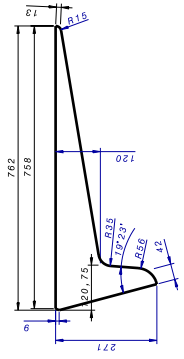
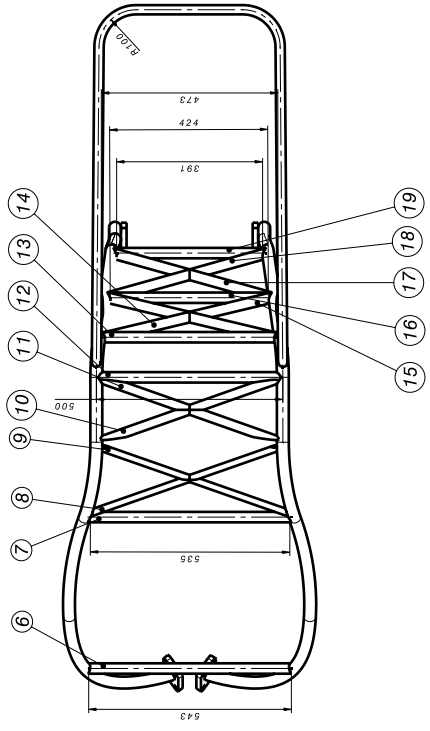
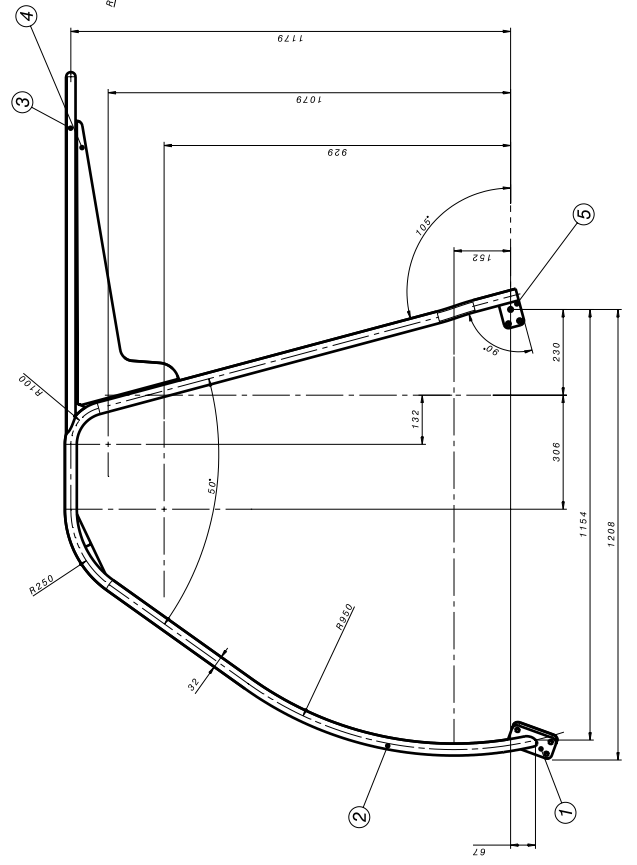
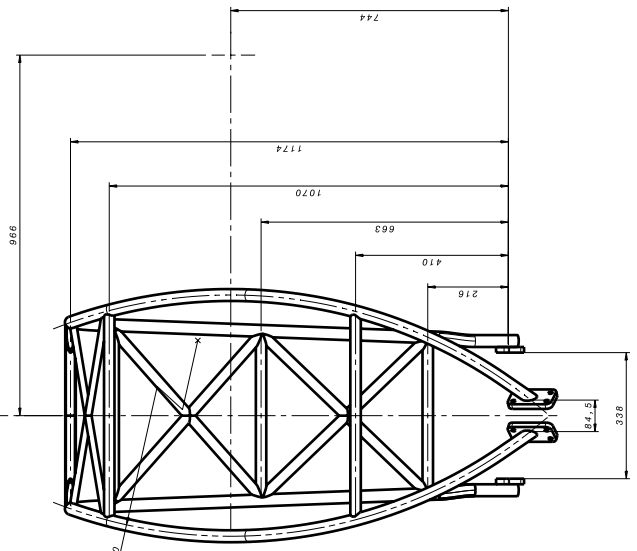
WSP

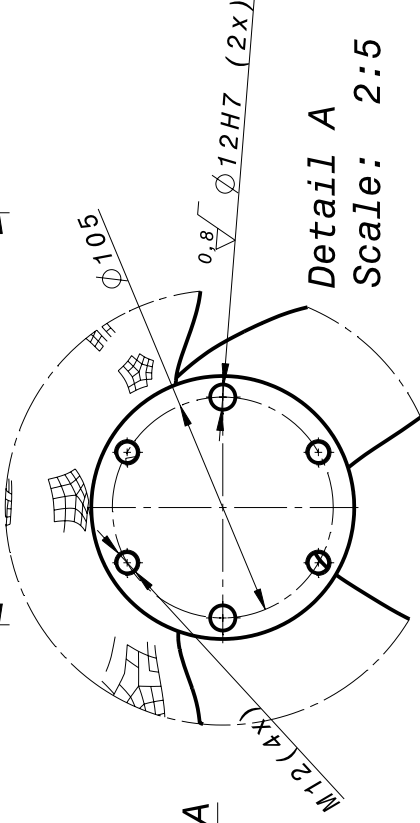
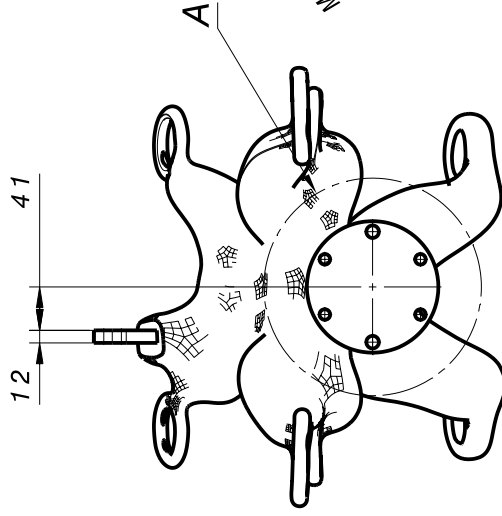
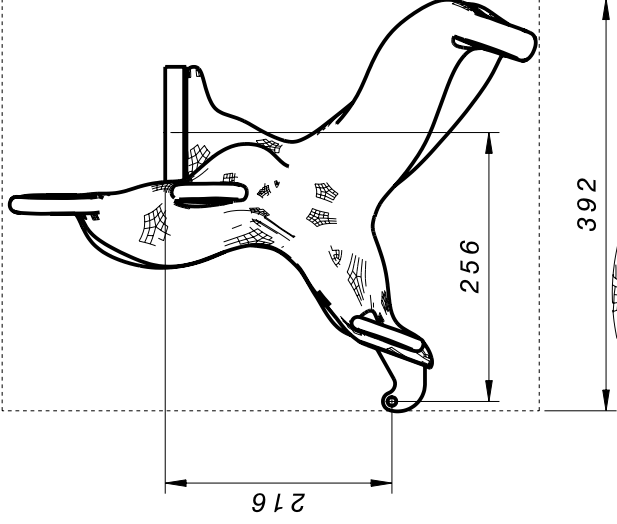
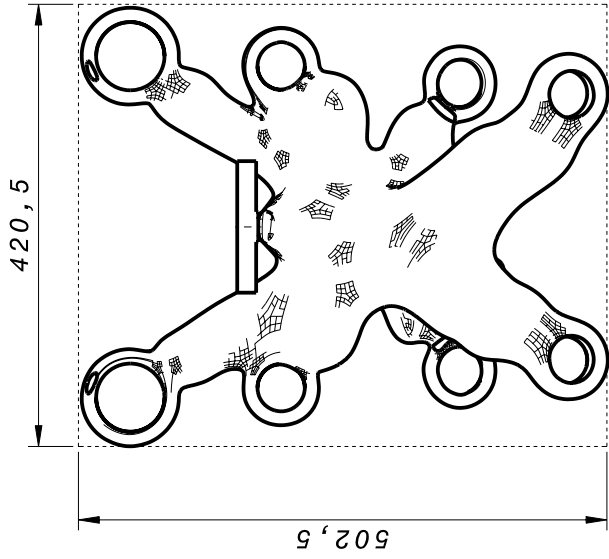
TRAIKE PROJECT
Upper Frame & Parts

DATE: 10/20/2011
TIME: 11:14:11
CLIENT: S&E 1000
PROJECT NO: 1000
DRAWING NO: 1000

SCALE: 1:1
SHEET: 1 OF 1

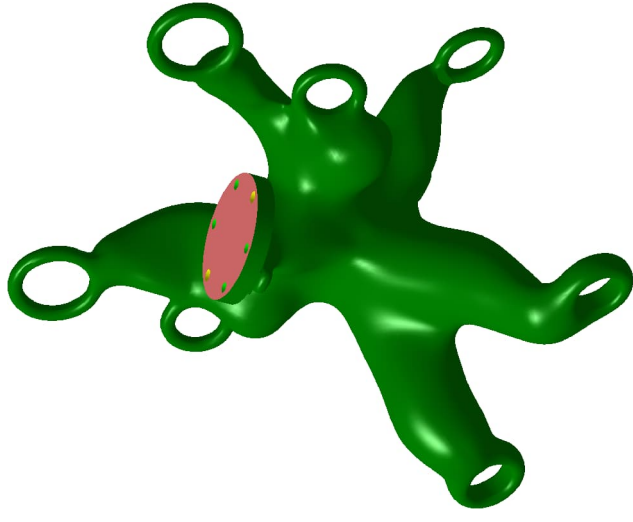
DESIGNER: [Signature]
CHECKER: [Signature]
APPROVER: [Signature]





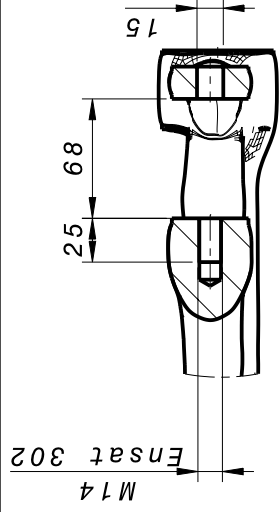
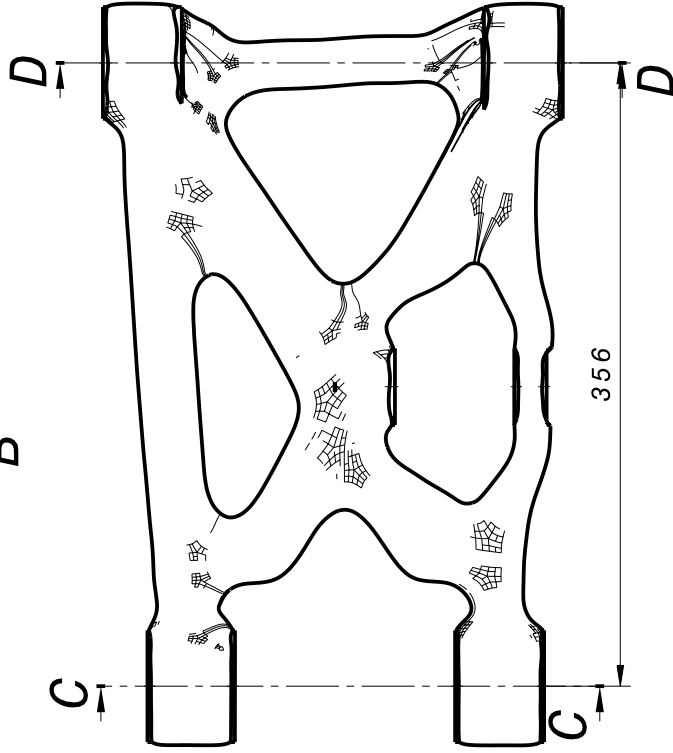
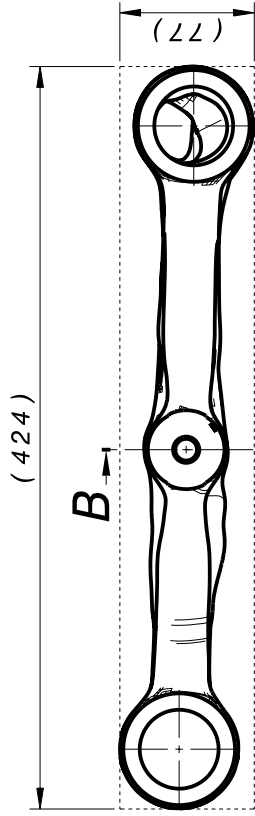
Detail A
Scale: 2:5

$3,2 \sqrt{0,8}$

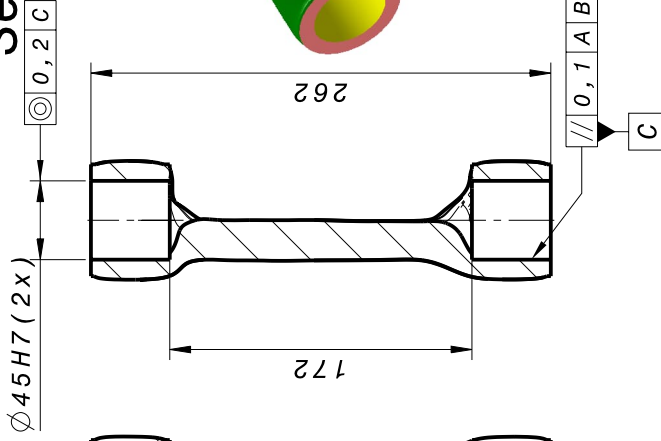


REV.	DESCRIPTION	Elaborate	Date
-	-	-	-
<p>Date: 2021/09/27 Title: TRIKE Project</p>			
<p>Design: PPROJETOS Suspension Frame</p>			
<p>Drawing: DDias</p>		<p>Material: SAE 8620</p>	<p>Sheet Nr: 1/1</p>
<p>Checker: DDias</p>		<p>Client: MAGNETTO</p>	<p>Escala: 2:1</p>
<p>Dimensions in Millimeters</p>		<p>MEASURES WITHOUT TOL. DIN 7168 - MEDIUM</p>	<p>Unit: --</p>
<p>ROUGHNESS</p>		<p>Position: 01</p>	<p>Drawing Nr. 3BBR2124075D5200_0201</p>
<p>All rights in this drawing belong to ABB LTDA. Designed by CAD system. Do not modify manually.</p>			

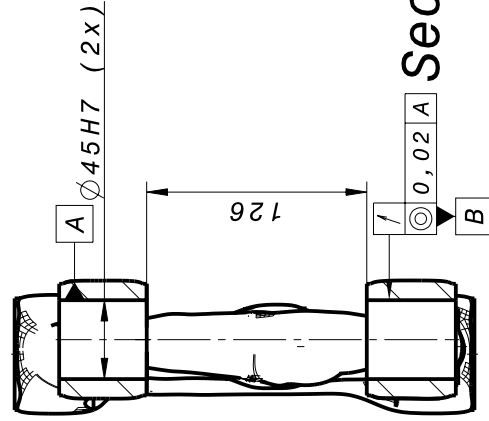




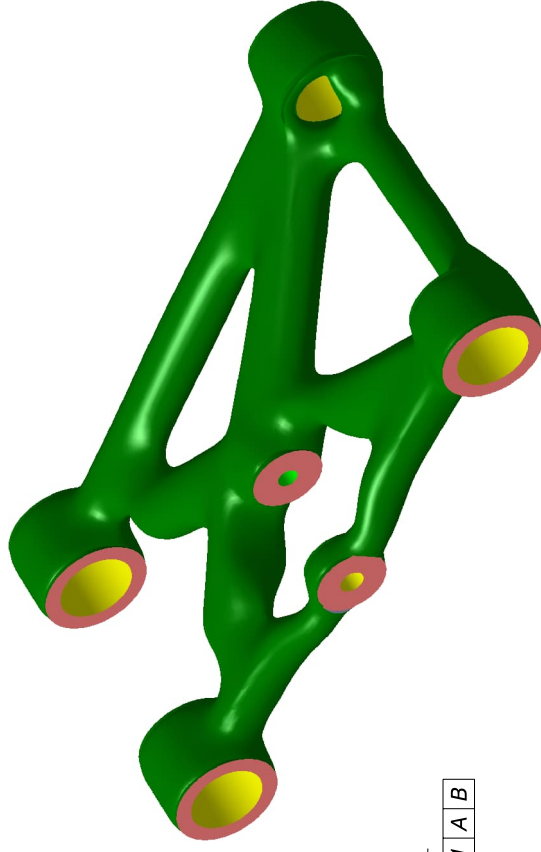
Section view B-B



Section view D-D



Section view C-C



3.2 [0.8]

REV.	DESCRIPTION	Elaborate	Date
-	-	-	-

Date: 2021/09/27		Title: TRIKE Project	
Design: PPROJETOS		Suspension Arm	
Drawing: DDias	Material: SAE 8620	Sheet Nr: 1/1	Escala: 2:1
Checker: DDias	Client: MAGNETTO AUTOMOTIVE	Unit: --	Position: 01
	MEASURES WITHOUT TOL. DIN 7168 - MEDIUM	Drawing Nr. --	
Dimensions in millimeters	ALL rights in this drawing belong to ABB LTDA. Designed by CAD system. Do not modify manually.		

